Quantification of thermal resilience in buildings

Evaluation of Building Envelope Performance and Operational Parameters

Master Thesis

Nathanail Tzoutzidis

Delft University of Technology

TU Delft

Quantification of thermal resilience in buildings

Evaluation of Building Envelope Performance and Operational Parameters

by

Nathanail Tzoutzidis

Student Number: 5611725

Mentors:

Simona Bianchi | Resilient Structural & Climate Design, TU Delft

Charalampos Andriotis | AI in Structural Design & Mechanics, TU Delft

External Advisor:

Jonathan Ciurlanti | ARUP, Amsterdam

November, 2022 - June, 2023

MSc in Architecture, Urbanism and Building Sciences (Building Technology)

Technical University of Delft (TU Delft)

TU Delft | ARUP

Preface & Acknowledgements

In an era of escalating climate change and its consequential impact on the built environment, the significance of ensuring thermal resilience in buildings cannot be overstated. As extreme overheating stresses become increasingly frequent and severe, the need for comprehensive strategies to assess and enhance thermal resilience has become paramount. This research endeavours to address this urgent challenge by developing a robust framework for quantifying the thermal resilience of buildings against extreme overheating stresses. By delving into various aspects of building performance, data analysis, and computational modelling, this study aims to contribute to the broader understanding and implementation of resilient building practices.

The topic engages various scientific disciplines associated with the built environment, including building physics, computational science, statistical techniques, and building performance efficiency. This aspect serves as a driving force for my interest in undertaking this research and developing innovative strategies and solutions to address the evaluation of thermal resilience performance in buildings during the initial design phase. Consequently, this endeavour aims to acquire comprehensive insights into building performance, enabling effective communication of the proposed design to stakeholders involved in a building project.

The successful completion of this research project has been made possible through the support and collaboration of numerous individuals. I would like to express my deepest gratitude to my research mentors, Dr. Simona Bianchi and Asst. Prof. Dr. Charalampos Andriotis, for their invaluable guidance, expertise, and encouragement throughout this journey. Their insightful feedback and unwavering support have been instrumental in shaping the direction and quality of this research. I would like to thank Jonathan Ciurlanti, my external advisor from ARUP, for his invaluable guidance and support in navigating the challenges of complex computational tasks. I am also grateful to the VR Lab staff and faculty of TU Delft, whose resources and facilities have provided a nurturing environment for my research endeavours. I extend my appreciation to Dr. E. Brembilla and PhD. Candidate P. de la Barra Luegmayer for sharing their knowledge about weather data sets. I would like to express my sincere gratitude to PhD. Candidate Ziead Metwally for sharing his knowledge about the sensitivity analysis process and providing me with useful insights about regression models.

Last but not least, I am indebted to my family and friends for their unwavering support, encouragement, and understanding throughout this research endeavour. Their belief in my abilities and their constant motivation has been a source of inspiration and strength. This research would not have been possible without the collective efforts, contributions, and support of all those mentioned above, as well as many others who have played a part in this endeavour. Their dedication and collaboration have been integral to the successful completion of this study, and for that, I am deeply grateful.

Nathanail Tzoutzidis
Delft, June 2023

Summary

Climate change and extreme heat are critical issues which have been faced all over the world. Consequently, designers strive to monitor and assess the performance of facades by developing environmental assessments at the early design stages, since design changes do not require many resources. Rapid urban expansion in many parts of the world is leading to increased exposure to extreme natural hazards, exacerbated by climate change. It is essential to come up with strategies for mitigating the vulnerability of the built environment. The concept of thermal resilience and adaptation to climate change have gained ground and international attention in the Architecture, Engineering and Construction (AEC) industry. Resilience is a multi-facet property which defines the vulnerability of the built environment. Although the qualitative assessment of resilience value, the quantification of urban resilience is not yet representative enough and there is a lack of calculating the resilience in the built environment. However, designers are called to develop building and planning proposals with taking into consideration the thermal resilience of buildings against extreme hazards. This thesis aims to fill the gap between the qualitative and quantitative evaluation of thermal resilience in buildings by considering the operational building performance and the thermal performance of the building envelope in case of extreme heat waves. Towards this direction, the most influential parameters of thermal resilience are identified by implementing a sensitivity analysis process, in the first part. Secondly, a quantification method is presented and the thermal resilience performance for buildings in Amsterdam is calculated. Last, this thesis attempts to develop a computational workflow in order to assist designers and engineers in defining the thermal resilience index from the early design stage. Defining a less computational cost and time-consuming workflow is also a goal. Due to time limitations, the multi-facet aspect of resilience and the difficulty of quantification of its indicators, this research focuses on the ex-ante evaluation of the building envelope by identifying its vulnerability to extreme heat waves.

Contents

Nomenclature

Abbreviations

Abbreviation	Definition
AEC	Architecture ,Engineering and Construction
BPS	Building Performance Simulation
EPW	Energy Plus Weather Files
TMY	Typical Meteorological Year
GCM	Global Climate Model
RCM	Regional Climate Model
GH	Grasshopper
HVAC	Heating, Ventilation and Air-conditioning
KPI	Key Performance Indicator
H	Humidex
HI	Heat Index
IOD	Indoor Overheating Degree
PMV	Predicted Mean Vote
SET	Standard Effective Temperature
WUMTP	Weighted Unmet Thermal Performance
RCI	Resilience Class Index
IPCC	Intergovernmental Panel on Climate Change
KNMI	Royal Netherlands Meteorological Institute
RCP	Representative Climate Pathways
GHG	Greenhouse Gas
UQ	Uncertainty Quantification
MC	Monte Carlo
LHS	Latin Hypercube
SA	Sensitivity Analysis
PCE	Polynomial Chaos Expansions
ACH	Air Change per Hour
ExFan	Exhaust Fan Ventialtion
COP	Coefficient of Performance
WWR	Wall-window ratio

Symbols

Symbol	Definition	Unit
t	Thickness	[m]
λ	Conductivity	[W/mK]
ρ	Density	[kg/m^3]
c	Specific Heat Capacity	[J/kgK]
T_{abs}	Thermal Absorbance	[-]
S_{abs}	Solar Absorptivity	[-]
V_{abs}	Visible Absorptivity	[-]
$U-vlaue$	Thermal Transmittance	[W/m^{2}K]
$R-value$	Thermal Resistance	[m^{2}K/W]
$G-value$	Solar Heat Gain Coefficient	[-]
V_{tran}	Visible Transmittance	[-]
Occ	Occupancy	[ppl/m^2]
SOL_{rad}	Solar Radiation	[kWh/m^2]
T	Temperature	[°C]
$Infil$	Infiltration	[m^3/s/m^2]
F/p	Flow/person	[m^3/person]
ACH	AirChange/Hour	[60q/V]

1

Introduction

Climate change and extreme heat are critical issues for the built environment. The global warming of the last century has currently reached a 0.2°C per decade and it is predicted that the global temperature will increase between 1.1°C and 6.4°C by the end of the 21st century compared to the period 1980-1999 (Pachauri & Reisinger, 2007). Gaffen and Ross (1998) and Kenward and Raja (2014) stated that the impact of climate change on heatwaves has already begun, as observed by the significant upward trend in the frequency of heatwaves from 1949 to 1995, indicating approximately a 20% overall increase in the number of heatwaves during that period. In addition, the projected population growth in urban areas is 68% of the world's population by 2050 (Heilig, 2012). The constant rising urbanisation and rapid urban expansion are leading to increased exposure of the built environment to extreme natural hazards, exacerbated by climate change (Jenkins et al., 2023). Cities consume the great majority – between 60% and 80% of energy production worldwide and account for roughly an equivalent share of global CO^2 emissions, according to Chaoui and Robert (2009). Zahra et al. (2017) mention that the building industry is responsible for 30% of the global annual greenhouse gas emissions and 40% of global energy consumption and 31% of all waste. Moreover, the facades are the most crucial thermal barrier in a building, defining how air moves in and out and driving spending on heating and cooling. As such, it plays a critical environmental role. Benardos et al. (2014) enhance the importance of facades, as they represent 25-30% of the total construction budget and their performance affects the energy consumption of a building and hence the operational greenhouse gas emissions. Taborianski and Prado (2012) stated that the type of façade has an influence on energy consumption during the building life cycle and, consequently, contributes to buildings' CO^2 emissions because these emissions are directly connected to energy consumption. In 2022, Favoino et al. (2022) noted that facade contributes to mitigating the risk related to climate change for different performance aspects, such as energy consumption and indoor comfort, hence the impact of facade design on the building resilience.

Rockefeller Institution in collaboration with Arup has been investing in research in order to come up with strategies for identifying the resilience factor and mitigating the vulnerability of the built envi-

Figure 1.1: The built environment is exposed to extreme heat waves.

ronment against climate change, since 2012 (Arup, 2012).

Nowadays, designers are called to develop building and planning proposals with taking into consideration climate resilience against extreme hazards and events. For this reason, researchers have been trying to define the resilience of buildings through their technical aspects by specifying their indicators and properties since 2003. This research thesis addresses the problem of identifying thermal resilience by quantifying its indicators on building scale, by calculating the energy demand and the indoor thermal comfort of buildings and assessing their vulnerability to overheating.

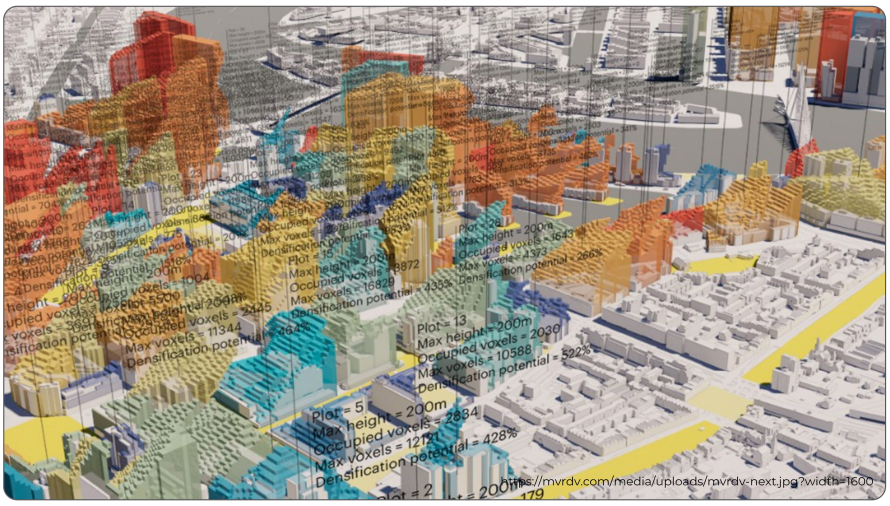

Figure 1.2: Environmental studies are embedded at the early stage of design.

1.1. Problem Statement

Quantifying thermal resilience requires precise calculations typically carried out in the final design stage when design elements, materials, and building properties are determined. This approach, however, offers limited flexibility, as making changes to the design at this stage demands considerable resources. Hence, performing assessments during the early design stage is more advantageous, even when material and building parameters remain undefined. Developing a framework for calculating thermal resilience in buildings is essential, as it should accommodate various design options, uncertainties, and probabilistic

scenarios. The importance of uncertainty in energy modelling is often undervalued. A model represents a simplification of reality and therefore it is important to quantify to what degree it is imperfect before using it in design, prediction and decision-making processes (Manfren et al., 2022). Deterministic energy simulations provide static performance of the indicators without considering future or uncertainty case scenarios.

Researchers at the MIT Concrete Sustainability Hub (MIT, 2017) argue that early-stage environmental studies are more valuable, as designers can more readily implement design changes and improve building performance without requiring substantial resources. Simultaneously, energy models have been developed to account for uncertainties during design and operation phases, incorporating complex interactions among various factors in the energy domain (Nik, Perera, et al., 2021). These models, which rely on stochastic rather than deterministic simulations, assist in developing strategies to address climate change and ultimately result in more resilient design choices. Nonetheless, the absence of adequate frameworks or methods for using climate data with extreme weather conditions in building simulations poses significant challenges in evaluating the climate resilience of the built environment.

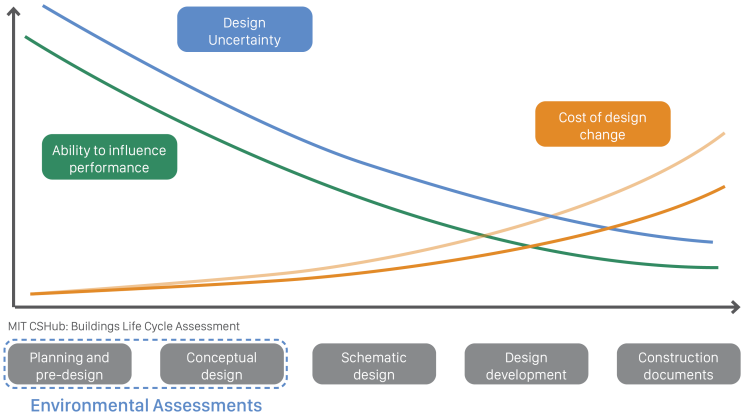

Figure 1.3: MIT CSHub: Buildings Life Cycle Assessment.

1.2. Scope

This study aims to gain new knowledge regarding the field of thermal resilience in buildings by pointing out the thermal resilience definition and stating its indicators that should be quantified. Moreover, this research attempts to evaluate the parameters that affect the indicator results by considering the results in a matter of uncertainty. Consequently, building performance simulations are applied to evaluate buildings' energy performance and understand how the uncertainty quantification process could be implemented in order to improve the decision-making process. The underlying assumption is that by employing a probabilistic approach to building performance simulations and incorporating the concept of risk, the energy performance gap can be quantified, precisely forecasted, and ultimately diminished. Moreover, implementing the theoretical knowledge into practice by developing a digital design tool for indicating buildings' vulnerability to indoor overheating by running energy and thermal performance simulations and hence predicting their performance against extreme overheating scenarios at the early design stage.

1.2.1. Research question and sub-questions

Realising the aforementioned theoretical background and problematic, the main research question and sub-questions of the thesis are stated as follows:

"*In what manner can a digital design workflow be devised to assess the thermal resilience of buildings against extreme heat wave stresses, and how it can assist designers and engineers in the decision-making process during the early design stage?*"

a. What are the thermal resilience definition and its indicators?
b. Which metrics should be quantified in order to evaluate a building's thermal performance?
c. What kind of weather data sets are suitable for thermal resilience quantification against extreme overheating hazards?
d. How uncertainty quantification can be implemented in the computational workflow?
e. Which are the major influential parameters that affect the building's performance against extreme overheating?

1.2.2. Objectives and Limitations

Objectives

The main purpose of this thesis is to bridge the gap between qualitative and quantitative assessment of thermal resilience in buildings and indicate the influence of facade performance on building's operational energy consumption. The research field focuses on the building envelope's vulnerability against long-term overheating stresses by predicting the building's energy performance under extreme weather scenarios while climate and design uncertainties are considered. In addition, the paper aims to purpose a computational workflow for developing an assisting tool for indicating buildings' vulnerability to heat stresses at the early design stage and give the ability to implement the same workflow to more building examples. Defining a less computational cost and time-efficient workflow for simulations is also a goal of the research.

Limitations

The research is based on the main assumption that the case study refers to a study of an office building in Amsterdam. Since it is not an already existing building but a hypothetical study and due to time limitations, the multi-facet aspect of the resilience definition resilience and the difficulty of quantification of its indicators, there is a need for setting transparent boundary conditions for this research.

To start with, the urban factors such as urban heat islands, view factors and micro-urban climate are neglected since they are related more to resilience with the aspect of urban scale, infrastructure and networks (Galanos & Chronis, 2022; Naboni et al., 2019; Nik, Perera, et al., 2021). Hence the research focuses on the building scale and more specifically the design case study refers to an open-plan, 8-story office building in Amsterdam. For this case study more assumptions have been made and hence the building geometry, its general dimensions and function are considered as design decisions. The main building has a rectangular plan of 45x30 meters with a central atrium of 24x15 meters and each floor a height of 4.20 meters. Since the research focuses on office building the operating schedule is defined

as 8 working hours per day and 5 days per week. Factors that are related to the material properties of the facade, the properties of the building envelope and the operational properties of the building are considered uncertain variables and hence the research focuses on those. More specifically, material properties such as thickness, conductivity, specific heat, thermal absorbance, thermal transmittance, visible transmittance and solar heat gain coefficient are examined. On the other hand, the hygrothermal property among the facade materials is neglected in the research. According to Ekström (2021) for exploring this field, a deep dive into facade materials properties and technical design variations of the facade is needed. Regarding the building envelope, properties such as the wall-window ratio and the infiltration ratio are examined but the thermal bridging is neglected in the research. Factors related to the thermal climate design such as indoor thermal comfort and HVAC systems are examined but on the contrary, factors of visual comfort such as artificial lighting and glare are neglected from the research since they are not closely related to the thermal resilience field. The aforementioned parameters are considered as uncertain factors and their effect on the performance of the building is evaluated. Another boundary condition is occupant activities and behaviour. Research has shown that the occupants' activities and behaviour significantly impact a building's energy use, although sampling daily data an annual time-frame is needed in this case (Ekström et al., 2020). Since the research is not based on real-time data the occupants' activity is considered as working standing or sitting in an open space office environment.

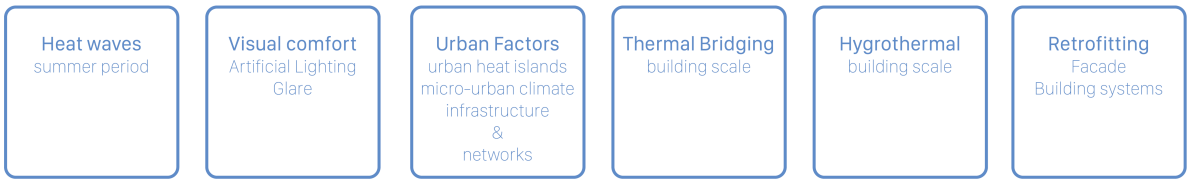

Figure 1.4: Limitations of this research.

A big part of the research is based on data that are produced from building energy and thermal simulations and hence weather data sets need to be examined apart from the building parameters. In order to perform building simulations with the main aspect the thermal resilience, weather data should consider overheating stresses. For this reason, weather data sets that refer to the location of Amsterdam were collected and the generation of the EPW file was based on those. The building simulations are held within a time range of 3-5 hottest days during summer.

Last, this research attempts to develop a computational framework for thermal resilience quantification and hence to indicate the thermal and energy performance of buildings during overheating events. In other words, the process is based on the ex-ante evaluation of the building's performance against overheating. Strategies for facade retrofitting and/or boosting buildings performance, such as PV panels implementation and energy batteries, are not part of this research.

1.3. Research method and case study

Since resilience is a complex term and is related to different sectors of the built environment, plenty of scientific papers and Doctoral Dissertations were founded for the seismic, flood, climate, infrastructure and resilience of urban networks. However, literature closely related to this topic is founded during the last two years. In general, considering the aforementioned scope of work, objectives and limitations of this research the literature spectrum relies on the following topics:

i. **Thermal resilience definition:** Clarify the definition of thermal resilience for this research and identify its indicators. In this first topic, the field of resilience in buildings is discussed with the main focus on the thermal performance of buildings. Indicators of thermal resilience are stated and the parameters that contribute to indicators performance are pointed out.

ii. **Weather data:** This topic refers to the generation of weather data sets that can be generated for extreme climate conditions by considering historical weather data and past events. Through this research, variant weather scenarios could be produced.

iii. **Building envelope and facade properties:** Energy simulations are part of the practical part of this thesis, for this reason, multiple simulation results of variant building properties respectively are discussed. Hence, the research focuses on the building envelope and material properties of the facade. These values are assigned to the simulation model, later on, in order to move forward to the case study and the computational workflow.

iv. **Uncertainty quantification:** As mentioned in the problem statement, material, building properties and climate factors are not certain for in case of extreme overheating events. Consequently, parameters of uncertainty are closely related to the topic of this research and quantification processes are explored. In short, methods for sampling and processing data via Python scripting are discussed.

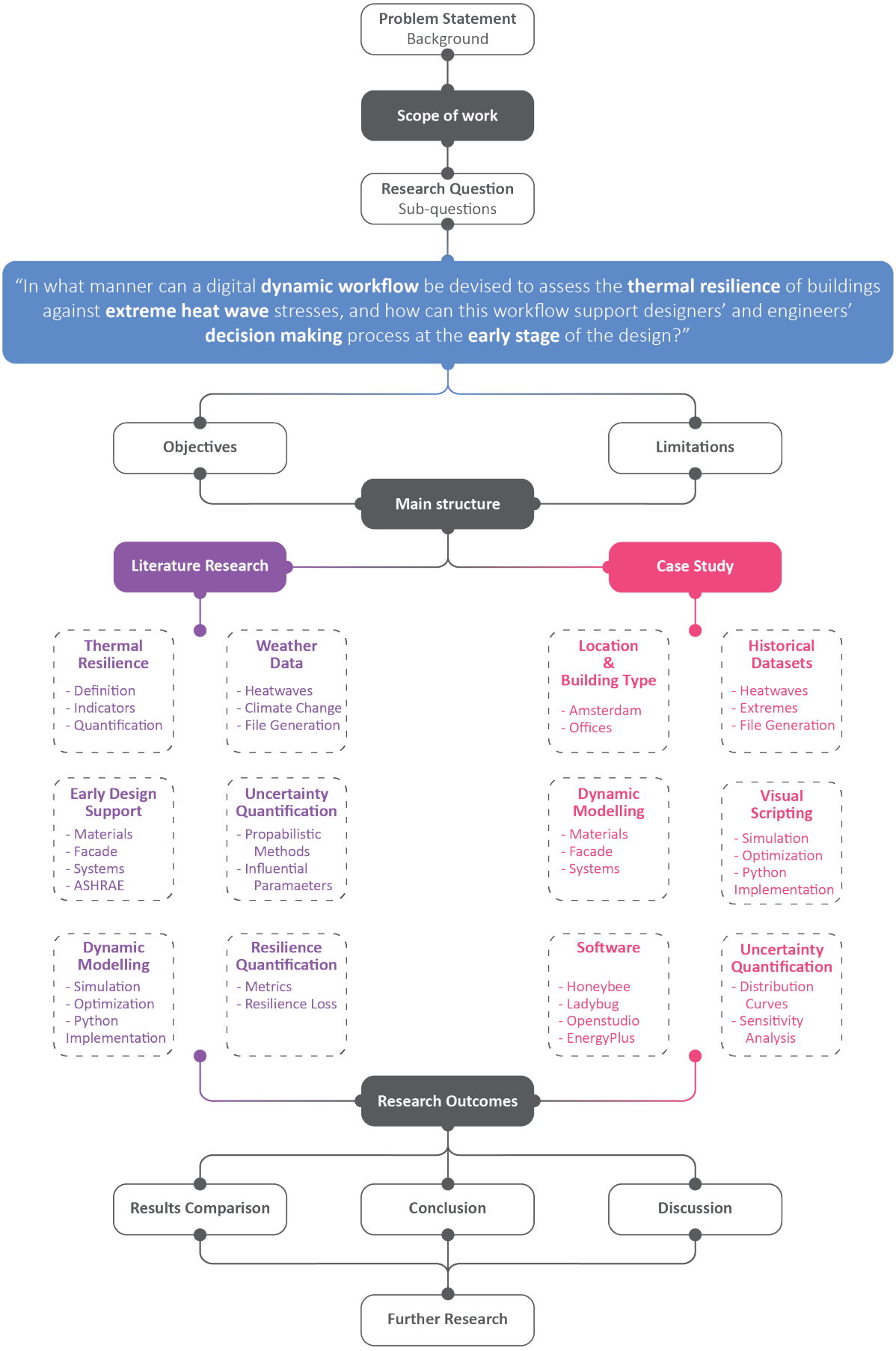

Figure 1.5: Research strategy diagram.

The main sources of this research are scientific papers gathered from Google Scholar, Research Gate and Elsevier. The Doctoral Dissertations of Abediniangerabi and Shahandashti (2022) and Ekström (2021), scientific papers from researchers of Leuven University, TU Delft, EPFL and ETH and consistent information from corporate research held by companies such as Arup, Perkings & Will are forming the main core of the literature research. In Appendix D.1 a literature map illustrates the references that have been studied during this research. The following terminology of *thermal resilience, resilience quantification, uncertainty quantification, predictive energy simulations, façade thermal performance, weather data, sensitivity analysis* were used as the main keywords of this search.

The implementation of the theoretical knowledge, of the topics mentioned above, into practice is the second part of this thesis. In general, digital models with 3D geometry of building prototypes and Visual Programming scripts are used in order to run energy simulations under different weather conditions that respond to possible future weather scenarios. Consequently, parameters of design uncertainties are needed to be considered for simulations for predicting the building's performance with a higher value of probability. More specifically, the assignment can be split into shorter individual tasks as mentioned bellow:

a. **Weather data:** Historical weather data is needed for getting information about the extreme heatwaves that occurred in Europe during the last decades. Historical weather data are used as a basis for generating a weather data set in which extreme climate conditions are included in order to run simulations and assess building's performance.
b. **Building and facade archetypes:** A digital model of office building with variant material properties is designed for covering a spectrum of facade materials in buildings. Here building envelopes differentiate because of the variant wall-window ratio and material properties.
c. **Building simulation:** Visual scripting and Python language are used for forming the energy and thermal simulation workflow by considering the climate and design uncertainties. Through this process, thermal resilience indicators are quantified in order to estimate the resilience loss of the office building.
d. **Uncertainty quantification:** The simulation outcomes are distributed in fitting curves in order to sample values that give results with 95% probability. Consequently, the results of thermal resilience loss are more accurate than deterministic simulation studies.
e. **Resilience quantification:** In this task, the simulation outcomes are compared with an optimised design of the office building and hence comparisons between an ideal and real performance are presented. Therefore, the conclusions can be made in order to help the decision-making process and assist designers in selecting the most valuable types of materials, glazing ratio and HVAC performance for their design.

Rhinoceros, Grasshopper, EnergyPlus and WallaceiX software are used for this assignment. In addition, Python libraries of eppy and sklearn used in complementary and post-processing tasks. Seaborn and Matplolib were used for data visualization.

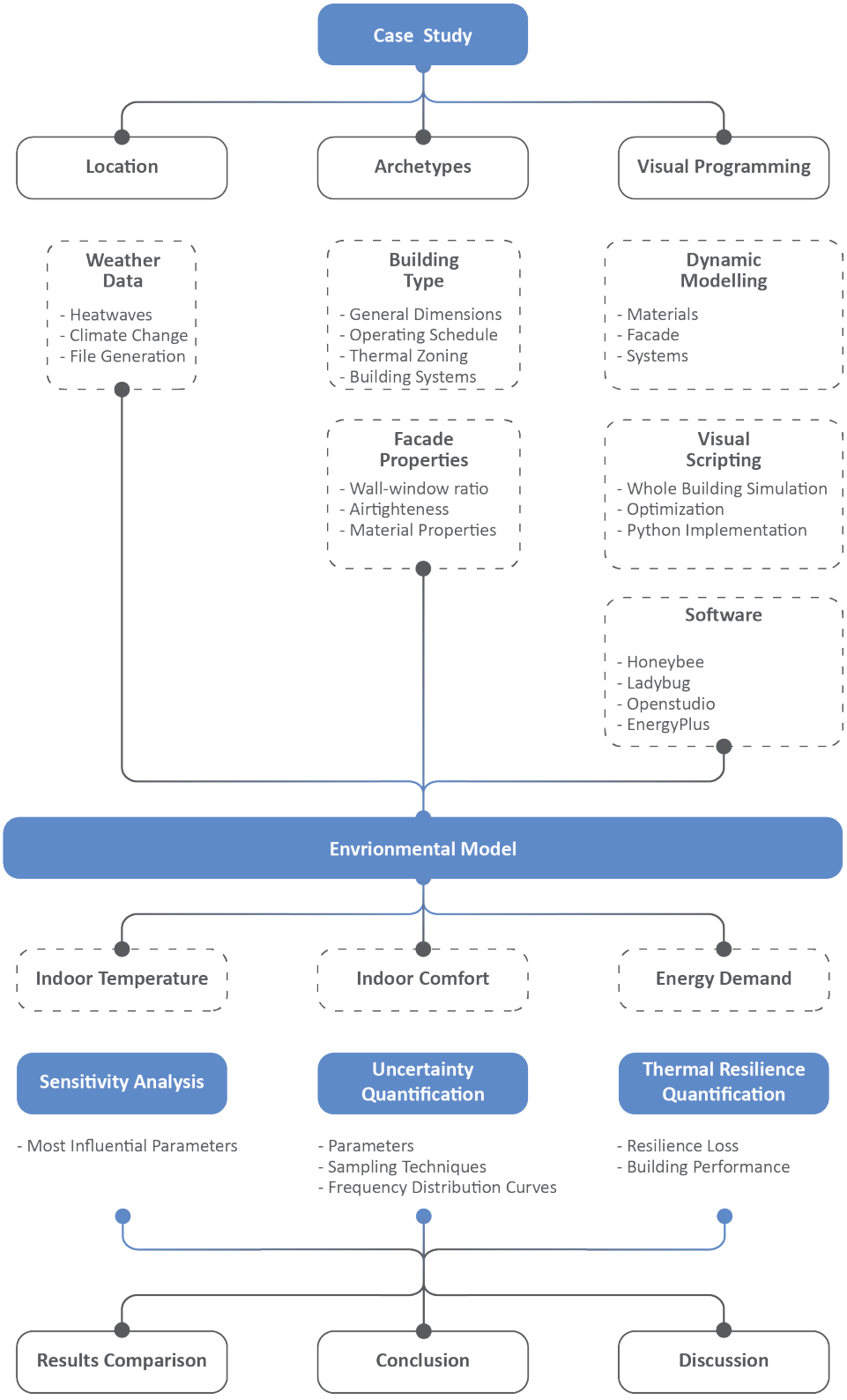

Figure 1.6: Design assignment methodology diagram.

1.4. Thesis Outline

The thesis report comprises by the following chapters.

Chapter 1. **Background:** Introduction to the topic of thermal resilience and building energy performance by considering climate and design uncertainties.The problem, scope of work, research questions, objectives and limitations are stated.

Chapter 2. **Literature review:** Gives the theoretical framework for the aforementioned fields of research based on the literature research.

Chapter 3. **Design Assignment:** Describes the overall practical implementation of the theoretical framework applied in this project. Hereby the results are compared and discussed in order to evaluate the validity of the process and gain knowledge for the implementation of thermal resilience quantification in the built environment.

Chapter 4. **Conclusion and Future work:** Presents the conclusions from the literature review and the produced results. Proposes identified subjects of interest for future research.

Chapter 5. **Reflection:** Describes the overall engagement of two departments of the Building Technology Master track by forming a multidisciplinary background to address the problem of climate change in the built environment. The graduation process and the societal impact of this graduation project are discussed.

2

Literature Review

The literature review of this research attends to the topics of resilience definition and quantification in the built environment. Scientific papers that concern resilience in a broader spectrum have been explored. In general, a significant amount of literature has been found for assessing resilience in the built environment against earthquakes, hurricanes, and floods by using qualitative or quantitative evaluation frameworks. Bruneau et al. (2003) introduced the resilience definition and stated a quantification methodology for evaluating the seismic resilience in buildings. Since then, the resilience qualitative and quantitative evaluation frameworks came to the foreground and studies conducted by researchers in order to explore this topic on different scales. Some of the scientific papers deal with the urban design and the CO^2 emissions in the context of climate change (Naboni et al., 2019), while some others (Sharifi & Yamagata, 2016) evaluate the resilience in urban scale by developing qualitative framework. In the same concept of a qualitative evaluation, Favoino et al. (2022) develops a framework for the resilience of facades and focuses on their structural and thermal performance. Panteli, Trakas, et al. (2017) evaluates the performance and quantifies the resilience of infrastructure power systems. Cimellaro et al. (2010) develops a quantitative framework for analytical quantification of seismic resilience for healthcare facilities. Other studies are focused on assessing the energy performance of buildings under the factor of climate change (Attia et al., 2021; Tavakoli et al., 2022). These refer to quantitative evaluation strategies for defining resilient cooling systems during overheating stresses. As the literature research indicates, building resilience is a complex multi-faceted issue ("Resilience (engineering and construction)", 2023) that must be evaluated considering multiple factors under various aspects that lean towards both macro- and micro-climatic contexts. However, as was clarified in the previous chapter, this research focuses on the quantitative evaluation of thermal resilience in a building scale by taking into consideration design and climate uncertainties.

In the following chapters, the topics of the resilience definition in the building scale will be discussed. More specifically, resilience definition, its dimensions and its stages are stated in the next chapter. Moreover, part of the research explores strategies for resilience quantification by calculating metrics related to resilience thermal factors. Subsequently, it is essential to identify the most influential

parameters that affect the results of thermal resilience indicators (Homaei & Hamdy, 2021b). Through the literature research, it is pointed out that the thermal resilience of buildings is affected by both design and climate factors (Nik, 2016). Therefore, the research explores the field of building and facade properties while attempting to observe climate data for synthesizing an overheat strike case. As stated in the problem formulation, there are inaccuracies between the building simulations results and actual performance, for this reason, this research explores the field of uncertainty among the design and climate factors (Sun et al., 2020) and hence uncertainty quantification strategies are discussed in the following chapters. However, this thesis focuses on thermal resilience on the building scale, the aforementioned framework can not be considered as aligned with this specific topic and hence the literature narrows down to studies that are closely related to thermal resilience by considering cooling loads and facade properties that affect the building performance.

2.1. Resilience

2.1.1. Definiton, Dimensions and Stages

Defintion

The concept of resilience is used in various research disciplines from environmental research to materials science, engineering, sociology and economics. Therefore there are variant definitions stated by the researchers. In general, resilience is related to the ability of a system to recover from a failure, cope with unanticipated dangers and bounce back to obtain its initial functionality. Arup (2015) presents the definition of resilience term as the capacity to adapt to changing conditions and to maintain or regain functionality and vitality in the face of stress or disturbance. It is the capacity to bounce back after a disturbance or interruption. However, this definition and others that can be found in scientific papers discuss resilience as a broad topic of the built environment and thus can not be considered sufficient enough for the topic of this thesis. Subsequently, resilience should be defined in the case of building level with rigorous terminology.

This research thesis attempts to define resilience at the building level. Bruneau et al. (2003) stated that seismic resilience is conceptualized as the ability of both physical and social systems to withstand earthquake-generated forces and demands and to cope with earthquake impacts through situation assessment, rapid response, and effective recovery strategies. In the field of building energy and thermal performance, Attia et al. (2021) developed a quantification framework for evaluating the resilient cooling of buildings against heat waves. His research states that resilience refers to the capacity of buildings and urban networks to withstand, absorb, adapt and recover from the effects of stress in a timely and efficient manner in order to continue functioning during natural hazards caused by climate change. Homaei and Hamdy (2021a) assessed the thermal resilience in buildings by establishing a benchmarking framework and labelling metric. This research defines the thermal resilience against extreme climate events as:

> *Resilience is the capability of the building to prepare, absorb, adapt and recover from disruptive events. In other words, resilience is the performance property of whether the building's performance is adequate enough against climate hazards by giving an indication of the building's future performance for mitigating the impact of extreme events.*

Dimensions

According to Bruneau et al. (2003), resilience for physical systems can be further defined by its properties. The four main dimensions (4Rs) of resilience - robustness, redundancy, resourcefulness, and rapidity - have been identified for both physical and social systems. Hereby those properties are defined as follows:

i. Robustness: strength, or the ability of elements, systems, and other units of analysis to withstand a given level of stress or demand without suffering degradation or loss of function.

ii. Redundancy: the extent to which elements, systems, or other units of analysis exist that are substitutable.

iii. Resourcefulness: the capacity to identify problems, establish priorities, and mobilise resources when conditions exist that threaten to disrupt some element, system, or other units of analysis; resourcefulness can be further conceptualized as consisting of the ability to apply material and human resources to meet established priorities and achieve goals.

iv. Rapidity: recovery, the capacity to meet priorities and achieve goals in a timely manner in order to contain losses and avoid future disruption.

Stages

According to Homaei and Hamdy (2021a), the response of a building to a disruptive event can be split into two stages. The phase when the building responds during the event and the phase when the building recovers after the event. The former includes the occurrence time in other words the duration of the unanticipated event and the latter evaluates the building performance considering the recovery time. The suggested framework involves simulating the building's performance during and after the disruptive event and utilizing appropriate metrics to quantify its thermal resilience. Various disruptive events can impact building performance, such as fires, windstorms, hurricanes, flooding, heatwaves, ice storms, power outages, and pandemics, and the test framework should reflect a fixed duration for each event (Attia et al., 2021). Resilience in the field of engineering encompasses multiple components. The initial component is vulnerability, which pertains to how susceptible a building system is to various types of shocks. This concept is considered crucial in climate change studies according to existing literature. Vulnerability refers to the system connected with specific hazards of concern and its associated attributes. The second stage is resistance, referring to a building system's capability to sustain the initial design conditions. The third element, robustness, refers to how the building system, along with its occupants, adjusts and adapts to shocks during critical performance conditions. Finally, the fourth aspect is recoverability, which refers to the nature and extent of a building system's recovery from shocks.

2.1.2. Indicators and Parameters

Indicators

Before discussing the quantification methods, the performance indicators that refer to thermal resilience should be pointed out. There are several Key Performance Indicators (KPIs) that can be used to evaluate the thermal resilience of buildings. Some of these KPIs include indoor temperature, thermal comfort, and energy consumption.

One of the KPIs for thermal resilience in buildings is indoor temperature. The study used dynamic

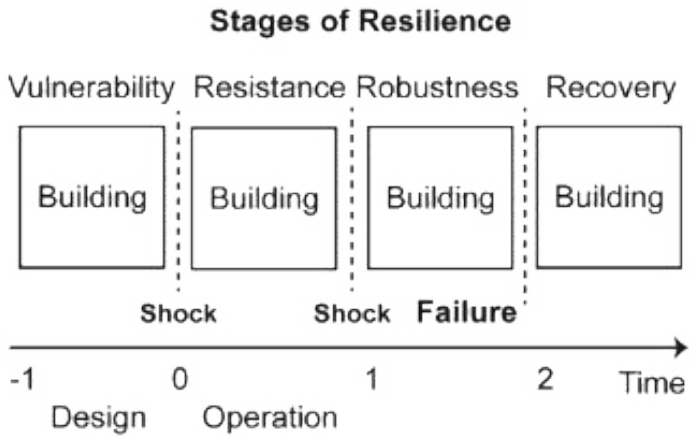

Figure 2.1: The stages and timeline of the resilience process. (Attia et al., 2021).

energy simulations to evaluate the thermal resilience in buildings and found that the indoor temperature was a critical KPI for assessing the building's ability to withstand heat waves(Homaei & Hamdy, 2021b). The main needs of building occupants are indoor thermal comfort which can be assessed by measuring the indoor operative temperature. Operative temperature is defined as the average of the mean radiant temperature and the ambient air temperature weighted by their respective heat transfer coefficients ("Operative temperature", 2022). Considering that cooling systems in buildings calibrate the indoor air temperature and hence the operative, the research explores the functionality of these systems and the energy consumption that is needed to achieve indoor operative temperature standards. Energy consumption is also a KPI for thermal resilience in buildings. Subsequently, it is crucial to consider the energy consumption apart from the indoor operative temperature. Graham et al. (2021) agrees and states that the most disruptive factors affecting building occupants' productivity are disruptions in thermal comfort. Therefore, it is important to evaluate the resilience of building performance from a thermal standpoint in relation to the building's energy performance. In that statement Homaei and Hamdy (2021b) agrees indoor operative temperature and energy consumption are considered indicators for assessing the thermal resilience evaluation in buildings.

This research focuses on evaluating thermal resilience through an office building case study. Most of the time during a day is spent around 87% indoors, and indoor thermal comfort is one of the most critical requirements of office building occupants and a crucial factor that can affect productivity (Homaei & Hamdy, 2021b).

Parameters

The aforementioned two main KPIs for assessing the thermal resilience performance can be affected significantly by building and facade parameters. According to Homaei and Hamdy (2021b) the performance of heating and cooling systems change the performance of those KPIs. The energy consumption is affected by the energy demand of the cooling system of the building. In this fact, there are building parameters that influence the performance of cooling systems and therefore the cooling set-point the air change rate and the air ventilation are parameters that can influence the cooling system. In addition, occupancy schedules and occupants' activity affect the indoor temperature (Graham et al., 2021).

Besides the functionality of the cooling system, the building envelope and its thermal performance

affect the indoor operative temperature (Feehan et al., 2021). Material properties, the glazing ratio, facade infiltration, thermal bridges and the air-tightness of the facade elements influence the heat transfer and the airflow from indoors to outdoors. These parameters and their evaluation are part of this study. Zhang et al. (2021) states that the thermal mass, with moderate to high absorptive capacity, can reduce heat gains to the indoor environment during heatwaves. However, some cooling or building designs might benefit the indicator of indoor temperature but can result in a negative impact on the energy demand.

2.1.3. Resilience Quantification

Besides the theoretical definition of resilience which delineates its qualitative aspect, researchers strive to come up with frameworks for calculating the resilience property in a quantitative manner. According to Hosseini et al. (2016), resilience quantification can be separated into two major categories with different approaches a. qualitative and b. quantitative assessments. The former area is based on the evaluation of resilience without numeric results and the latter is dependent on evaluation frameworks with rigorous calculations. Bruneau et al. (2003) formed the most representative general-based resilience evaluation framework in the field of seismic resilience which used the total impact e.g. performance losses during and after the disruption. This quantification definition calculates the performance curve that presents the quality of the building system in relation to time. As presented in the diagram 2.2, the performance curve can variate from the initial performance of the building during a disruption event. Hence, resilience can be quantified by calculating the inner area of this chart by measuring the definite integral of performance of 100% minus the real performance curve.

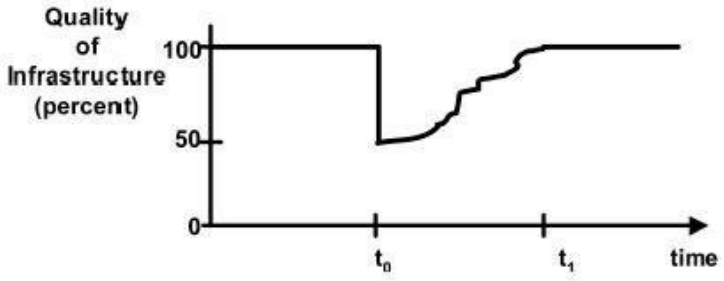

Figure 2.2: Resilience quantification (Bruneau et al., 2003).

$$R = \int_{t_0}^{t_1} [100 - Q(t)]\, dt \tag{2.1}$$

According to Bruneau et al. (2003) to achieve a holistic understanding, both aspects of the qualitative and quantitative assessment frameworks must be thought out. The resilience Bruneau's triangle assesses the field of seismic resilience and is a representative general-based method, which uses the total impact, such as performance losses during and after disruptions, to measure seismic resilience. This method is adopted by other researchers for expanding this concept for calculating the Resilience Loss in other fields of the built environment. Panteli, Mancarella, et al. (2017) develop an assessment framework of quantifying resilience in the context of power systems for both operational and infrastructure integrity. In this research, the resilience *triangle* is expanded to resilience *trapezoid* 2.3 and it is quantified by

using time-depend resilience metrics that are introduced to capture the critical systems degradation and the recovery features. In addition, resilience enhancement strategies are analysed by using this evaluation framework. The resilience trapezoid used quantification grid resilience by the introduction of a set of time-dependent metrics called the $\Phi\Lambda E\Pi$ metric system, which is based on the speed Φ and the magnitude Λ of the damaged grid functionality, the duration of the damaged state E, and the recovery speed Π.

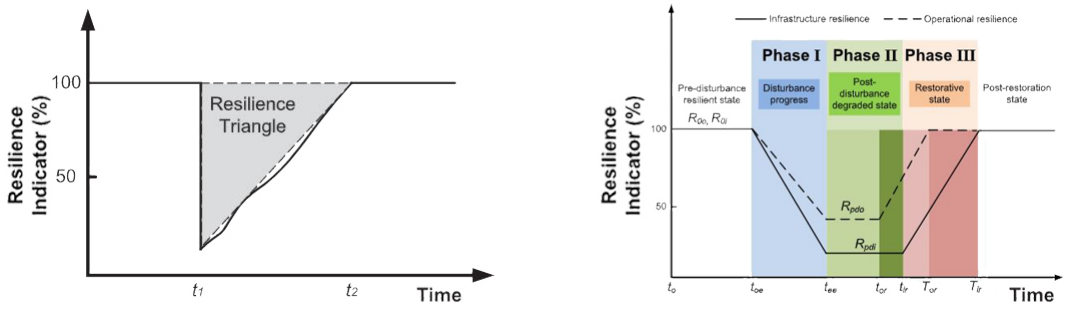

Figure 2.3: Resilience triangle and multi-phase resilience trapezoid. The smaller the area gets,the more resilient grid will be. (Panteli, Trakas, et al., 2017).

In the context of the built environment and energy resilience against extreme events is enhanced by the research of Zhou (2022) which contributes to developing a quantification evaluation framework for the survivability of energy systems. The enhancement of energy resilience can be categorized into three different types based on the phase of the extreme event: preparation for resilience before the event, actions and survivability during the event, and service restoration after the event 2.4.

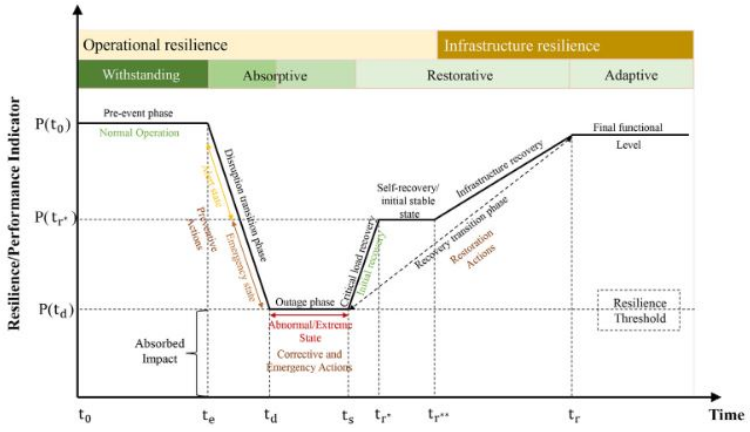

Figure 2.4: Resilience performance curve for building energy systems (Zhou, 2022).

Homaei and Hamdy (2021a) have adjusted these metrics for the quantification of different resilient abilities (i.e. preparation, absorption, adaptation, recovery). Their evaluation framework evaluates the thermal resilience in the building level during and after the disruptive event by calculating the indoor operative temperature 2.6. This framework is based on the performance of the operative indoor temperature with respect to the thermal performance of the building envelope, the level of occupancy, the operating schedule of the building and the performance of the building energy systems.

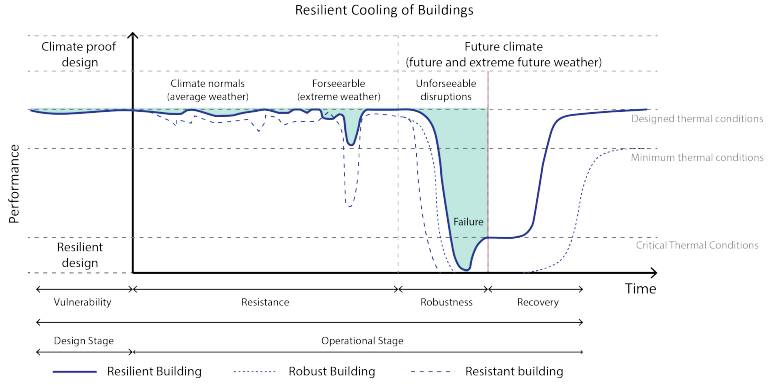

Figure 2.5: The components of a resilience definition (Attia et al., 2022).

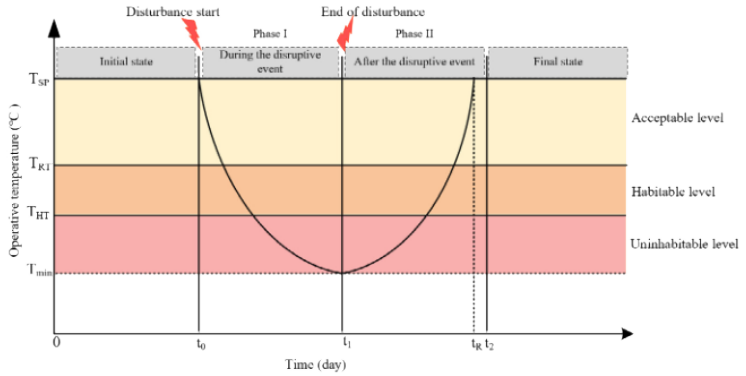

Figure 2.6: Multi-phase thermal resilience curve (Homaei & Hamdy, 2021b).

Metrics

An evaluation of the likelihood, potential vulnerability, and consequences of each risk using metrics or an assessment could aid in prioritizing the examination of risk factors and strengthening building resilience ("U.S. DoE", 2022). This measurement of building resilience can assist owners in making informed decisions to safeguard their assets, provide a better understanding of the resilience of the built environment and complement the current assessments of building sustainability.There have been several studies that have examined the evaluation of resilience in various fields. Hosseini et al. (2016) identified two main types of resilience assessment methods: qualitative and quantitative. Qualitative methods do not use numerical data to evaluate resilience and may include approaches such as conceptual frameworks or semi-quantitative indices.Resilience metrics are essential for quantifying resilience by calculating the performance of its indicators. These metrics should indicate how far and how low the building's performance deviates from the targets. Homaei and Hamdy (2021a) states that resilience quantification is needed to be captured during and after the disruption event based on simulation results. In this chapter, qualitative and quantitative metrics related to building thermal performance are discussed.

Favoino et al. (2022) in collaboration with the Eckersley O'Callaghan engineers, developed a qualitative framework for building thermal resilience which is focused on the evaluation of the facade performance. The assessment consists of two parts: the climate risk assessment and the mitigation strategy assessment ("A tool to improve climate resilience of facades", n.d.). This numerical framework (2.8) evaluates the likelihood of climate stressors, which were defined from 1-insignificant to 5-extremely high,

by their impact and consequences on the functionality of the facade.

Figure 2.7: Mitigation strategy diagram by Eckersley O'Callaghan engineers.

This framework gives an indication of whether the functionality of the facade under the climate stressors was minor or catastrophic by a numerical metric with a range from 1 to 5. Through this assessment, it is possible to identify a specific risk for each design option and ways for reducing or eliminating the consequences of the climate stressor and assist the stakeholders in the decision-making process (2.7). Although this numerical framework gives numerical indications it is not adequate enough for resilience quantification because it does not constitute a rigorous calculation methodology. However, this research contributes to the conceptualisation of evaluating thermal resilience in buildings as it is used to indicate the major facade parameters that affect thermal stresses.

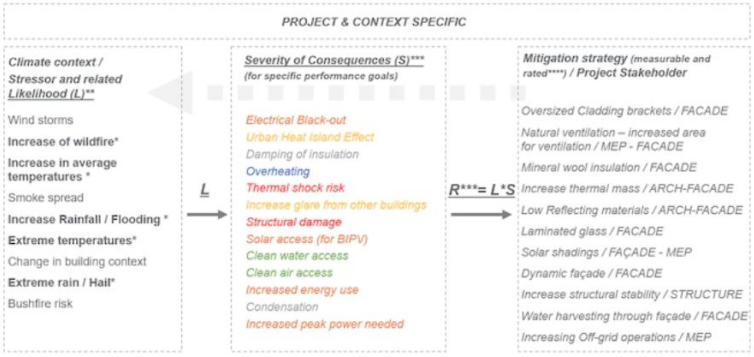

Figure 2.8: Qualitative framework Favoino et al. (2022).

Apart from the aforementioned qualitative framework, this research explores qualitative thermal resilience metrics. Bennet (2016) used the Energy Plus building performance simulator ins order to evaluate the resilience of high-rise residential buildings in case of power outages. This research is based on the handicaps of poor insulating properties of the facade materials and the high solar transmittance of glazing. Therefore, the heat loss can be high and consequently, high levels of discomfort and high energy consumption during operation can occur. Besides their poor performance in normal operation, these buildings are vulnerable to power failures during overheating stress. The research describes a

methodology to evaluate buildings' thermal resilience by quantifying the metrics of thermal autonomy and passive survivability. The results have shown that thermal autonomy does not consider a sufficient level the occupant interaction. Moreover, the results suggest adaptive opportunities of the building envelope with regard to maintaining indoor comfort. Sun et al. (2020) provided a methodology for modelling and analysis of thermal resilience and energy-efficient buildings. The case study of a nursing home was used for implementing the assessing methodology evaluating retrofit scenarios for improving thermal resilience, reducing the cooling demand and increasing energy efficiency. The metrics for assessing thermal comfort in buildings can be divided into two major categories, the biometeorological indices and the heat-budget models. The former is based on simplified metrics of the air temperature (heat index) () and humidity (humidex) (Steadman, 1979). The latter are complex indices that include all important meteorological and physiological parameters. According to the Energy Department of the United States the metrics of Heat Index (HI), Humidex (H), and Standard Effective Temperature (SET) are needed to be defined for evaluating thermal resilience in buildings calculated.These have been adopted by government agencies and industry ("U.S. DoE", 2022).

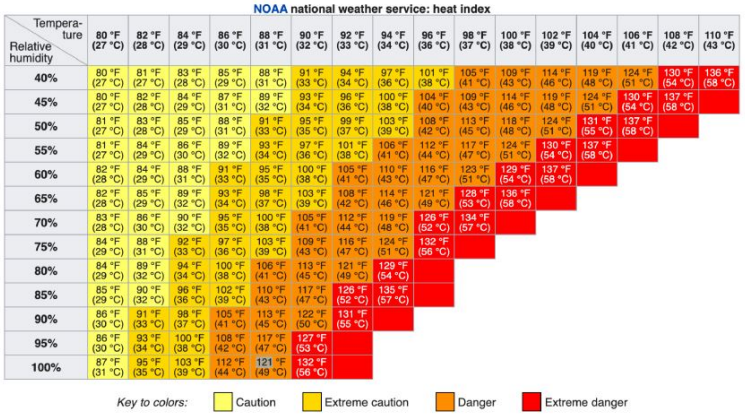

Figure 2.9: Heat Index lookup table. The HI effects on human health are categorized into five levels: Safe, Caution, Extreme caution, Danger and Extreme danger.

The Heat Index (HI) is a metric that combines the air temperature and the relative humidity for evaluating the level of human comfort. In other words, it calculates how the temperature feels like to the human body. This metric is used in the United States as an indicator of heat stress. In the HI table 2.9 the correlation of temperature(°C) and relative humidity (%) is presented. The calculation is based on the regression equation of Rothfusz (2.2) and provides results for the accumulated hours of all the occupants of a space or a thermal zone. Moreover, the Rothfusz regression is not valid for extreme temperature and relative humidity conditions beyond the range of data considered by Steadman (1979).

$$\text{Heat Index} = c_1 + c_2T + c_3RH + c_4TRH + c_5T^2 + c_6RH^2 + c_7T^2RH + c_8TRH^2 + c_9T^2RH^2 \quad (2.2)$$

Where:

T: ambient dry-bulb temperature (°F)

RH: relative humidity (%)

c1 = -8.78469475556	c2 =1.61139411	c3 =2.33854883889
c4 = -0.14611605	c5 = -0.012308094	c6 =-0.0164248277778
c7 =0.002211732	c8 =0.00072546	c9 =-0.000003582

The Humidex (H) is an index that is used in Canada to describe how hot the weather feels like to the average person, by combining the effect of heat and humidity. This index is a dimensionless quantity based on the dew-point temperature ("U.S. DoE", 2022) and can be calculated by the formula 2.3 and indicates levels of discomfort as they presented in table 2.10.

$$\mathrm{H} = T_{air} + \frac{5}{9}\left(6.11 * \exp\left(5417.7530 * \left(\frac{1}{273.16} - \frac{1}{273.15 + T_{dew}}\right)\right) - 10\right) \tag{2.3}$$

Where:

T_{air}: the air temperature in °C

T_{dew}: the dew-point temperature in °C

exp : 2.71828

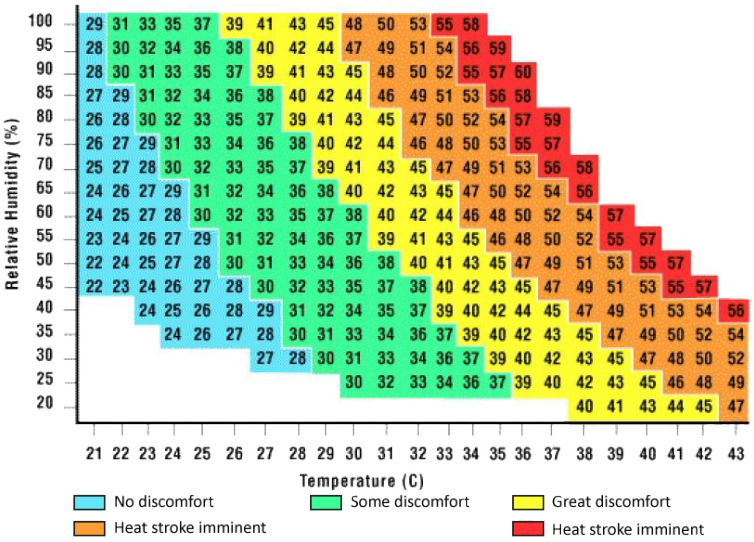

Figure 2.10: Humidex lookup table. Humidex from Temperature and relative Humidity Readings.

The Standard Effective Temperature (SET) is a metric of human response to the thermal environment and its calculation is similar to Predicted Mean Vote (PMV) as it is based on heat-balance equations that incorporate personal factors of clothing and metabolic rate. SET is widely used in cases of power outages in order to maintain safe thermal conditions. The EnergyPlus software calculates the SET metric in relation to time ("U.S. DoE", 2022). A simplified metric that considers only temperature is passive survivability and because of this limitation can not be considered as comprehensive enough for evaluating thermal resilience (Katal et al., 2019).

According to Homaei and Hamdy (2021a), these simplified metrics are neglecting the building thermal zoning and thus it is not possible to indicate rigorous evaluation and results. Besides those were used for quantifying the resilience during the disruptive event and neglected the post-event phase. Referring to heat-budget models, Predicted Mean Vote (PVM), Operative Temperature (OT) and Standard Effective Temperature (SET) are widely adopted for thermal comfort assessment. According to ASHRAE

(2010) are more suitable for evaluating the comfort level of the occupant rather than survivability under extreme conditions. Hamdy et al. (2017) quantify the thermal resilience in a case study of Dutch dwellings by using the Indoor Overheating Degree (IOD) as a metric indicator which considers different thermal comfort thresholds for different thermal zones over the frequency of overheating. The IOD (2.4) quantifies the overall risk by taking into account both the intensity and the frequency of indoor overheating. All the aforementioned metrics can help to benchmark different designs from the resilience perspective and give a more informative approach to the design process.

$$\mathrm{IOD} = \frac{\sum_{z=1}^{Z} \sum_{i=1}^{N_{occ}(z)} [(T_{fr,i,z} - TL_{comf,i,z}) t_{i,z}]}{\sum_{z=1}^{Z} \sum_{i=1}^{N_{occ}(z)} t_{i,z}} \tag{2.4}$$

Where:

T_{fr}: free-running operative temperature

TL_{comf}: thermal comfort temperature limit

N_{occ}: intensity of overheating during the occupied period

z: building zones

Hamdy et al. (2017) states that the IOD increases as far as the Ambient Warmness Degree (AWD) increases. Subsequently, the dwellings can perform differently under the stresses of global warming. Hence with stricter overheating stress cause higher values than the overheating. Dwelling with higher solar heat gains and low heat transmission is at high risk than ground floors, especially in dwellings with low insulation and low solar protection. In case of no mechanical ventilation, the risk is significantly higher. Ventilative cooling and solar protection are the most effective adaptation measures to mitigate the consequences of global warming. However, the potential of ventilative cooling decreases as global warming increases and hence this type of cooling would not be sufficient for keeping the indoor temperature stabilized under 24°C. Subsequently, active cooling should be established in buildings.

Homaei and Hamdy (2021a) proposes a methodology, as presented in 2.11 to measure and classify the thermal resilience of buildings, which can help protect building performance against uncertainties and disturbances. The proposed methodology uses the weighted net thermal performance (WUMTP) to quantify the deviation from thermal targets and penalize them based on the phase, hazard level, and exposure time of the disruptive event. This metric is a multi-zone measure that considers not only the performance during the disruptive event (phase I) but also the recovery phase (phase II). Apart from the resilience quantification, this research attempts to classify the buildings according to thermal resilience by forming a benchmark labelling. There are two main considerations for this metric. In comparison with the previous metrics, the WUMTP metric can be used with respect to the building characteristics such as building envelope, ventilation systems and occupancy hours and hence it can be used for a multi-zoning case with different thermal conditions. By changing one of these factors can affect the thermal resilience of a building. Therefore, it could be used as a metric system for evaluating the thermal resilience of the whole building. Moreover, the metric is quantified with respect to the disruptive event, the phase of the event, the hazard of the event and the time of exposure to the hazard.

The metric uses the indoor operative temperature as a performance indicator. By conducting dynamic building simulations, where parameters which affect the operative temperature can be set as

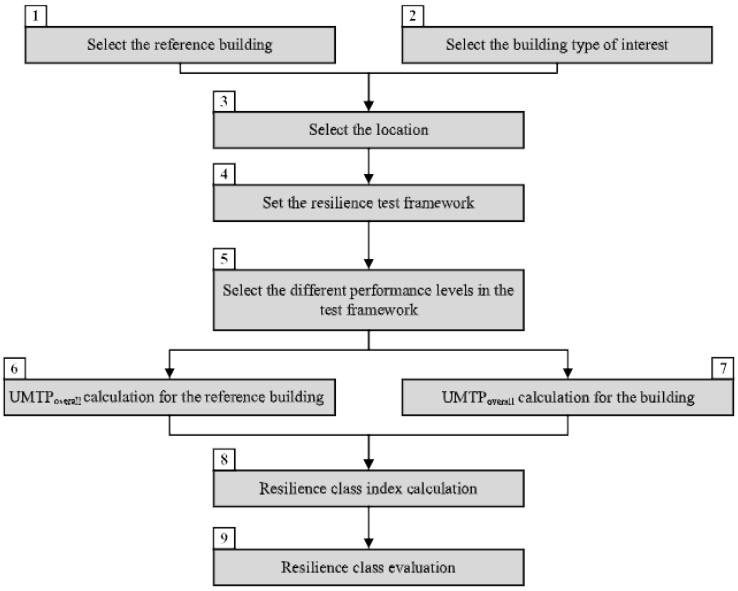

Figure 2.11: Resilience calls index quantitative framework as stated by Homaei and Hamdy (2021a).

variables, performance curves are generated depicting the operative temperature fluctuation over time Homaei and Hamdy (2021a). The simulation-based approach is preferred because it allows for easy control of building boundary conditions and the evaluation of building performance under disruptive events. The suggested resilience test framework involves a fixed-duration disruptive event and simulates the performance of the building during and after the disruptive event. The WUMTP calculation is divided into the following stages (2.12). At the initial stage ($0 \leq t < t_0$), the building operates before the disruptive event based on a temperature set point. The second stage, which represents phase I ($t_0 \leq t < t_1$), is placed between the start and the end of the disruptive event. Here, the indoor temperature deviates significantly from the initial slight fluctuation (around the temperature set point target). Based on the definition of resilience, at this phase, the building absorbs the impact and then adapts to the disruptive event. In phase II ($t_1 \leq t < t_2$), the curve indicates the building's performance after the disruptive event and lasts until the building reaches the performance level of the initial state. In the final stage ($t > t_2$), the building continues to operate based on the initial set point temperature. In addition to these stages, four different performance thresholds are forming a multi-phase resilience calculation and they are presented in the diagram 2.12. Those are the set-point temperature threshold (T_{sp}), which presents the temperature at the set-point target. According to Homaei and Hamdy (2021b) this set-point for office buildings is set to 21°C. The robustness threshold (T_{rt}) of 23°C includes any point of the performance curve that exceeds the (T_{sp}) and defines the acceptance level of performance. The performance threshold of habitability (T_{ht}) defines any performance that is at the uninhabitable condition for the occupants. Last, the (T_{min}) is the minimum performance of operative temperature. This proposed methodology and the metric system Although, the proposed method (Homaei & Hamdy, 2021a) calculates the thermal resilience for building simulations during winter, the metric was adopted for the thermal resilience quantification in case of summer heat waves. For this reason, the threshold figures were adapted to the case of indoor overheating, hence the T=23°C, T=26°C and T=29°C for the case study which is presented in Chapter 3.

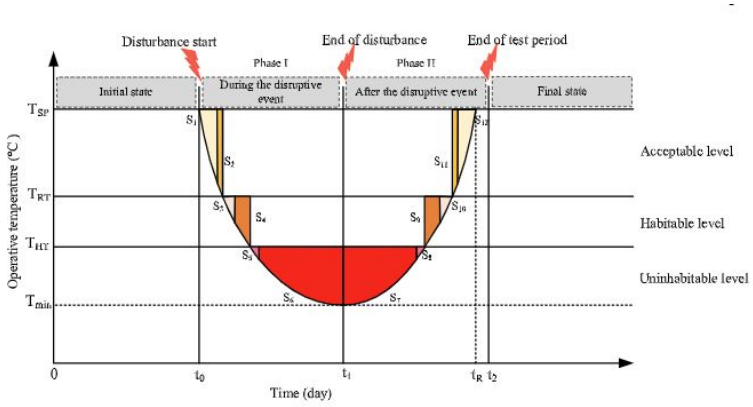

Fig. 3. Differentiation of 12 various segments in resilience test framework.

Figure 2.12: WUMTP metric calculation by Homaei and Hamdy (2021a).

$$\text{WUMTP} = \sum S_i W_p W_h W_e \tag{2.5}$$

For the calculation of WUMTP, the temperature values are multiplied by a penalty-weighted factor 2.13) in order to consider the increase in stress over time of disruption.

As mentioned above, the WUMTP metric can be translated into a benchmark label 4.4 system similar to energy labelling systems and can be incorporated in the design, planning, and operation of buildings, as well as in energy performance certificates. Therefore, valuable information can be provided to designers and engineers enhancing the decision-making process at the early stage of the design. Subsequently, building design can be ready to prepare for and adapt to disruptive events. Through this calculation, the resilience class index (RCI) is defined 2.6. However, The methodology is limited to residential buildings but can be extended to other types of buildings by setting new assumptions regarding thermal comfort conditions for each building type. It only quantifies thermal resilience for residential buildings during heating seasons and needs adjustments for cooling seasons in regions with hot and humid weather. It also only considers temperature and not other factors that can impact thermal resilience such as humidity, which requires further research. Moreover, Homaei and Hamdy (2021b) suggests the implementation of PV panels and/or battery storage for restoring the thermal performance and hence minimizing the duration of Phase II.

$$\text{RCI} = \frac{\sum(S_i W_p W_h W_{e_{ref}})}{\sum(S_i W_p W_h W_e)} \tag{2.6}$$

The method for rating a building's resilience is similar to energy labelling (Homaei & Hamdy, 2021b), which rates a building's energy consumption and potential for energy-saving measures. Buildings are assigned an energy performance label based on a scale from A to G, with A-rated buildings being the most energy-efficient. The energy performance of a reference building is evaluated, and the actual building's performance is compared to it to determine its label. This same strategy is used for resilience labelling, where an ideal reference building is chosen based on standards, and the building to be rated for resilience is compared to it in a test framework subjected to a disruptive event.

Sun et al. (2020) stated that energy efficiency is not uniformly beneficial for thermal resilience. For instance, the factor of air infiltration through the facade, which is state-of-art for energy efficiency

Table 1
Associated penalties for different segments inside the resilience test framework.

Segment	Penalties		
	Phase penalty (W_P)	Hazard penalty (W_H)	Exposure time penalty (W_E)
S1	0.6	0.1	2
S2	0.6	0.1	8
S3	0.6	0.2	10
S4	0.6	0.2	20
S5	0.6	0.7	20
S6	0.6	0.7	40
S7	0.4	0.7	40
S8	0.4	0.7	20
S9	0.4	0.2	20
S10	0.4	0.2	10
S11	0.4	0.1	8
S12	0.4	0.1	2

Figure 2.13: WUMTP metric calculation by Homaei and Hamdy (2021a).

Table 2
Resilience classes for buildings labelling.

<3.6	RCI		Class A+
<2.4	RCI	≤ 3.6	Class A
<1.5	RCI	≤ 2.4	Class B
<0.9	RCI	≤ 1.5	Class C
<0.6	RCI	≤ 0.9	Class E
	RCI	≤ 0.6	Class F

Figure 2.14: WUMTP metric calculation by Homaei and Hamdy (2021a).

practices, made it more difficult to expel the high indoor temperature. Moreover, the measures of his research varied by changing multiple parameters such as the air-conditioning and the outdoor temperature. Resilience standards and metrics are needed to follow the building energy codes in order to achieve adequate levels of thermal resilience from the early design stage.

2.2. Weather Data

2.2.1. Heat waves in Europe

Analysing and generating weather data was a part of this research. In this chapter, sources for obtaining weather files and methods for generating weather files are discussed. The thermal resilience of a building is quantified under overheating stresses, for this reason, historical weather data are examined. As mentioned in the introduction, the frequency and duration of heat waves have increased during the last decade. Specifically, the heatwave which occurred in 2003 in Europe lasted from the 20th of July until the 20th of August and the highest temperature of 37.8°C was recorded on the 7th of August. During the summer of 2019 2.15, two heatwaves occurred in Europe during June and July and the temperature rose up to 39.3°C. Three years after, multiple heatwaves occurred in short period of time each one but the high temperatures occurred from June until August. The highest temperature in the Netherlands was 39.5 °C ("2022 European heat waves", 2023). According to the Intergovernmental Panel on Climate Change (IPCC) (Pörtner et al., 2019), the frequency of extreme case scenarios is expected to increase in the near future because of climate change. Extreme heatwave events are occurring more frequently

and last longer, in comparison with the pre-industrial era (Homaei & Hamdy, 2021a). The Copernicus Climate Change Service stated that 2019 was the warmest year on record for Europe with June being the hottest month ("C3s releases European State of the climate to reveal how 2019 compares to previous years", n.d.). Such events affect the cooling and ventilation system and as a result, require high demand energy to mitigate the significant rise of the indoor temperature. Therefore, can lead to thermal discomfort in buildings.

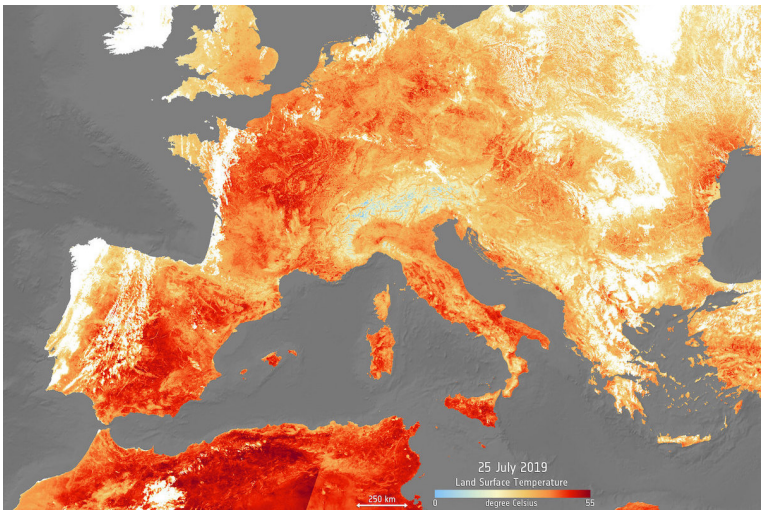

Figure 2.15: A heat map shows Europe on July 26, 2019, in the midst of an extreme heat wave that saw temperatures reach as high as 41°C in Paris, France. Copernicus Sentinel data (2019), processed by ESA(CC BY-SA 3.0)

Historical weather data can be retrieved by the official website of Climate Explorer by Royal Netherlands Meteorological Institute (KNMI, 2023). Libraries for variant climate models of CMIPs and Cordex scenarios with monthly, daily and hourly data of extreme temperature values can be found.

2.2.2. Climate uncertainties

The modelling uncertainties when assessing the impact of weather on the resilience of buildings, can decrease the accuracy of the modelling output. This is mainly because of the lack of data and of the unpredicted behaviour of the weather(Panteli, Trakas, et al., 2017). For this reason, sensitivity studies are required to evaluate the impact of the assumptions made in weather modelling. The sensitivity studies would help understand the importance and effect of each modelling aspect and parameter on the modelling output. This will guide the more effective and systematic collection of data that would increase the accuracy of the simulation output.

The Intergovernmental Panel on Climate Change (IPCC) synthesis report offers quantifiable climate data that can be re-used to estimate the likelihood of punctual and global climate events depending on the project location (Favoino et al., 2022). Representative concentration pathways (PCP), presented in the picture 2.16, represent different scenarios for addressing the uncertainties in future concentrations of greenhouse gas (GHG) Moazami et al. (2019). Those scenarios are called Global Climate Models GCMs and their outputs represent averages over a region with a spatial resolution of 100-300km2 am monthly temporal resolution. These data resolutions are not suitable for direct use in BPS tools that require local weather data with hourly or sub-hourly resolution. Therefore, GCM data need to be downscaled to the appropriate spatial and temporal resolution. There are two main approaches to downscale GCM

outputs and generating data with a finer temporal and spatial resolution. These are dynamical and statistical downscaling (Nik et al., 2017). The RCP 4.5 is described as a moderate scenario and the RCP 8.5 as a scenario with a high concentration of CO^2 emissions, while the RCP 2.6 is considered as the one with the lowest concentration. According to Nik (2016), the RCP 4.5 and/or RCP 8.5 scenarios must be included in the process of downscaling weather data from the Global Climate Model (GCM) to the Regional Climate Model (RCM) for generating future weather data.

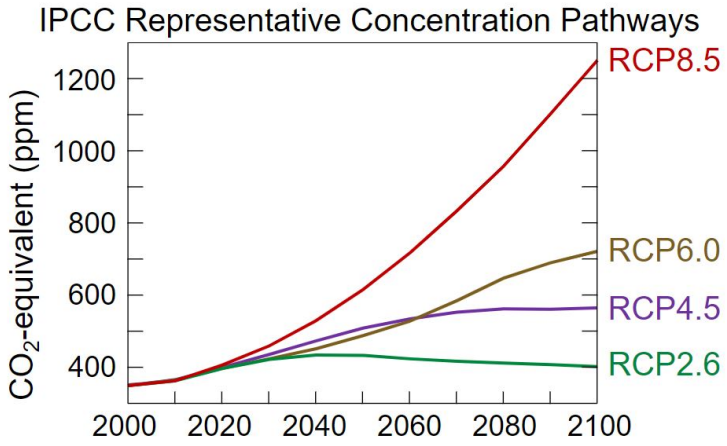

Figure 2.16: Representative concentration pathways (PCP) as defined by the IPCC.

Climate uncertainties can affect considerably estimations of the energy demand, as shown by (Vahid, 2012) through the implementation of several future climate scenarios, based on the 4th Assessment Report (AR4) of IPCC and with different spatial resolutions. The adopted temporal resolution can also affect the assessment results considerably. This illustrates the critical situation for energy systems to cover peak demands in future (Nik, 2016). The key to the climate resilience assessment is the proper linkage between climate and energy models. Besides considering climate uncertainties, it is important to adopt a suitable temporal resolution for the analyses to reveal the risk of extreme events. This allows counting for 'unprecedented' extreme events which are physically 'plausible' and reflected by future climate models (Nik, Perera, et al., 2021).

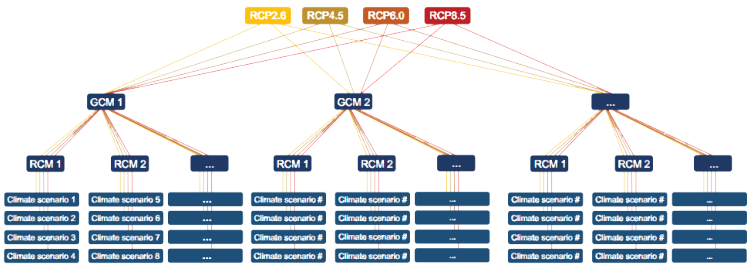

Figure 2.17: Future climate projections can be generated by using the RCPs of IPCC in GCMs. RCMs are used to downscale GCMs dynamically with fine spatial and temporal resolution, enabling a physically consistent representation of climate variations and extremes. (Nik, Perera, et al., 2021).

2.2.3. Climate models & weather datasets

Climate is a very dynamic system and studying its behaviour depends highly on the selected temporal and spatial resolutions. By realizing the importance of climate change adaptation in the built environment and following the advances in computing future climatic conditions, which has resulted in higher availability of future climate data sets, assessing the probable impacts of climate change has turned out to be an interesting research topic for the field of energy consumption and buildings (Nik, Perera, et al., 2021). There has been significant progress in developing climate models and projecting future climate conditions over the last two decades. Moreover, in the recent past, energy models have been developed to consider uncertainties at the design and operation phases including many complex interactions among different actors within the energy domain(Nik, Perera, et al., 2021). Linking these models to properly understand and quantify the impacts of climate change on the energy system brings unprecedented opportunities to assess and improve the design and performance of energy systems (Nik, Perera, et al., 2021).

Global climate models (GCMs) are numerical models of the physical processes that characterize the global climate system, including the atmosphere, oceans, cryosphere and land surface. Buildings are affected by the local climate, and some assessment methods may require environmental data even at the sub-hourly resolution. Probabilistic approaches are usually taken into account for the impact assessment of climate change, considering several climate scenarios and uncertainties. The climate research community are focused on GCMs and RCMs. An RCM (with a spatial resolution of 20–50km) is usually nested in a GCM (with a spatial resolution of 100–300 km) and driven by the conditions of the global climate at the boundaries of the RCM domain. RCMs can reproduce realistic regional climate, especially with regard to extremes (Nik, Perera, et al., 2021). Impact assessment of climate change is usually performed by means of the climate data generated by Global Climate Models (GCMs) (Nik, 2016). The GCMs cannot be considered as adequate for building simulations because of the coarse spatial and temporal resolution. For this reason, regional and national scales, where Regional Climate Downscaling (RCD) provides projections with much greater detail and more accurate representation of localized extreme events (Gregory et al., 2007). While future climate information can only be

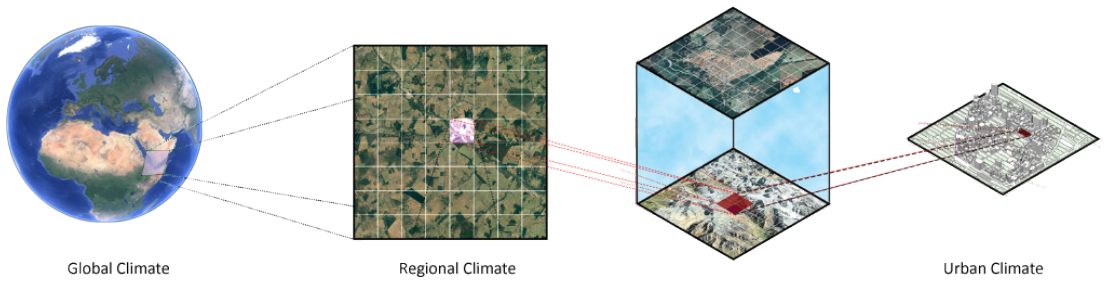

Figure 2.18: Global to regional climate(Nik, Perera, et al., 2021).

provided by GCM and/or RCM, the past/present data climate can be represented by historical observations or GCM/RCM simulation for the historical climate. A common approach in energy studies is to use a one-year typical weather data set to represent climate over a 30-year period, known to be a Typical Meteorological Year (TMY) (Nik, Perera, et al., 2021). TMY helps to represent typical conditions for the past/current climate and limits the calculation load; however, it is unable to fully represent

extreme conditions. Typical Meteorological Year (TMY) data sets rely on statistical measures mean and a maximum of dry-bulb temperature, dew-point temperature, wind speed and solar radiation over a span of 30 years. However, those neglecting weather extremes conditions because they include only average outputs.

The morphing technique however reflects only changes in the average weather conditions and neglects changes in future weather sequences. For example, it is not possible to see changes in extreme climatic conditions for the morphed data, though extremes will be more often and stronger in the future (Nik, 2016). Dynamic downscaling of GCMs by means of regional climate models (RCMs) has the advantage of generating physically consistent data sets across different variables (Giorgi, 2006). RCMs provide weather data with suitable temporal (down to 15 min) and spatial resolutions (down to 2.5 km2) for direct use in building and energy simulations (Rummukainen, 2010). Most of the Synthesizing weather data sets techniques for energy simulations are based on the statistically downscaled GCM data. One approach for creating weather files is integrating the monthly mean changes from GCMs into the existing TMY by means of the morphing technique (Chan, 2011). Downscaling can be done dynamically using RCMs or statistically (stochastic methods or morphing) (Yassaghi & Hoque, 2019). In this process EPW files can be created suitable for building simulations.

To evaluate and quantify the thermal resilience in buildings against extreme heatwaves by developing dynamic energy building simulations, the following weather data sets are typically needed to be embedded to EPW files ("U.S. DoE", 2022):

Dry-bulb temperature : The temperature of the air as measured by a thermometer with a dry sensing element.

Wet-bulb temperature: The temperature of the air as measured by a thermometer with a wet sensing element. This is a measure of the humidity of the air.

Relative humidity: The ratio of the partial pressure of water vapor in the air to the saturation pressure at the same temperature.

Solar radiation: The amount of solar energy that reaches the Earth's surface, typically measured in watts per square meter.

Wind speed and direction: The speed and direction of the wind at a given location.

Atmospheric pressure: The pressure exerted by the atmosphere at a given location.

Precipitation: The amount of rain or snow that falls at a given location.

Cloud cover: The fraction of the sky that is covered by clouds at a given location.

2.2.4. Synthesizing weather data

The averaging process of creating TMY files based on 20-30 years of historical data or future-generated weather data, which usually excludes extreme values. These methods are based on synthesizing typical weather files with extreme cold and extreme hot years. Nik (2016) used a similar process for creating future weather files by synthesizing data sets of typical weather files with extreme cold and hot with a temporal resolution of a month. With this process, it is possible to achieve accuracy similar to Regional Climate Data. Climate uncertainties are included by taking into consideration of different climate RCPs. To obtain a fine spatial and temporal resolution the use of downscaling techniques is required.

The results (Moazami et al., 2019) proved that building robustness cannot be assessed only under typical weather files. The relative change of peak load for cooling demand under near future extreme conditions can still be up to 28.5% higher compared to typical conditions. Only the generated weather files generated that are based on dynamical downscaling and that take into consideration both typical and extreme conditions are the most reliable for providing representative boundary conditions to test the energy robustness of buildings under future climate uncertainties.

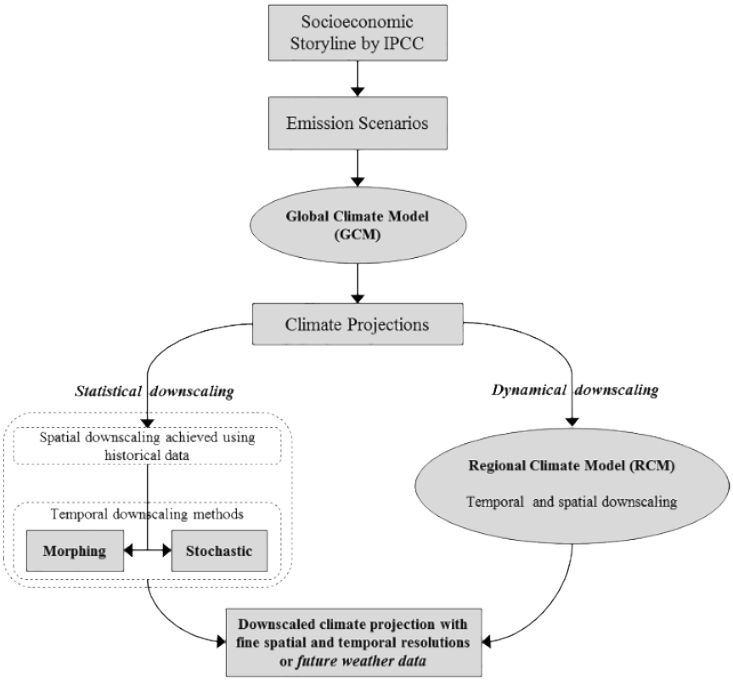

Figure 2.19: Global Climate Model downscaling for future climate projections(Moazami et al., 2019).

Dynamical downscaling

Dynamical downscaling produces local or regional information using Regional Climate Model RCM. RCMs are numerical models that require explicitly specified boundary conditions from GCM, hence they provide a finer resolution of 2.5 klm2. Many advantages but needed many resources (computational power, large storage) for the creation of data sets. This type is nested into a GCM and hence its quality lies on the accuracy of the GCM. Ensembles and Euro-cortex are projects that produce probabilistic projections of climate for Europe to inform researchers and decision-makers in order to quantify climate uncertainties by combining different GCM and RCM pairings.

Statistical downscaling

Statistic down scaling derives regional or local climate variables form larger-scale climate data using stochastic approaches. The complexity of dynamic downscaling make the BPS users to favor statistical downscaling, This approach is much simpler than dynamical downscaling however it does not provide high availability of hourly data. The statistical downscaling can be done with morphing and stochastic generation of data sets. The former uses algorithms for applying changes on monthly variations of GCM or RCM output from a location. CCWorldWeather Generator tool uses the morphing method to generate EPWs. It allows the user to generate future weather files for worldwide locations within

three-time slices: 2011-2040 (20s), 2041-2070 (50s), 2071-2100 (80s) and EPW files are freely available. It transforms an original EPW typical weather file into future weather data, formatted in the EPW format and so ready for use in BPS tools. Jentsch et al. (2008) describes in detail the potential source of inaccuracy in the outputs of the tool due to the possible time-frame difference in the morphing process. Arup and Argos analytics developed the Weathershift tool (Dickinson & Brannon, 2016). This applies the morphing method to the outcomes to create climate change weather EPW files for EnergyPlus simulations. The tool provides future projection weather data for three time periods: 2026–2045(referred as'2035s'), 2056–2075 (referred as '2065s'), 2081–2100 (referred as'2090s'). The latter, based on statistical analyses of recorded climate data and they can provide weather variables using just a few independent variables such as solar radiation or solar radiance. Meteonorm is a combination of a climate database spatial interpolation tool and a stochastic weather generator. Meteonorm can calculate typical year switch hourly resolution for any site and canal so be used for climate change studies. Instead of using weather data from typical weather files, it generates weather data by using GCMs for every decade from 2010-2100 Nik (2016). Those models produce hourly data that can be used as input for building performance simulations.

Hybrid downscaling

Is an approach for reducing the computational resources and storage space required in dynamic downscaling. The outputs of an RCM are stored at coarse spatial and temporal resolution for further downscaling with statistical process. UKCP09 provide future weather data on a monthly basis with a spatial resolution of 255 km2. Those are statistically downscaled later on to hourly or daily temporal resolution at 5klm23 spatial resolution. This method is capable of providing high resolution weather data for several years into the future. For translating weather files into EPWs which are used for building simulations principles of the typical meteorological year is needed to be followed. (12 months and a conventional period of 30 yr). In those approaches generation of extremes can be included.

Most of the above-mentioned approaches are based on the statistical downscaling of GCMs and in the case of dynamic downscaling, based on the daily or monthly temporal resolution of RCMs. Many of these methods neglect the probable climatic variations in different time scales, e.g. from seasonal to hourly, and hence it is not possible to estimate the probable extreme conditions (Nik, 2016). However, Nik (2016) suggests an approach for the impact assessment of climate change on buildings and their energy performance, based on creating three sets of weather data out of RCMs: (1) typical downscaled year (TDY), (2) extreme cold year (ECY) and (3) extreme warm year (EWY). The weather data sets are created using one or several RCMs.

2.3. Uncertainty quantification

Uncertainty quantification (UQ) is the field of studying and analyzing the sources of uncertainty and variability in mathematical models and simulations. In building energy simulations, UQ involves quantifying the uncertainties in the inputs, parameters, and models that can affect the energy performance predictions of a building. UQ is becoming increasingly important in building design and energy retrofit projects as it helps to identify and reduce the risks of performance gaps between the predicted and actual energy performance of buildings. By reducing these uncertainties, UQ can improve the accuracy and reliability of energy performance predictions, reduce the risk of performance gaps, support

decision-making, and optimize building performance. Uncertainties are connected with the concepts of reliability and robustness (Janssen, 2013). Reliability focuses on the probability of failure during a given time period, while robustness delineates the probability of the performance of a system in time. This research explores the field of thermal resilience by the aspect of robustness in the building performance rather than reliability and hence on the general uncertainty analysis outcomes rather than the low probability of failure events. In probabilistic building simulations, Monte Carlo appears to be universal and progressively since can be a reliable assessment of heat transport through the building materials and building components and the whole building performance can lead to sustainable and durable performance. Most of the related parameters for building simulations such as material properties, boundary conditions and human activity can be characterised as stochastic variables. Multi-performance processes that are based on uncertainty scenarios and optimizations should be integrated as part of the design process of new buildings Bianchi et al. (2022). In order to support the decision-making process comprehensive and robust procedures should be implemented in order to compare the performance of possible design solutions. For this reason, the involvement of probabilistic analyses in the process of building energy simulations for the calculation of the energy performance is rising in the last years (Sun et al., 2020).

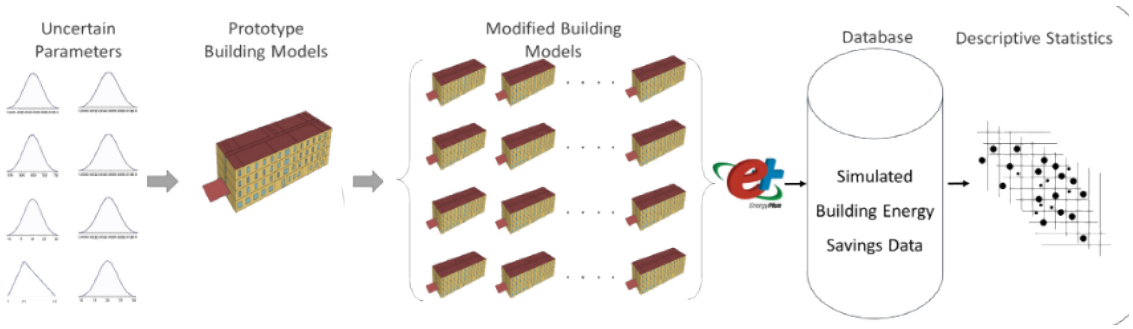

Figure 2.20: Evaluation of Uncertain parameters (Abediniangerabi et al., 2021).

To assess and manage uncertainties in a conceptual framework, three major steps need to be taken (2.21). The first step (A) involves defining the problem, including the input and output variables, model specification, and interest in measuring output uncertainties. The analyst can choose which variables are uncertain or fixed, and all uncertain inputs include parametric and model uncertainties. In this step, fixed variables are considered negligible with respect to the output variables of interest. The second step (B) requires the quantification of uncertainty sources, which involves defining probability density functions of uncertain inputs with simplified correlation structures. This step involves gathering information through direct observations, physical arguments, or direct estimations, and may require multiple computation sources. The third step involves the propagation of uncertainty (C) which is necessary to map the uncertainty of the outputs into the uncertainty measures in the outputs. At this point, data sampling techniques are required. Finally, sensitivity analysis (SA) is implemented in order to understand how uncertainties in the model outputs can be apportioned to the different sources of uncertainties in the model inputs (Saltelli et al., 2008). Finally, sensitivity analysis (D) is implemented to understand how model output uncertainties can be apportioned to different sources of uncertainties in the model inputs. This analysis is crucial for determining the most influential variable inputs, and involves statistical treatment of the input and output relations.

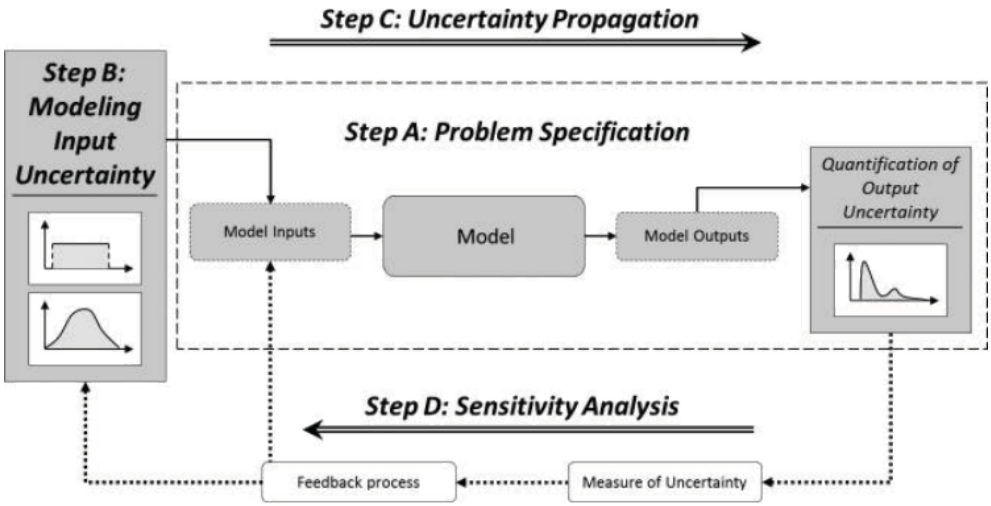

Figure 2.21: Generic conceptual framework for uncertainty (Punzo et al., 2014).

The uncertainty quantification process has been used in several building simulation studies. Ekström et al. (2021) used the Monte Carlo method for 1000 simulations using the probability distributions that were quantified at the energy simulation process. The number of simulations were depended on the balance between producing enough output data and in order to achieve an adequate spread of the results and the computational time. The results from the BPS were used to quantify the probability of failure. The simulation results were presented as probability density functions to depict the difference between the design options (Ekström, 2021). The selection of input data for building a predictive model is contingent on the purpose of the study, which can either be benchmarking or evaluating actual performance. Stakeholders determine the study's scope, depending on their values, which establishes the project's design criteria and limitations, as well as the techniques employed to anticipate the performance criteria.

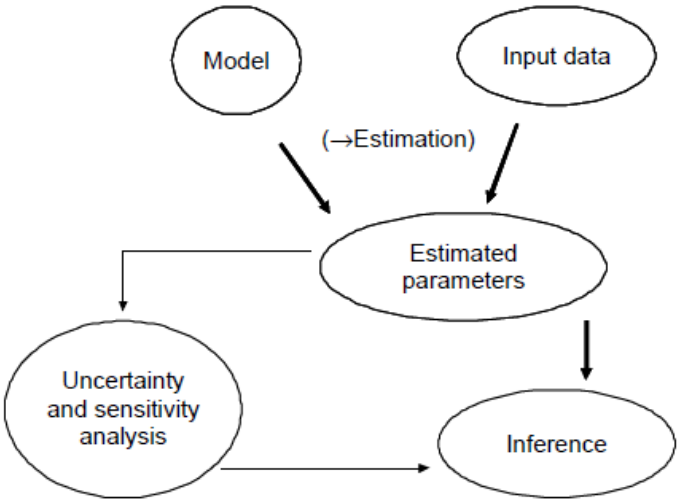

Figure 2.22: Uncertainty and sensitivity analysis diagram ("Introduction to Sensitivity Analysis", 2007).

2.3.1. Sensitivity Analysis

One-at-time (OAT) sensitivity analysis

In the OAT sensitivity analysis, the study analyzes the variance in the model outputs due to the variation of one input parameter at a time, while the remaining parameters are fixed in certain values(Punzo et al., 2014). This process can be presented in the matrix 2.7 for a case of SA of multiple parameters. For instance, every variable may take only two values, 0 and 1, and only one variable changes its value among consecutive simulations. While OAT analysis has limitations, variance-based analyses can address these limitations and are simple to conduct. Additionally, these methods enable the identification of important factors in a rigorous manner, thereby making the ranking process unambiguous.

$$\begin{bmatrix} 1 & 0 & 0 & 0 & 0 & ... & 0 \\ 1 & 1 & 0 & 0 & 0 & ... & 0 \\ 1 & 1 & 1 & 0 & 0 & ... & 0 \\ 1 & 1 & 1 & 1 & 0 & ... & 0 \\ ... & ... & ... & ... & ... & ... & ... \\ 1 & 1 & 1 & 1 & 1 & ... & 1 \end{bmatrix} \begin{pmatrix} b_0 \\ b_1 \\ ... \\ b_k \end{pmatrix} = \begin{pmatrix} y_1 \\ y_2 \\ ... \\ y_{k+1} \end{pmatrix} \tag{2.7}$$

Variance-based sensitivity analysis

A variance-based method is a probabilistic approach which quantifies the input and the output uncertainties as probabilistic distributions and it decomposes the output variance into parts which are dependent on input variables and combinations of variables ("Sensitivity analysis", 2023). The major advantages of using variance-based SA are the model independence, the capacity to capture the influence of the full range of variation of each input factor, the appreciation of interaction effects among input factors and the capacity to tackle groups of input factors (uncertain factors) ("Variance-Based Methods", 2007). On the other hand, variance-based methods require high computational costs because they require efficient algorithms for their computation. This analysis is based on first-order and higher-order effects of the variables on the outputs. Moreover, the concept of uncertainty importance is embedded into the initial variance-based mathematical model. By the implementation of the Sobol method, the study is enhanced with Monte-Carlo and hence the computing of sensitivity measures for a group of factors is possible.

Sobol' indices (Marelli, Lamas, et al., 2022) are based on the idea of defining the expansion of the computational model into numeric samples of increasing dimension. The total variance of the model is described in terms of the sum of the variances of the samples. Through the Sobol' indices method, the variance decomposition leads to sensitivity measures that represent the relative contribution to each group of variables $\{X_{i1}, \ldots, X_{ix}\}$. The index with respect to one variable $\{X_i$, is called the first-order Sobol' index and represents the effect of $\{X_i$. The total Sobol' (2.8) index of input variable $\{X_i$ is the sum of all the Sobol' indices involving this variable:

$$S_i^T = \sum_{\{i_1,\ldots,i_s\} \supset i} S_{i_1,\ldots,i_s} \tag{2.8}$$

Black-box models sensitivity analysis

All metamodeling techniques for computing sensitivity indices are based on fitting a model approximation based on Monte Carlo or quasi-Monte Carlo sample. In addition, metamodeling techniques compute more quickly than the conventional variance-based techniques ("Factor Mapping and Metamodelling", 2007). Metamodels are surrogate models which are built to substitute for computationally intensive simulation models. Metamodels can be built with a variety of strategies (e.g. simple linear regression) and purposes to perform a sensitivity analysis. One approach to conducting sensitivity analysis on complex black-box models is to utilize a metamodel that can approximate the model's output. By doing so, the time needed to perform the analysis can be significantly reduced as the metamodel can be used in place of the original model(Punzo et al., 2014). This technique is gaining traction among researchers due to the appealing qualities of certain metamodels. According to (Marelli, Lamas, et al., 2022) surrogate models such as Polynomial Chaos Expansion (PCE) or Kriging can be used in order to compute the Sobol' indices with low computational cost to carry out SA.

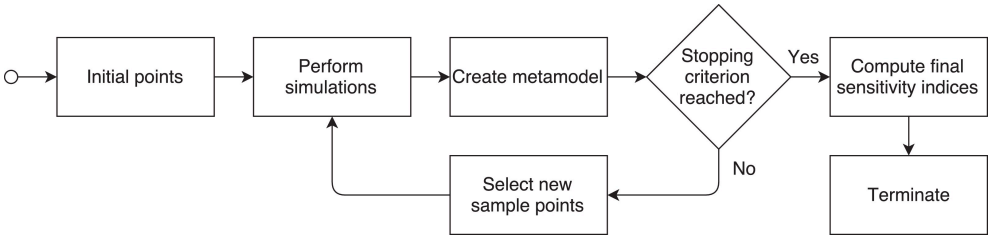

Figure 2.23: Sequential sensitivity analysis of expensive black-box simulators with metamodelling (Van Steenkiste et al., 2018).

Polynomial Chaos Expansion (PCE) metamodel is possible to calculate the Sobol' indices analytically from its coefficients. The metamodel should be created before defining the sensitivity analysis (Marelli, Lamas, et al., 2022). Monte Carlo simulation leads to computationally expensive models and a mathematical function is required to be used in order to obtain sensitivity analysis results. In this thesis the results were generated from the Grasshopper simulation model hence a mathematical function for calculating the indoor temperature was created but this is considered a simplification method for defining the Sobol' indices. In this case, the required mathematical function was replaced by the PCE metamodel. According to Marelli, Lamas, et al. (2022), the PCE metamodel should be created before defining the sensitivity indices. Metamodelling or surrogate modelling attempts to substitute the stochastic modelling to inexpensive-to-evaluate surrogate models (Marelli, Lüthen, et al., 2022). PCE model is a powerful technique that aims to provide a functional approximation of a computational model by using a series of input data. The Polynomial Chaos expansion Y=M(X) (2.9) is defined as (Marelli, Lüthen, et al., 2022):

$$Y = M(X) = \sum_{\alpha \in N^M} y_\alpha \Psi_\alpha(X) \tag{2.9}$$

Where:

$\Psi_\alpha(X)$: are the multivariate polynomials with respect to $\alpha \in N^M$

y_α: are the corresponding coefficients

Once the polynomial coefficients are known the metamodel can be evaluated with the respect to

X vector, while the samples are weighted by their coefficients. This process can be used effectively for calculating the PDF of the model accurately by using large Monte Carlo samples of the inputs. There are two principles for calculating the coefficients; *projection* and *regression*. Projection methods compute the coefficients by numerical integration, while the regression methods formulate a system of linear equations and solve the system with linear regressions (Marelli, Lüthen, et al., 2022).

2.3.2. Data sampling

Simulations with analytical techniques (2.20) are recommended for resilience studies as the climate and design uncertainties are complex systems with a variant and stochastic nature (Abediniangerabi et al., 2018). According to Ekström et al. (2021), one technique to overcome this unreliability of the BPS results is to perform uncertainty analysis, based on probabilistic methods to include uncertainties in the predictions. Tian et al. (2018) put on display the implementation of uncertainty analysis in data models and sampling methods.

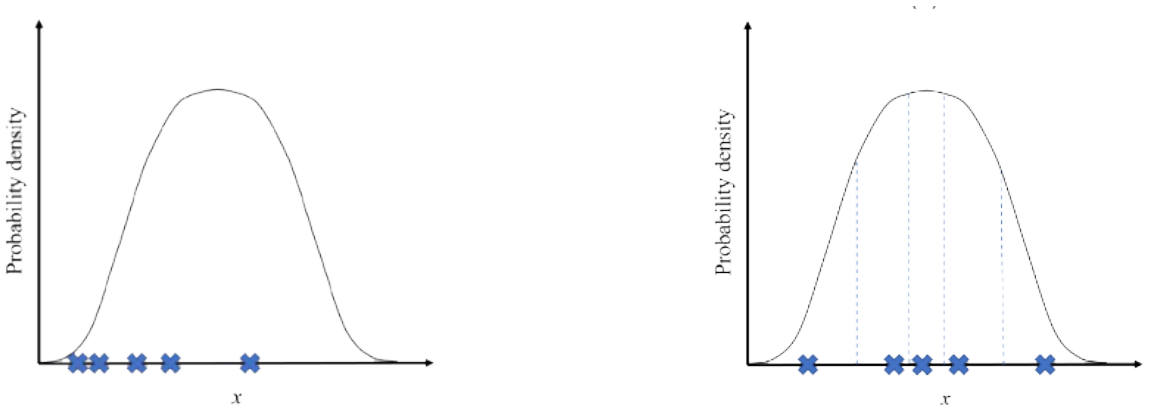

(a) Monte Carlo random sampling. **(b)** Latin Hypercube stratified sampling.

Figure 2.24: Monte Carlo and Latin Hypercube sampling from probability density curves (Lovreglio et al., 2019).

Monte Carlo (MC) simulation and Latin Hypercube sampling (LHS) are both widely used techniques for uncertainty quantification in thermal and energy dynamic building simulations (Sheikholeslami & Razavi, 2017). Both techniques are useful for generating input variables that can be used to simulate various scenarios and evaluate the sensitivity of the model output to changes in these variables. However, the MC method of random sampling often requires multiple repetitions, and may not cover the entirety of the sampling space. LHS addresses this issue and is more effective, uniform and orthogonal (2.24). This approach involves dividing the cumulative probability distribution range into probable subregions (2.25) of equal size and then performing stratified sampling within each interval (Lovreglio et al., 2019). LHS has been preferred by many researchers due to its ability to improve the sampling efficiency and reduce the number of simulations required to achieve a certain level of accuracy (Tian et al., 2018). Moreover, LHS provides more even sampling in high-dimensional spaces compared to other sampling methods. This means that LHS can capture more accurately the underlying distributions of the input variables and the correlations between them. Janssen (2013) states LHS needs on average 10 times less sampling points in comparison of MC random sampling.

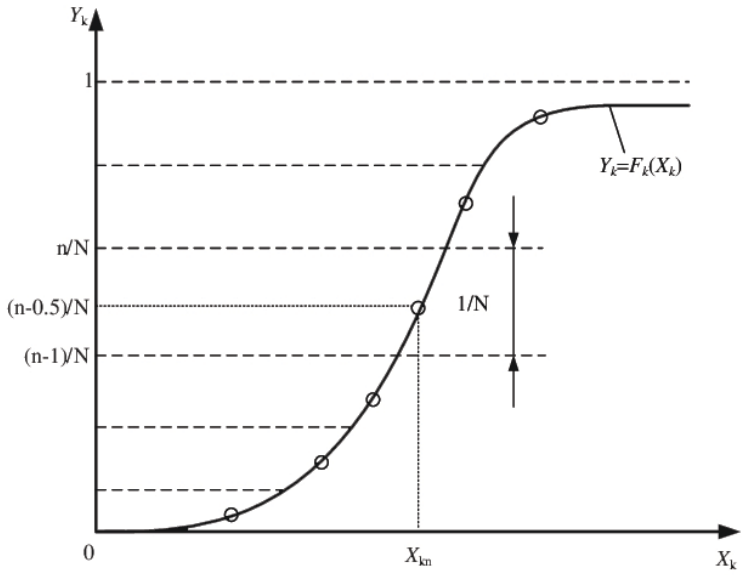

Figure 2.25: Latin hypercube sampling from a cumulative distribution function (Xiao et al., 2020).

Before implementing the MC or the LHS techniques, the *mean*, μ, and the *standard deviation* of the samples is need to be defined. Hence, the range and the distribution of the sample population are tuned accurately. The *standard deviation*, σ, can be calculated by the following formula ("Standard deviation", 2023):

$$\sigma = \sqrt{\sum_{i=1}^{N}(x_i - \mu)^2 \frac{1}{N}} \tag{2.10}$$

$$\mu = \frac{1}{N}\sum_{i=1}^{N} x_i \tag{2.11}$$

Where:

σ: is the standard deviation of the samples

x_i: a curtain value from the population of samples

N: is the size of the population sample

μ: is the the population mean

2.4. Concluding remarks

Concluding remarks from the literature research are discussed in this section. Findings literature help the research process in order to address the main research question and sub-questions. Besides, the findings feedback on the implementation of the theoretical framework to practice for evaluating the thermal resilience in buildings.

Resilience definition was first defined against seismic stresses and this main approach is adopted by other researchers and engineers for addressing resilience in other fields of the built environment. The definition of thermal resilience in buildings against overheating stress that is best aligned with this research is stated by Homaei and Hamdy. Thermal resilience is the property of whether the building's performance is adequate enough against climate hazards by giving an indication of the building's possible performance for mitigating the impact of extreme events. This property can be described by the main four dimensions (4Rs) of robustness, redundancy, resourcefulness and rapidity. Those are related to the strength of a system to withstand a hazard, which elements of the system can be substituted, the capacity and sources that are needed to overcome these stresses and the time of recovery. The evaluation of thermal resilience in buildings consists of phase I, before the disruption event (*resistance*), phase II, during the disruption event (*robustness*) and phase III which includes the post-event performance of the building (*recovery*).

For assessing thermal resilience in buildings Key Performance Indicators are defined in the previous sections. Indoor thermal comfort in relation to the building's energy consumption during the occurrence of the disruption event are the indicators that can be quantified and hence numeric results can be generated that can lead to valuable arguments at the end of this research. Moreover, the KPIs depend on the building system parameters (e.g. ventilation and cooling systems), material parameters of the building envelope (e.g. material properties and glazing) and the building schedule (e.g. occupancy levels, the activity of the occupants and operational time). These indicators are quantified by using metrics as mentioned in the previous chapters. The thermal resilience quantification method can be adopted by the initial Bruneau's quantification theorem since this approach can be adjusted for quantifying resilience in other fields of the built environment. The proposed metrics of thermal resilience are the Heat Index (HI), Humidex (H), Standard Effective Temperature (SET), Indoor Overheating Degree (IOD) and the weighted unmet thermal performance (WUMTP) for addressing a building's performance in terms of indoor thermal comfort. However, each metric has its own limitations. For instance, the HI is stated as simplified and as a metric that can not be applied in the case of extreme temperatures. In the calculation of H, although the effect of heat and humidity are considered, the performance of the building envelope and the building systems is neglected. The SET metric calculates the thermal comfort with respect to the human response to the thermal environment, but it neglects the thermal zoning in the case of whole building simulation. On the other hand, the IOD can be implemented in a multi-thermal zoning building and depends on the calculation of the operative temperature (T_{oper}) during the time. However,in extreme overheating stresses cause higher values than overheating. The metrics of passive survivability and thermal autonomy are stated to be simplified because they are only focused on thermal performance during the disruptive event. The WUMTP evaluates thermal multi-phase resilience by calculating the T_{oper} in the case of whole building multi-zone simulation. Moreover, this metric can be converted to benchmark labelling, called as Resilience Class Index (RCI).

Weather data can be generated for different climate future scenarios with respect to RCPs as stated by IPCC. In this process, GCMs need to be scaled down to RCMs and then RCPs scenarios are required in order to achieve coherent weather datasets for different weather scenarios. This process is essential in order to generate weather files of high spatial and temporal resolution. The scaling of the Climate Models can be achieved by downscaling the model either with dynamic or statistical methods. The former requires the handling of large datasets and hence needs many computational resources, while the latter is used by variant weather generators that can produce EPW files which are necessary for building performance simulations (BPS). Moreover, a hybrid method is used. Most of the weather generators use the statistical downscaling method by using the morphing technique. In this process, a typical meteorological year (TMY) weather file is used as a base and the morphing technique is implemented by considering different climate scenarios with respect to GHG emissions and location of interest. There are plenty of sources where TMYs can be found on the web for instance, EnergyPLus and OneBuilding libraries contain world-wide TMY files. Apart from scenarios of climate change, historical weather data for every year can be found on the KNMI official website. Large libraries are compiled with the contribution of climate institutions, climate studies and observatories. More specifically, historical weather files of the years 2003, 2019 and 2022 that contain extreme weather values can be found for the location of Amsterdam. These contain information about the dry-bulb temperature, wet-bulb temperature, relative humidity, precipitation, cloud cover and solar radiation, properties that are essential for creating EPW files.

Uncertainty quantification (UQ), is important in building design and energy projects as it helps to identify and reduce the risks of performance gaps between the predicted and actual energy performance of buildings. By reducing these uncertainties, UQ can improve the accuracy and reliability of energy performance predictions, reduce the risk of performance gaps, support decision-making, and optimize building performance. The conceptual framework of uncertainty consists of the problem formulation step, where the model calculates the output with respect to input variables and hereupon probabilistic density functions define the uncertain inputs. The propagation of uncertainty step is necessary to map the uncertainty of the outputs. Then, the sensitivity analysis (SA) step indicates the apportion of uncertainties in the model outputs and determines the most influential input variables. There are two main types of SA, the one-at-time and the variance-based. The first method analyzes the variance in the model outputs due to the variation of one input parameter at a time, while the remaining parameters are fixed in certain values. The main limitation of this approach is that the inputs are correlated with the outputs in a univocal manner. The variance-based SA can overcome this limitation because first and higher-order indices are computed. Hence the study can generate multi-correlation results a. between inputs and outputs and b.among each variable with other variables. There are also other methods of SA that can be used in the case of black-box models. Here, the Sobol' indices are computed by the assistance of a surrogate or metamodel that can be trained and tuned in order to estimate the model's outputs based on the variables. In this method, Linear, Gaussian regression and Polynomial Chaos Expansion (PCE) models can be used. During the aforementioned UQ processes data sampling is essential. The most common sampling methods are the Monte-Carlo (MC) and the Latin Hypercube (LHS). With MC random samples can be selected from density distribution curves of input variables, while the LHS is based on stratified selection of values. Most of the researchers use the LHS because of its high efficiency and accuracy compared with the MC.

3

Case study

This thesis addresses the thermal resilience in buildings and implements the theoretical framework into practice by exploring the performance against extreme overheating events of a mid-rise office building, that is located in Amsterdam. For this practice, weather data are generated in order to compute EPW files that include extreme climate scenarios. In the beginning, the CCWorldWeatherGen tool is used for generating weather files of extreme future climate scenarios under the impact of RCP8.5. However, as presented in the flowing chapters, this method was discarded because of the invalidity of the computed results. For this reason, the research focused on historical weather in the Netherlands which is obtained by the KNMI. Hereupon, the higher values of these data sets are compared and converted to an EPW format. In the next part, the simulation model is created and adjusted with the desired design, material and building properties. All these, are distinguished into design options standard parameters and variables which are tuned in order to meet values that exist in building norms like ASHRAE 2017. Once the simulation model is created, the script for evaluating the thermal resilience indicators of thermal comfort and energy consumption is prepared. Hence, thermal resilience metrics, in this case, the indoor operative temperature comfort and energy use intensity, can be computed for the whole building. In the next step of the workflow, one-at-time and variance-based sensitivity analysis (SA) methods are implemented in order to indicate the variables that have a significant impact on the metrics. For this process, multiple simulations are computed in order to generate an adequate number of samples. The simulation outputs are used for the probabilistic assessment and uncertainty quantification (UQ). The SA and UQ outcomes are used to assign specific values to variables to run the final simulations and compare the newly computed results with an ideal optimised performance of this particular building.

3.1. Methodology and workflow

The main methodology for quantifying thermal resilience is described in this chapter and consists of four major parts that are related to weather data collection and modification, 3d digital model of the office building, a simulation model via visual scripting and post-processing of the simulation outcomes with Python in order to compare the resilience loss of different cases. In short, the first part of the research explores the field of climate sources in order to get valuable information about the weather data that can be used for assessing thermal resilience. In the next step, the building geometry, general dimensions and the number of floors are defined. Moreover, the main building and material properties of the facade are presented in order to point out the challenges, the assumptions and the limitations that are considered for this case study. Building thermal zones, building envelope properties, building schedule and HVAC system structure are set up for the building simulation model.

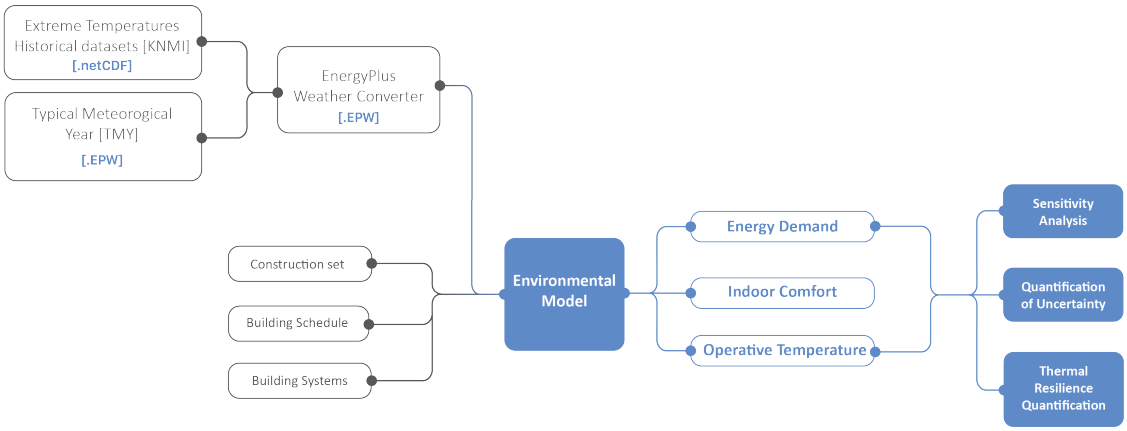

Figure 3.1: General methodology workflow diagram used in this case study. A detailed diagram is presented in Appendix C.4.

Assumptions were made in order to distinguish the design decisions from the building parameters and variables that influence the metrics of thermal resilience indicators. In the beginning, a shoe box was simulated and then the process was applied to the whole building for generating the final results of this research. Simultaneously with the simulation workflow, the implementation of the uncertainty quantification in the whole process is explained. The uncertainty quantification process is used in order to map the density of the uncertain parameters (variables) in relation to the results. This process is split into smaller tasks in which one-at-a-time and variance-based sensitivity analysis are needed for indicating the most influential parameters to the results. Sensitivity analysis results are visualised either with correlation matrices or with box-plot charts. During the process, Monte Carlo (MC) and Latin Hypercube (LHS) sampling methods. In the last part, the parameters that give significant divergence to the results are pointed out, thus building simulations are held only by considering the variant values of the most influential parameters. These results are compared with an optimised performance of the building and hence the resilience loss is quantified by calculating the outcomes of cooling and ventilation energy demand and indoor operative temperature.

3.2. Weather data generation

As mentioned in the previous chapter the case study refers to an office building in Amsterdam. Thus, weather data sets from variant sources were collected and analysed in order to generate an EPW file that is suitable for this research. In general, the main principle is firstly to define the overheating stresses in the climate data file and transfer this information to a TMY file in order to generate an EPW that works with EnergyPLus software for the building simulations. However, before using the weather data sets an assumption is needed in order to define the concept of the overheat stresses and how can they be identified within a weather data set. According to Cheung and Jim (2019), there are thermal sensation thresholds defined by Physiological Equivalent Temperature (PET). As presented in the table 3.1, these thresholds are split into two categories of cool-cold temperatures and warm-hot temperatures. The outdoor temperature of 29°C is considered as thermal sensation comfort threshold and hence is used for defining the warm, hot and extremely hot temperatures during the summer period.

Thermal sensation	Physiological stress	Range (°C PET)
Very cold	Extreme cold stress	< 4
Cold	Strong cold stress	4 to 8
Cool	Moderate cold stress	8 to 13
Slightly cool	Slight cold stress	13 to 18
Neutral (comfortable)	No thermal stress	18 to 23
Slightly warm	Slight heat stress	23 to 29
Warm	Moderate heat stress	29 to 35
Hot	Strong heat stress	35 to 41
Very hot	Extreme heat stress	> 41

Table 3.1: Thermal sensation and thermal stress classification scale of PET (Cheung & Jim, 2019).

Another assumption is made about the duration of the heat stresses in time and is based on Attia's statement. In order to calculate the thermal resilience in buildings the building simulations should not be held in instant temperature values that exceed a certain threshold but in a period of time when the heat wave occurs and hence a specific time frame should be defined.

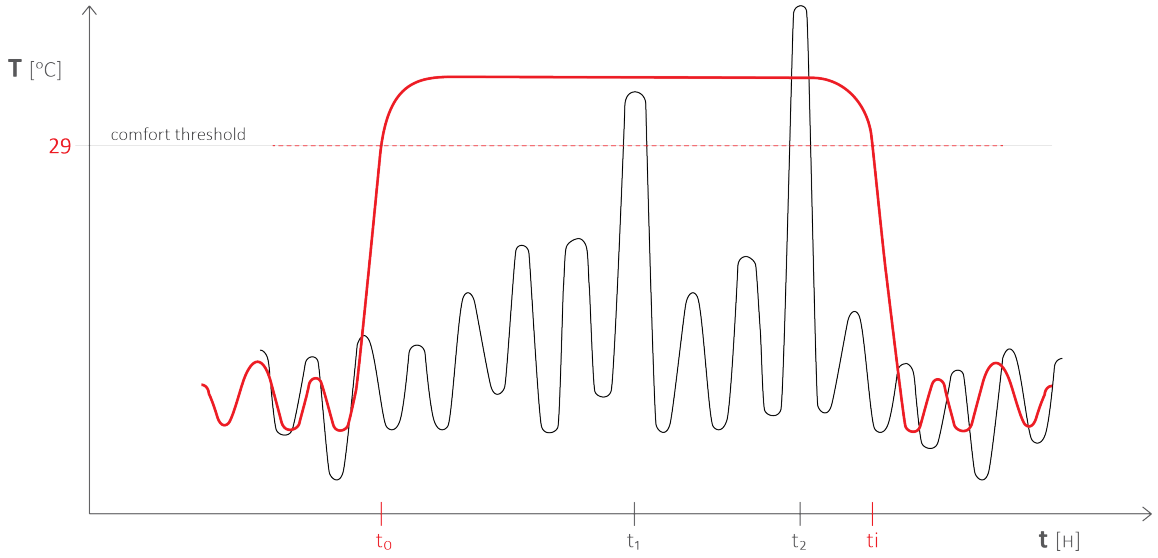

Figure 3.2: Concept diagram for defining the time frame of overheat stresses for this research.

By considering those two facts, a concept diagram 3.2 presents a hypothetical temperature fluctuation and the threshold of 29°C. Although, the outdoor temperature in the instant moments of t_1 and t_2 exceeds the outdoor thermal threshold of 29°C, this time frame between t_1 and t_2 is not considered as a continuous overheating event. Hence, the hypothetical heatwave is defined from the constant temperature above the certain comfort threshold and the time period between t_0 and t_i is considered the occurring time of extreme climate conditions.

After forming this assumption, the incoming weather data are explored in order to find temperatures above 29°C for a certain period of time during summer. Multiple sources of weather data sets were used in order to achieve the generation of a valid EPW file. In the first method, the generator (CCWorldWeatherGen) tool is used. As described in the previous chapter the generator uses a TMY file as a base and generates weather data according to different RCP scenarios. In this part, the most unpropitious scenario RCP 8.5 was used in order to generate EPW files that consider extreme temperatures and CO^2 emissions. The generated files are presented in the diagram B.3a in comparison with the TMY weather file. The diagram presents TMY weather data and generated data by the CCWorldWeatherGen tool for three different RCP scenarios (4.5, 6.0, 8.5). The diagram B.3b illustrates more clearly the comparison of weather data. The generated data have significantly higher values but those are proportional to the data of the TMY file which is expected because the generator uses the morphing method for synthesizing data.

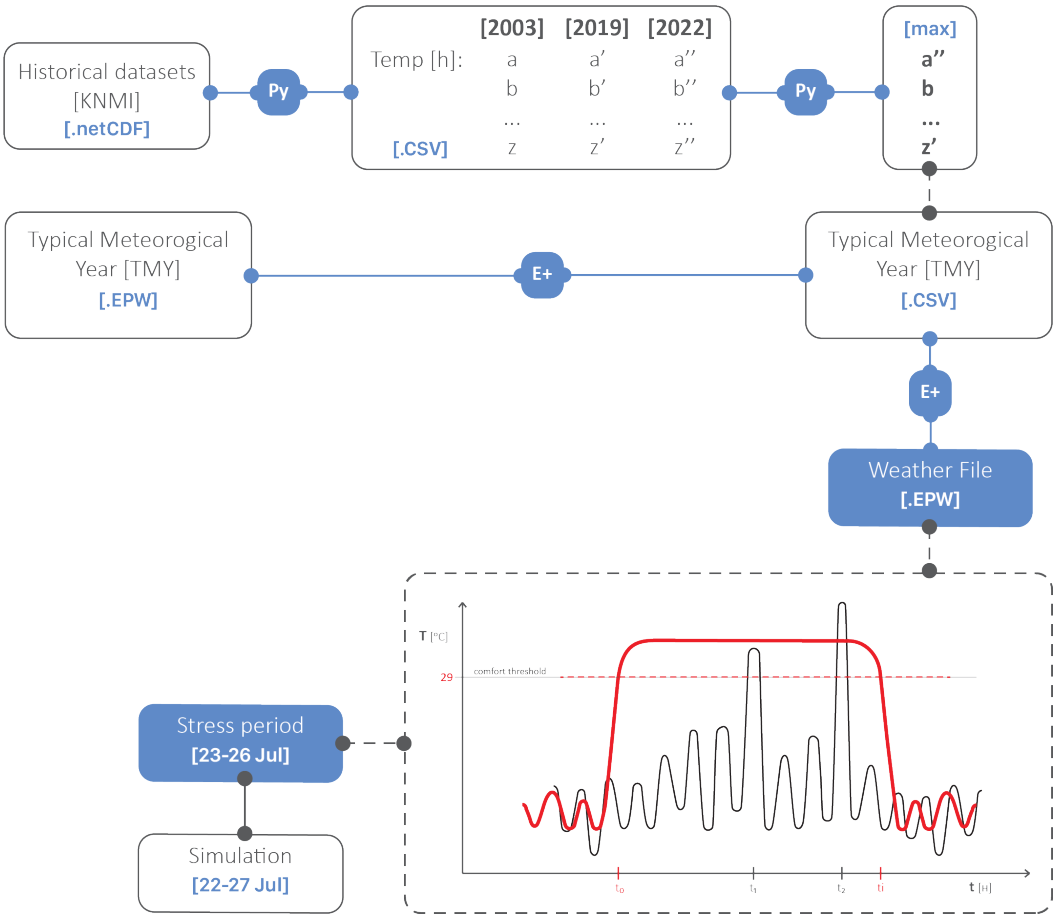

Figure 3.3: Selection of the higher values among three weather files of the heatwaves 2003, 2019 and 2020.

Subsequently, although the RCP scenarios are valid, the final outcome can not be considered as accurate because it is not affected by historical weather data of heatwaves. Furthermore, the generator generates weather data in a proportionally increasing manner to the initial values. Besides, the CCWorldWeatherGen tool has a strict step-by-step process and the results can be affected only by variant RCPs files and other weather data sets can not be complementary included in the process. The generated weather data by the CCWorldWeatherGen tool are presented in Appendix B.3.

As the first attempt was not valid, the research was focused on historical weather data. As mentioned in subsection 2.2.1 on page 24, extreme heat waves in 2003, 2019 and 2022 have occurred in Europe. Weather data sets were collected from the Royal Netherlands Meteorological Institute (KNMI) for these years (Appendix D.3). These are presented in the following diagram 3.4 and can be compared with the TMY. In the next step, the temperature values from all three data sets are compared and the highest values are chosen and used for generating an EPW weather file for this research. The comparison and the selection of the highest values are done by using the Python script as presented in Figure 3.3.

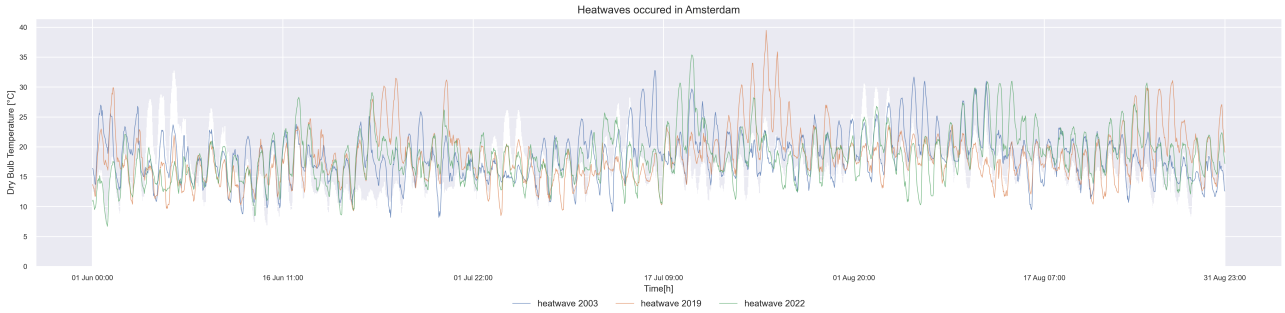

(a) Chart of TMY and heatwaves that occurred in Amsterdam during summer.

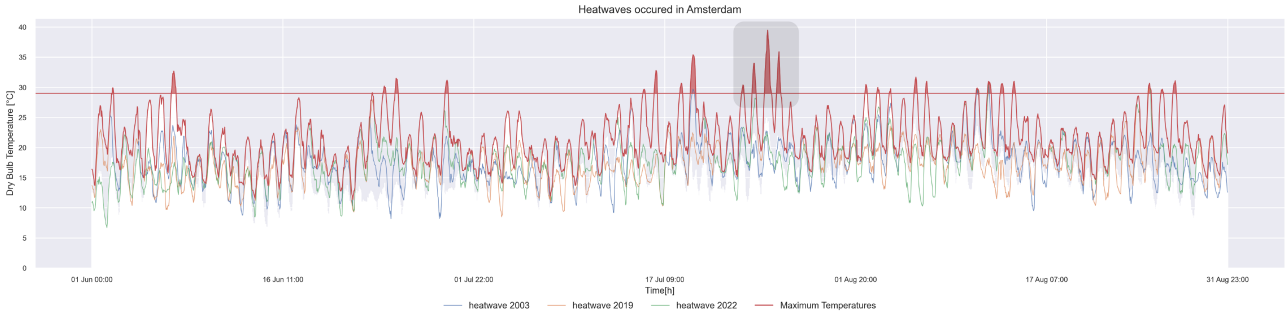

(b) Extreme temperatures during summer. The generated data are illustrated with the red line. The selection of the heat-stress period is based on the frequency of temperature over the threshold of 29°C. The selected heat stress period is pointed out.

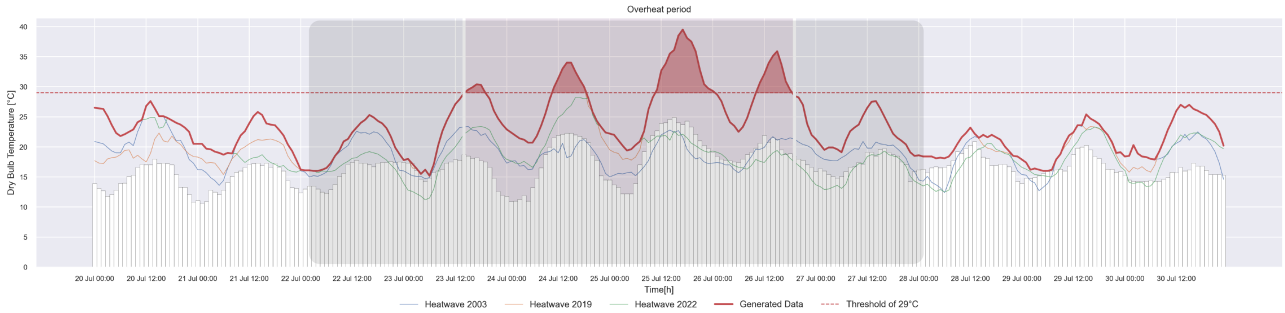

(c) Zoom in to the region with the most temperatures beyond the thermal threshold. One day before and one day after are included in the simulation process.

Figure 3.4: Extreme temperatures generated from historical weather data. Appendix B.4c

At this point, it is valuable to present the selected extreme temperatures with the outdoor comfort temperature threshold of 29°C. In the diagram 3.4, most of the temperatures that are constantly over the comfort threshold are depicted during the days of July. Therefore the building simulations, which are presented in Section 3.3.2, are held within the time frame from 23^{rd} to 27^{th} of July.

After the collection and evaluation of historical weather data, the EPW file is created. For this process, multiple software is used but the main principle of using the initial TMY file as a basis remains the same (Figure **??**). First, the initial EPW file with the TMY data is converted to a CSV file via the Energy Plus Weather Converter. The weather data with extreme values are embedded into the CSV manually. More specifically, dry bulb temperature, solar radiation and humidity values are modified for the time period of summer. As long as all the values are embedded into the CSV, the file is converted to EPW by using the Energy Plus Weather Converter. During this process, alternatives and different approaches were attempted by modifying directly the EPW either with Python or with Notepad++ but the generated file occurred errors during the simulation process.

3.3. Definition of the design

3.3.1. Building

A mid-rise office building, located in Amsterdam is used as a case study for this thesis. This eight-story office building consists of a rectangular plan geometry of 45x30 meters and a central atrium of 22x15 meters which expands to the whole height of the building. The floor height is defined at 4.2 meters and the vertical circulation through floors is served by two main cores that are located in the western and eastern parts of the building.

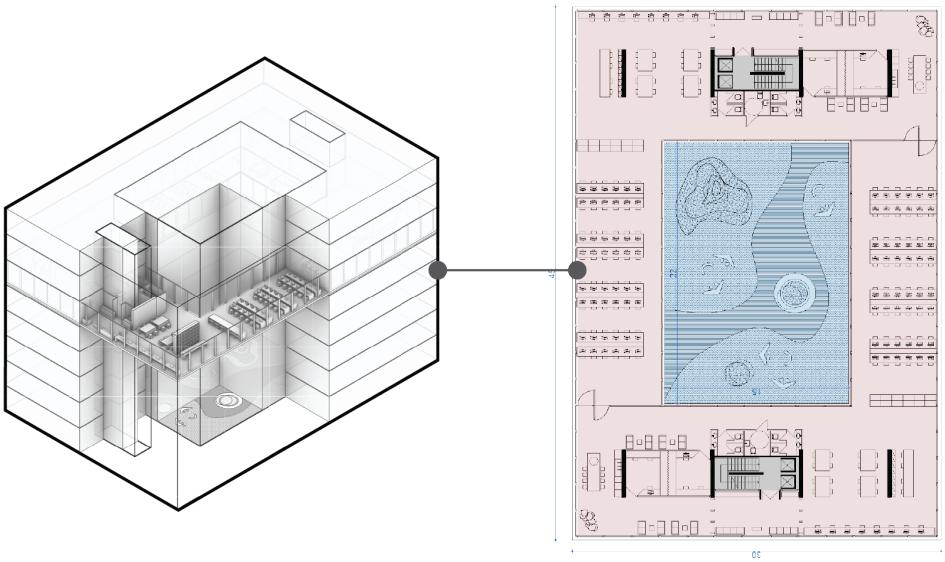

Figure 3.5: Building geometry and plan. Open-plan offices, a central atrium and two cores constitute the main areas. General building geometry properties and plan dimensions are presented in the table D.1.

Besides the general geometry and the type of the building, assumptions were made also for the facade elements and materials. The main facade system consists of pre-fabricated elements and in this case,

the main material is concrete. Moreover, thermal insulation covers the whole exterior facade surface area and a final layer of aluminium cladding is added for finishing. Between the concrete and thermal insulation layers, a cavity space is also considered. Air sealant tape and vapour open water membrane layers are considered as lines of defence in the technical design of the facade. The opaque materials are defined by their discrete material properties of thickness, conductivity, density, specific heat gain coefficient, and thermal, visible and solar absorbance. Hence, the material U-values and thermal mass are dependent on these. The glazing elements are defined by the wall-window ratio (WWR) and the thermal transmittance property (U-value), solar heat gain coefficient (SHGC) and visible transmittance (Vis_{trans}). Therefore, these material properties are assigned as variables to the final simulation model for the whole building simulation. The properties of interior floor slabs are defined by their thermal resistance properties (R-values) and are considered standard parameters in the model.

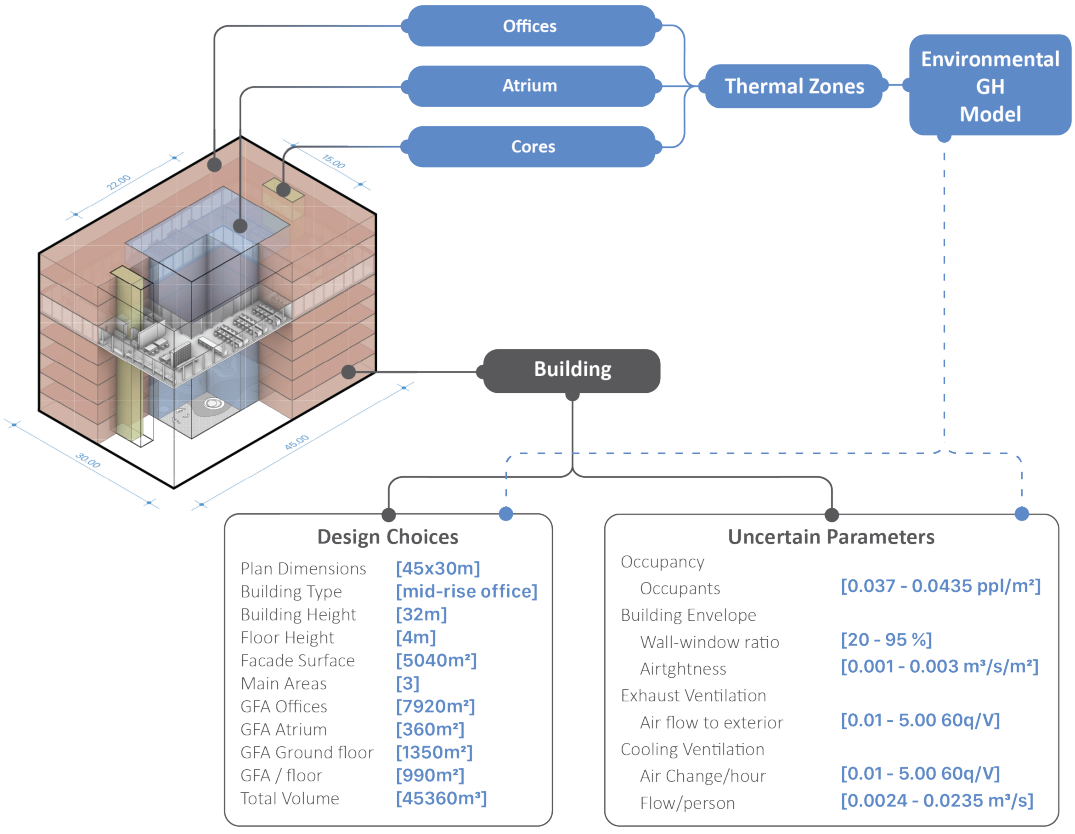

Figure 3.6: The main areas of the building are considered as separate thermal zones in the environmental model. Occupancy, wall-window ratio, air-tightness, exhaust ventilation, cooling system and flow per person are variables of the problem.

Apart from the building materials, general operational building properties and ventilation system properties are assigned to the model in order to define the case of the office building of around 300 occupants. More specifically, the features of heating and cooling set-points, infiltration rate, building operating hours, people per square meters (ppl/m^2) and air change per hour (ACH) constitute the operational and exhaust ventilation (ExV) properties of the building. All of the aforementioned properties are tuned within a range of values that are based on ASHRAE 90.1 building norms and they are presented in the table D.2 in Appendix D.

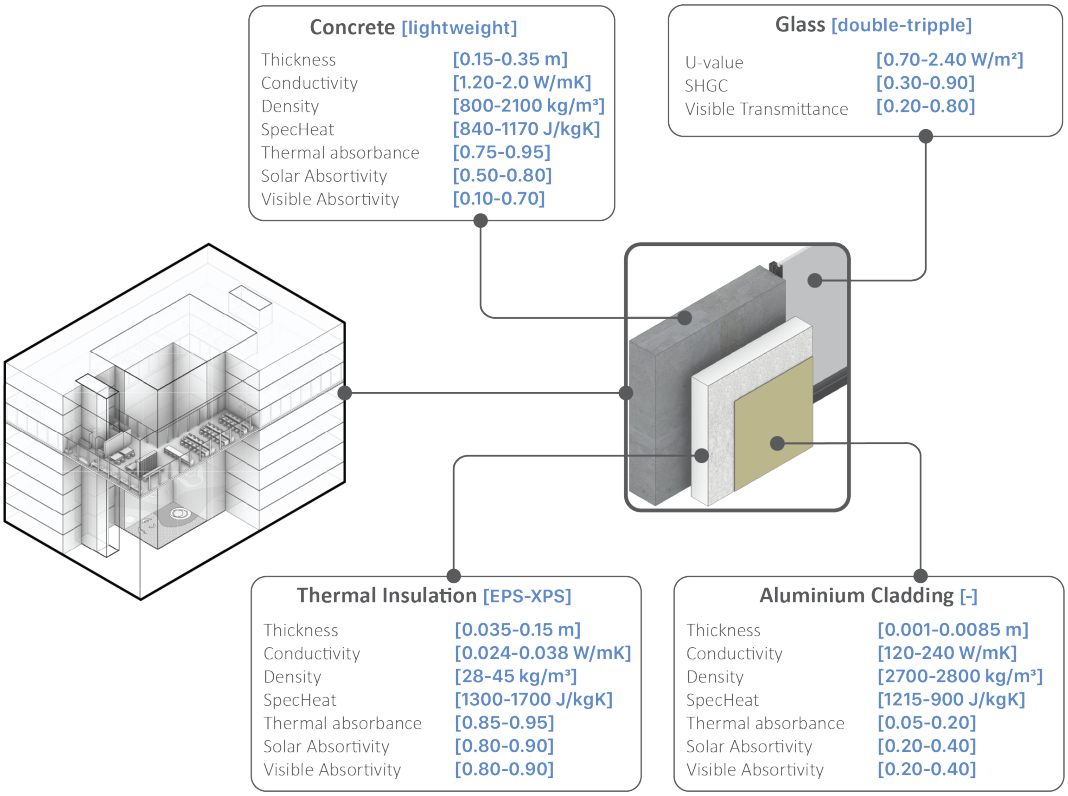

Figure 3.7: Facade and material properties are considered as variables of the problem. See Appendix D.2 for a detailed overview of all building and material properties values.

At this point, it is worth mentioning that the Grasshopper model offers the option to define all properties for both opaque and aperture materials either by their discrete properties or by their R and U values. At the beginning of the simulation process, the simulation workflow run in a shoe-box model (part of the building) in order to define the number of variables that best fit to simulation outcomes. Hence, both ways of setting only discrete material properties and generic properties are attempted. By setting all materials with their discrete properties the iteration number of simulations is immensely large and could not be considered as a realistic case scenario considering time constraints. In contrast, by setting all materials with their generic properties of R and U values, the iteration number of simulations would not be adequate enough for obtaining valuable results. Material properties are described in material brochures standards and norms by their discrete values in the case of opaque materials while by their U-values in the case of glazing. Hereby, a decision is made in order to set a useful simulation model for designers and engineers in which the calculated values and the generated results are interpreted to values that are applied to the design and calculation process. Subsequently, the opaque materials are defined by their discrete properties and the glazing parts by their U-values and hence the iteration number of simulations is sufficient and handleable time-wise.

3.3.2. Structure of the Simulation Model

A dynamic building simulation model in the visual programming language, in this case, Grasshopper (GH) is created for developing dynamic building simulations. As a whole, the main core of the script consists of Honeybee (HB) components and libraries from the Ladybug tools (LB) plug-in in order

to define the energy simulation model and the thermal zones for the whole building. In the second part, the plug-ins of Open Studio (OS) and EnergyPlus (E+) are used for tuning the variables and generating results. The weather data sets are assigned as EPW files to the GH script and are linked with the E+ simulator. In addition, the Colibri (COL) iterator plug-in is used for running the whole workflow in loops and hence, multiple simulations can be run and their results can be stored in a CSV file automatically. Complementary Python components are developed for adding more features and functions to the energy model and to the simulator script, such as the ACH, ExV, Economizer (ECO) and Coefficient of Performance (COP) (See Appendix A.1).

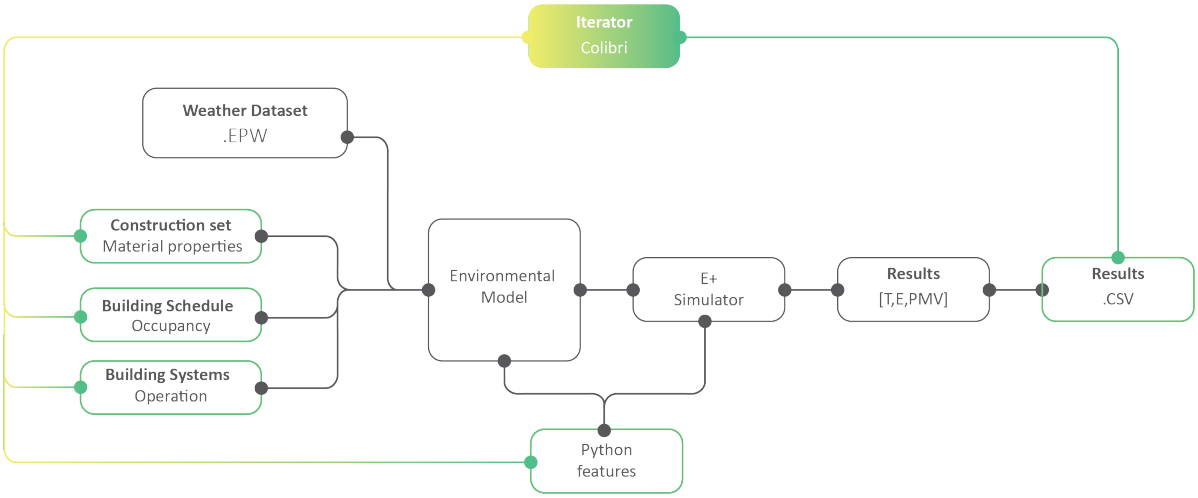

Figure 3.8: Overview of the simulation model. Colibri runs multiple iterations according to the inputs. The generated data is saved in a CSV file. The Grasshopper script is presented in Appendix A.2.

More specifically, in the first part of the script the basic building geometry is generated. Here, the main dimensions of the plan, the floor height, the building height and the atrium are created. Once the main geometry is set, the generation of the energy model for the building follows. At this stage of the model, it is essential to set correctly the thermal zones for the building which depend on the architectural plan and the room separation. As long as open-plan offices are selected for this case study, each floor is considered as a separate thermal zone. The atrium and the cores are considered as separate thermal zones as well. The model recognises the adjacencies between different thermal zones, as a result, exterior and interior surfaces are defined correctly.

At this stage, building and material properties are defined and assigned to the HB thermal zones. The default building schedules by LB libraries (ASHRAE 90.1) are used and adjusted to the desired options in order to be aligned with this particular type of building (see section 3.3.1). In short, the occupancy schedule, the infiltration, the heating and cooling set points, the lighting, the equipment and the ventilation loads are set to the building properties. Moreover, the exterior elements of the building envelope and the interior elements, such as the interior floor slabs and the interior walls of the atrium are defined by the construction set in respect to material properties. The aperture dimensions of the building envelope and the atrium walls are set by the WWR. A customised ideal air system is introduced to the energy model with different features for the offices' thermal zones and the atrium. The flexibility of this element is enhanced by linking a Python component which uses data from the IDF

file of E+ and hence features such as ACH, ECO, COP, maximum and minimum indoor temperature operating set points of the air system can be dynamically defined.

Once all the settings are set, the second part of the GH is ready to be adjusted as well. At this stage, the main OS plug-in uses the E+ software as a background task. Simulation parameters, such as the EPW file, the simulation period, the ambient shadow and reflections and the temporal frequency of the generated results are tuned. Particularly, the EPW file with extreme temperatures as mentioned in 3.2 is linked, the simulation period is set from 22^{nd} to 27^{th} and the generated results are set to hourly frequency. The simulator generates an SQL file from which all calculations can be extracted and can be used for post-processing. Since the main scope of this research is thermal resilience quantification, the metrics of thermal resilience indicators and energy loads are calculated. For obtaining more accurate results factors such as the human activity and clothing insulation parameter are defined for this particular occupancy level and activity. Metrics of Predicted Mean Vote (PVM), indoor Operative Temperature (T_{oper}) and End Use Intensity (EUI), Cooling and Ventilation loads are calculated for the whole building and for each floor.

3.4. Computational workflow

As explained in the previous section, the calculation of thermal resilience metrics and energy loads depends on the material and building properties variables. For this reason, it is essential to identify the most crucial parameters that have a significant effect on the results in order to distinguish the final variables from the standardized parameters. Subsequently, sensitivity analysis is held for this scope before running the final simulations for the thermal resilience quantification of the office building. In section 3.5, the whole process of one-at-a-time and variance-based sensitivity analysis is presented and the variables with significant variance to the results are concluded.

Since the Uncertainty Quantification (UQ) of the design parameters is part of this research, a probabilistic quantification process is implemented in the next part after the sensitivity analysis. Once the most influential parameters are clarified, their probability to generated results is evaluated. In building energy simulations, UQ involves quantifying the uncertainties in the inputs, parameters, and models that can affect the energy performance predictions of a building. By reducing these uncertainties, UQ can improve the accuracy and reliability of energy performance predictions, reduce the risk of performance gaps, support decision-making, and optimize building performance. In practice, distribution density curves of the variables that achieve a high sensitivity score are created with respect to their range of input values and simulation outcomes.

In the last part of the workflow (section 3.6) thermal resilience quantification is described. As mentioned above the simulation model calculates hourly results for the thermal resilience metrics of Predicted Mean Vote (PVM) and Indoor Operative Temperature (T_{oper}) and results for the energy cooling and ventilating loads. Through the quantification process, the thermal comfort outcomes are correlated with the energy loads and both generate the thermal resilience performance curve of this particular building. However, these results need to be compared with an ideal case scenario in which the building achieves 100% of its performance. For this reason, an optimisation generative algorithm for this building is implemented by using the WallaceiX (GH plug-in).

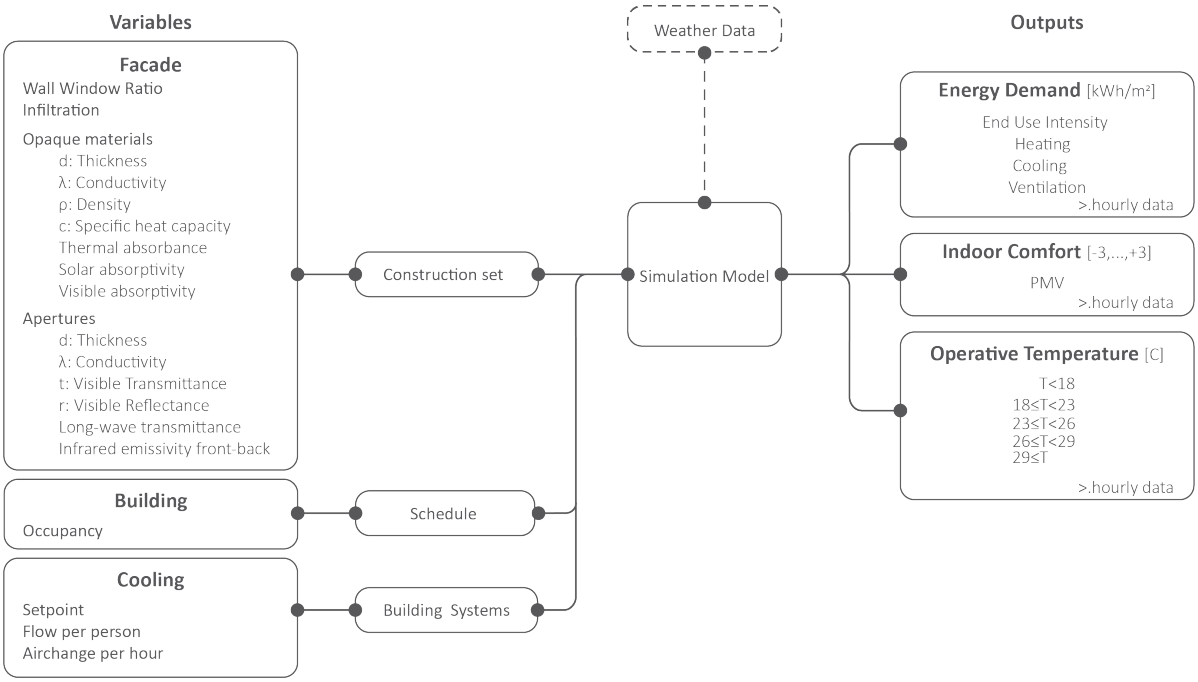

Figure 3.9: Computational workflow diagram. The variables of the problem are assigned as inputs in the workflow and hourly data are generated. The detailed diagram can be found in Appendix C.5.

In the last part, the optimisation outcomes and the simulation results are transmitted to Python for post-processing. Thereupon, performance curve charts of the optimised and the simulated case scenarios are created and the difference in their numerical hourly values is calculated and hence the resilience loss. At this part, simulations with certain values for each building parameter can run, and be extracted to Python hence thermal resilience is evaluated by making comparisons among different design cases. For instance, thermal resilience performance on different office floors can be evaluated by associating them with variant wall-window ratios of the facade.

3.5. Sensitivity analysis

After generating the EPW file, creating the 3D digital model, the visual scripting simulation model and adjusting the necessary parameters and variables, the part of the simulation process is presented in the following sections. As mentioned in the introduction, one-at-time and variance-based SA are presented. Three attempts of this analysis are computed in order to define the variables that best meet the simulation criteria, of obtaining an adequate number of results considering time constraints (See Appendix D.2). In short, the model could be established either by defining the materials with their discrete properties (e.g. thickness, conductivity, density etc) or with their thermal properties (e.g. U and R values), as a result, the simulation model could have 26 or 34 variables and hence the simulation time is affected significantly (Appendix D.2). Considering, both obtaining an adequate population sample and time limitations the final simulation model is adjusted to 30 variables (See Appendix D.2). All these are evaluated through the SA and then their probabilistic distribution curves are computed

in order to generate results of 95% of probability in the second phase.

As mentioned in 3.3.2, the performance of the simulation model is dependent on multiple variables that define either the building envelope material properties or the operational use of the building. At this part of the research, it is crucial to explore the importance of each variable to the study and the influence of each on the results. For this reason, sensitivity analysis is implemented in the workflow by working in three different methods. The first method refers to one-at-a-time sensitivity analysis, the second to variance-based by using a simplification of mathematical function for calculating the indoor operative temperature and the third one calculates the Sobol' indices by using the generated data from building simulations.

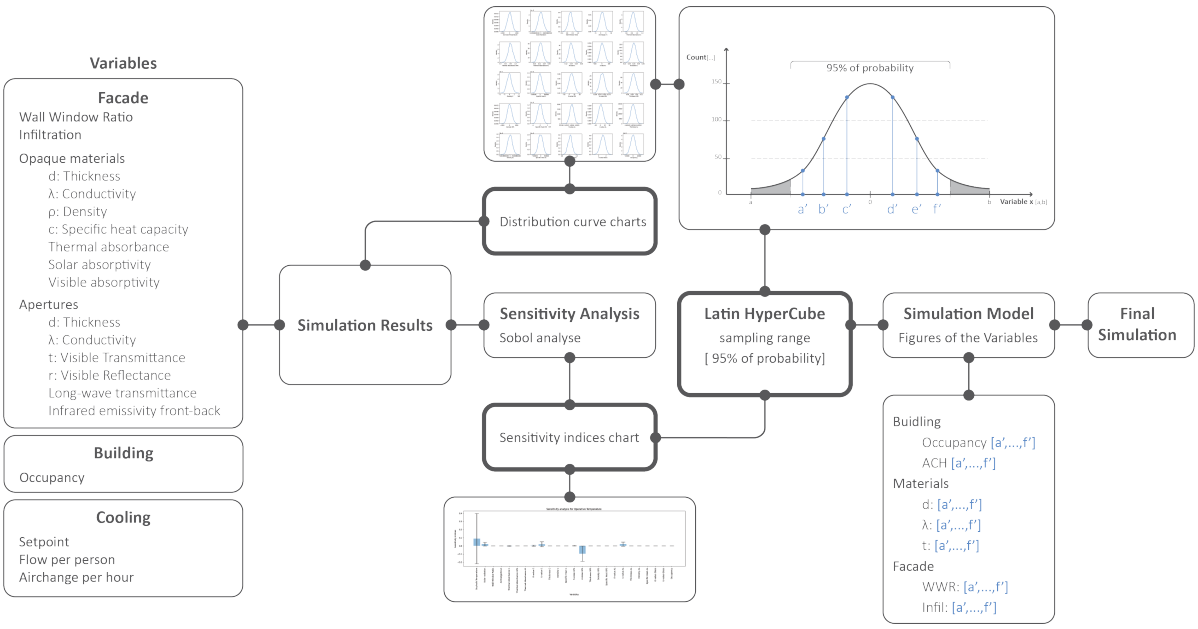

Figure 3.10: Post-processing simulation results for sensitivity analysis and uncertainty quantification tasks.

3.5.1. One-at-a-time sensitivity analysis

For the one-at-a-time sensitivity analysis each variable is defined by a minimum, maximum and mean from the range of values as presented in 3.3.1. In this process, the simulation model, in which 34 variables are assigned, run multiple iterations and produced results with a sample size of 146. Each time the model assigns to the first variable the minimum value and to the other variables their mean value, then it assigns the maximum value to the first variable and to the other variables their mean value. This process iterates for all the variables of the model until their minimum and their maximum values are assigned. As shown in the correlation matrix 3.11a the properties of thickness, conductivity, density, occupancy, WWR and ACH influence most of the generated results. These values are presented extensively in the table D.5.

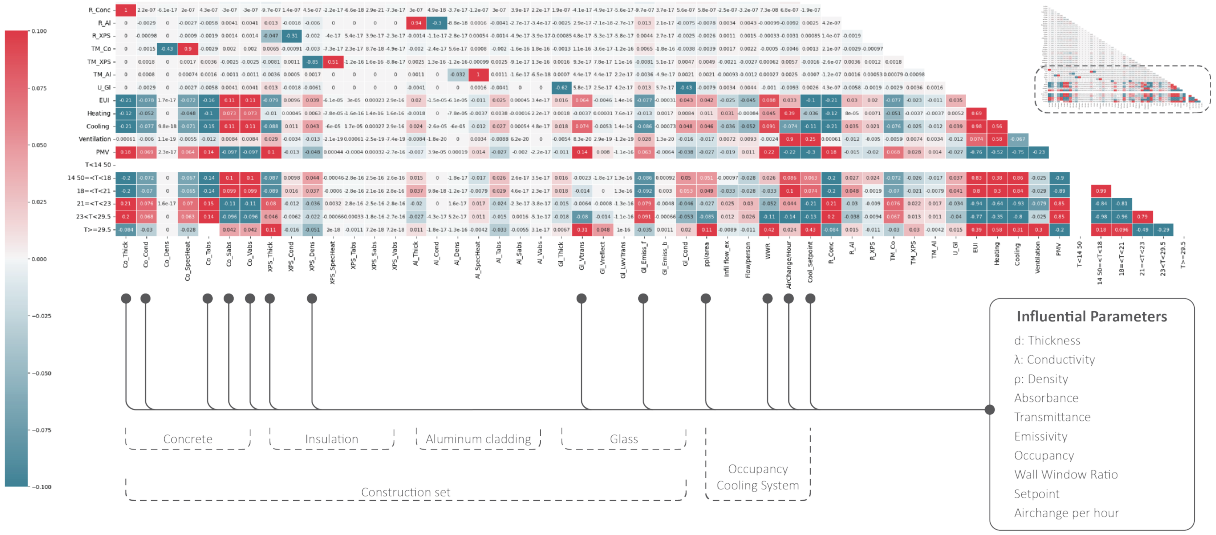

(a) Correlation matrix of 34 variables.

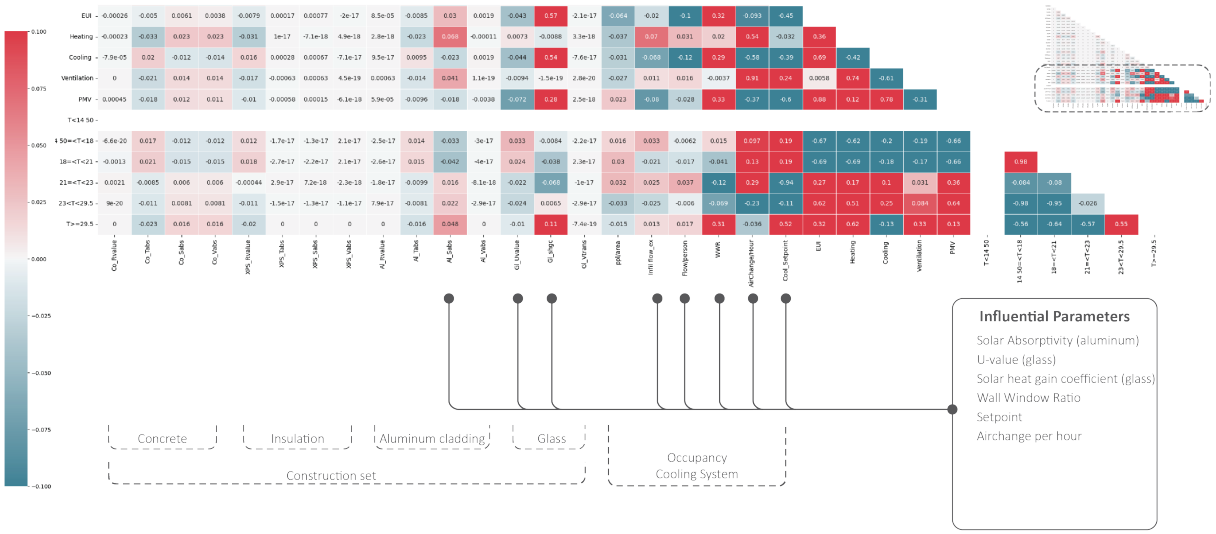

(b) Correlation matrix of 26 variables.

Figure 3.11: The entire correlation matrices are presented in Appendix F.2.

The same process run for another simulation model which consists of 26 variables. In this case, the material properties consist of their thermal resistance (R-values) and thermal transmittance (U-values) in which the properties of specific heat, conductivity, and thickness are already considered. The correlation matrix 3.11b of this simulation model shows that the properties of thermal transmittance (U-values), solar heat gain coefficient (SHGC), WWR and ACH are critical. These values are presented extensively in the table D.4.

3.5.2. Variance-based

Implementation of a math function.

Variance-based sensitivity analysis was held in Python with the main goal to calculate the Total Order of Sobol' indices, which define the most influential parameters. In this attempt, it is important to set up a calculation function within the Python script that calculates the operative temperature and the

energy demand by setting up different values for each variable. The mathematical function is based on thermal equations that are adopted from the field of building physics and they are presented in Appendix E.

$$T_{oper} = \frac{a_{rad} T_{facade\,in} + a_{conv} T_{air\,in}}{a_{rad} + a_{conv}} \tag{3.1}$$

Where:

a_{rad}: radiation heat transfer coefficient

$T_{facade\,in}$: surface temperature of the facade inside

a_{conv}: convection heat transfer coefficient

$T_{air\,in}$: indoor air temperature

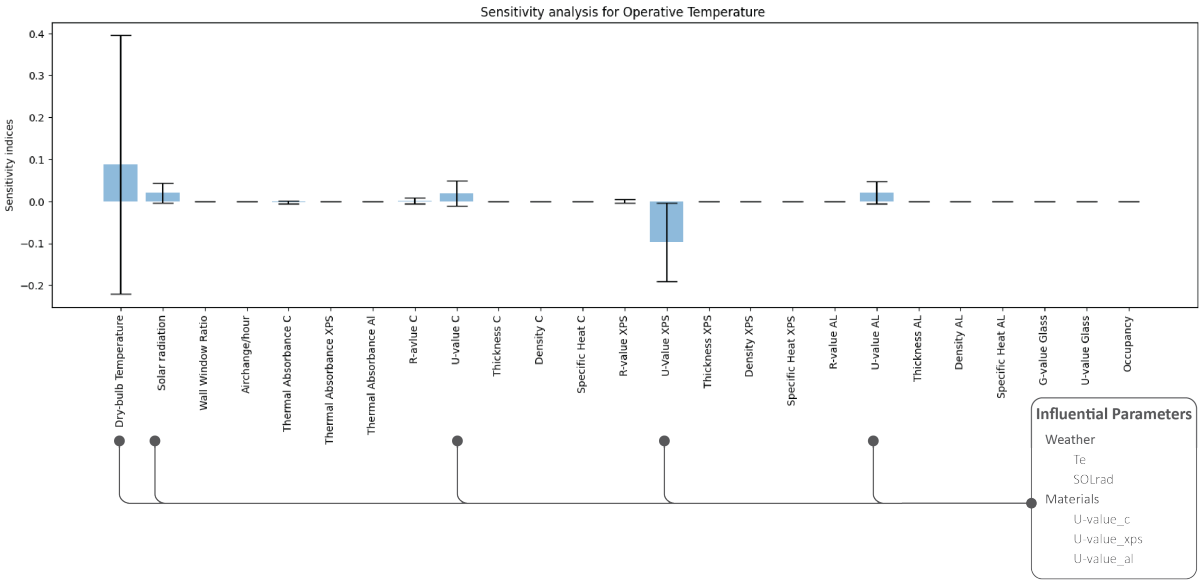

Figure 3.12: Total order Sobol' indices. Python script can be found in Appendix A.2

The building physics equations consist of the following variables and the numeric values are assigned to them as presented in the table D.6. In the beginning, the mathematical function for calculating the indoor operative temperature is set and the mean (mu) and standard deviation (sigma) are calculated from the samples of variables. Then the function for calculating the operative temperature is used as an iterative process for all values of variables and hence Sobol' indices were calculated (3.18a).

Through this process, the parameters of exterior temperature, solar radiation and thermal transmittance values (U-values) are stated as the most influential to the results. However, the divergence of the sensitivity indices is significant, thus the validity of those is doubtful. Because of using the simplified equation from building physics and/or the small population size (150) of the variables affected the calculation of Sobol' indices for operative temperature. For this reason, the influential parameters that are stated above can not be considered as valid.

Black-box

In the following attempt more simulation results were generated and the variance-based sensitivity was held by considering the simulation inputs and outputs. The simulation model generated 3470 outputs for each of the calculated metrics (see 3.3.2) and hence the population size for the Sobol' indices calculation is considered adequate enough for getting valid results. The simulation process is split into six simulation models that run simultaneously in order to generate an adequate sample size of results. More specifically, each simulation model is run by using five variables and five values for each one. The rest of the 30 variables are set with standard mean values. The main simulation outputs calculate the metrics (as mentioned in 3.3.2) of cooling and ventilation demand, indoor operative comfort (T_{oper}) and predicted mean vote (PVM). The simulation inputs and outputs of these six files are combined into one CSV and are imported to Python for post-processing. Before conducting the calculation of Sobol' indices, the type of distribution and the bounds of data needed to be defined for each variable according to the simulation results. Then the simulation data are split into training and testing sets in order to train a Gaussian Regression model that is essential to compute the Sobol' indices. More specifically, the Radial Basis Function reads the samples that were stored in CSV file previously, finds the underlying patterns between the simulation inputs and outputs and trains the Gaussian regression. At the same time, the Saltelli sampling technique for selecting each time a sample and with the assistance of the Gaussian metamodel the Sobol' index is computed. The process is explained in detail in Appendix A.3.

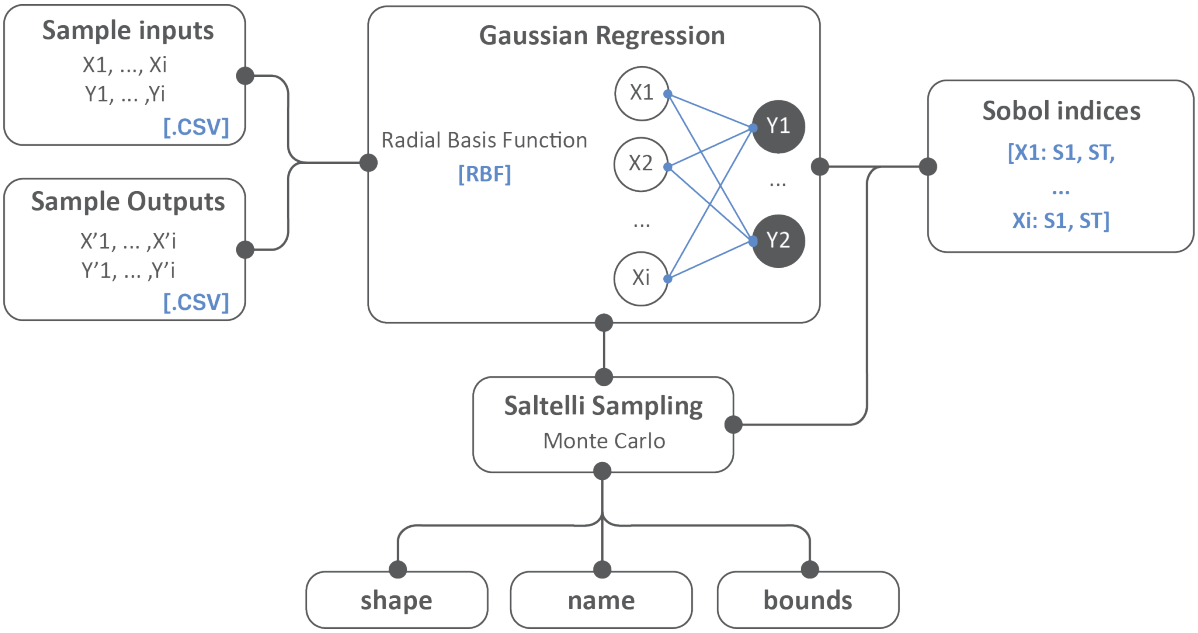

Figure 3.13: Workflow of performing SA by using the simulation inputs and outputs as a black box.

Before conducting the Sensitivity analysis, the accuracy of the model is examined. The following diagrams illustrate the comparison between the actual simulation and the predicted values for each sample. Considering the low value of the Mean Squared Error (MSE)(3.52e-16), the model is accurate enough to compute the Sobol' indices. This fact agrees with the presented diagrams below.

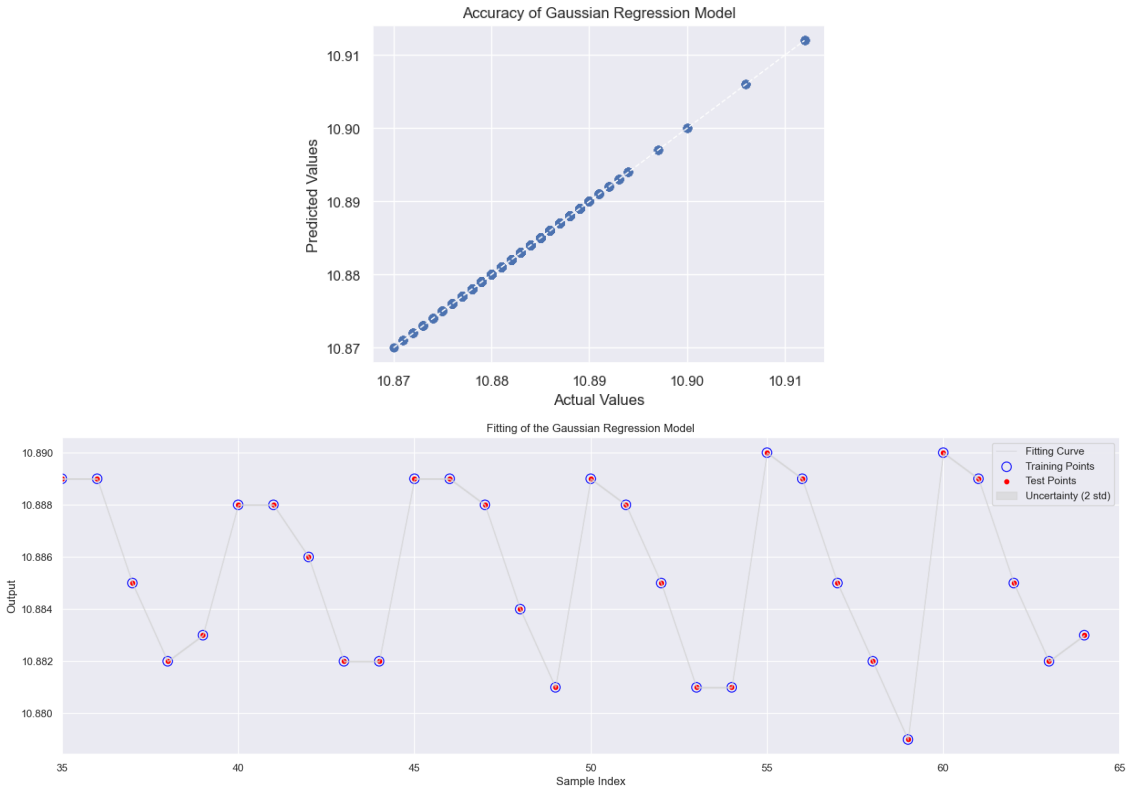

Figure 3.14: Predicted and simulation values of the Gaussian Regression model (See Appendix F.3). The Python script can be found in Appendix A.3.

The correlation matrix (3.15) illustrates the variables with the highest variance on the calculated results. The properties of conductivity and density of the main material of the structure, in this case, concrete, and the thermal insulation are highlighted with brighter colours than the other properties. Moreover, the thermal transmittance (U-value) of glass and the solar heat gain coefficient (SHGC) are crucial for the calculations. The wall-window ratio and the performance of the ventilation system have significant importance to the results.

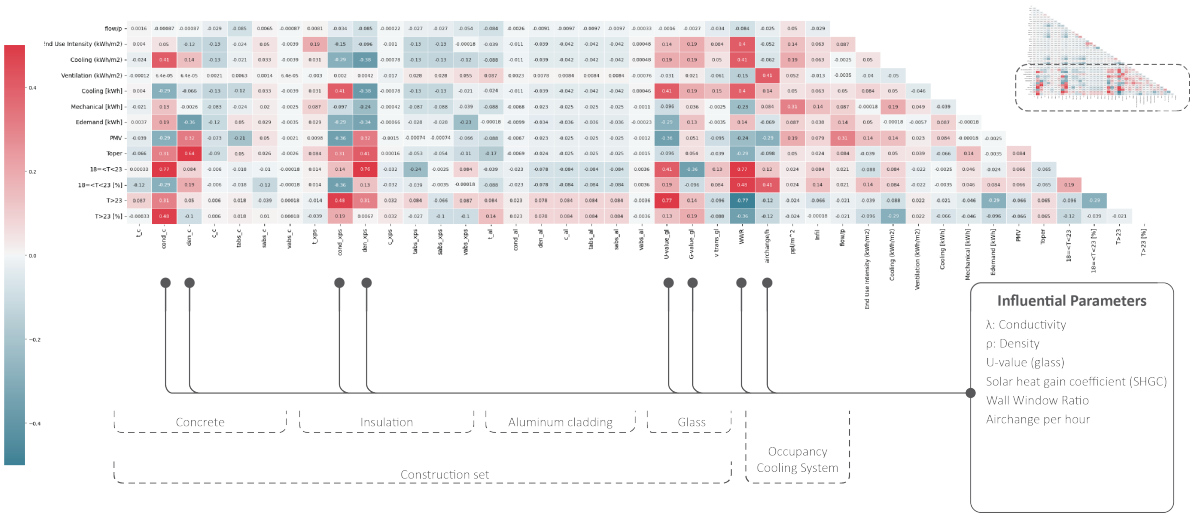

Figure 3.15: Correlation matrix of variables and calculated results. Appendix F.1

The simulation results were analysed for observing the inter-relationships among the problem variables and their influence on the simulation outputs. The diagram 3.16 shows that the building operational parameters and the glazing parameters after directly the simulation outputs, while the facade material properties are interrelated.

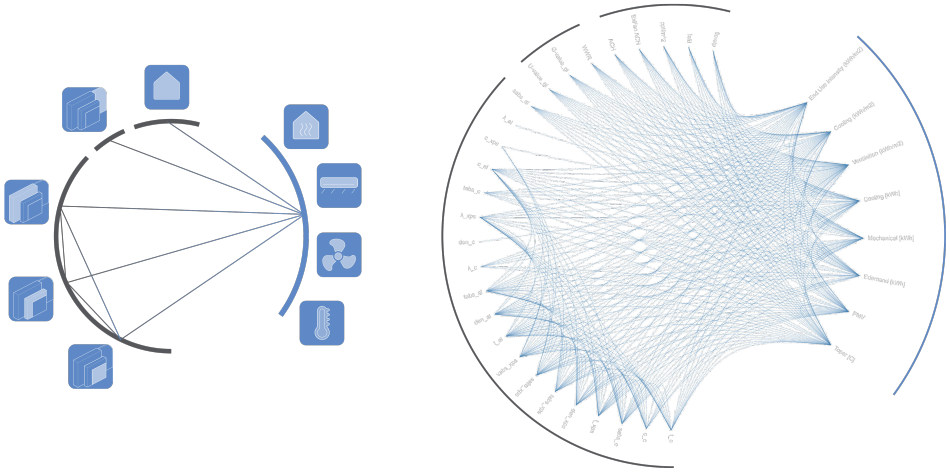

Figure 3.16: Edge Bunding Diagram that presents the inter-relationships among problem variables.

Apart from the results of the correlation matrix, it is valuable to mention the results from the Sobol' sensitivity analysis. In this analysis, the problem variables are defined with total-order and first-order indices. Total-order indices are a type of sensitivity analysis metric used to evaluate the influence of each input variable on the output of a model while taking into account all possible interactions with the other variables. In contrast, first-order indices only consider the direct effect of each input variable on the output of the model, ignoring any interactions with other variables. First-order indices are calculated by varying one input variable at a time while keeping all other variables constant. Total order indices, on the other hand, are calculated by varying all input variables simultaneously. The variables in which the boxplot is higher indicate the higher relative importance of the input to the variation of the output (C.2). For this task, the total-order indices are used for comparing the variables of this problem.

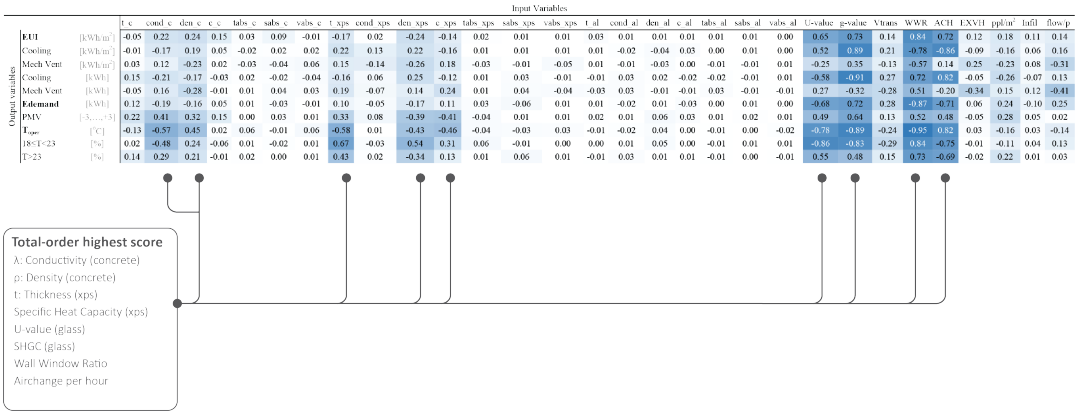

Figure 3.17: Sensitivity Coefficient chart. Sobol' indices scores of problem variables.

For this process the Sobol' indices are evaluated for the Energy demand (3.18b), the EUI (3.18c) and the Operative temperature (3.18a). The evaluation of the indices with respect to the Energy demand results showed that the wall-window ratio, the U-value, the SHGC, the visible transmittance of glass and the air change per hour affect most the results. Most of the rest variables score a lower total-order score. However, the indices of thermal conductivity (λ) and density variables of concrete and insulation are slightly higher. Similarly, the total-order indices are depicted in the chart for the EUI. In the total-indices boxplot regarding the operative temperature results, the same glass properties and glazing percentage reached the highest score among the rest variables. In addition, the properties of thermal conductivity and density of concrete are significantly high and slightly higher than the thickness, density and specific heat capacity of the insulation material. In the 3.17 all the variable Sobol' indices are presented. Conductivity, density and thermal absorbance of concrete and insulation material have significant variances in the results. In addition, the WWR, U-value and SHGC of glass are important for building simulations.

The boxplot charts indicate the total-order index score for every variable of the problem. The height of the box indicates the relative importance of the input variable in explaining the variation of the output. Therefore, the higher the boxplot is, the larger the Sobol' index and hence the variable's influence on the computed results respectively. The Saltelli function picks 3470 samples from a variable (same as the number of simulation results) and with the assistance of the prediction model the Sobol' indices are computed. As a result, the total-order indices for each variable result in a divergence range, which is presented with the *whiskers*, while the blue *box* represents the 75% of the entire sample size. The box is defined by the lower and upper *quartile*. The line inside the box represents the *median* value of the data (See Appendix C.2). Overall, the ACH reaches the highest Sobol' indices score and the glazing properties of WWR, U-value and G-value influence significantly the results. The facade material properties of concrete conductivity and density and the thickness, density and specific heat of the thermal insulation materials cause moderate influence on the final results. On the other hand, the rest variables of the problem achieve a low score.

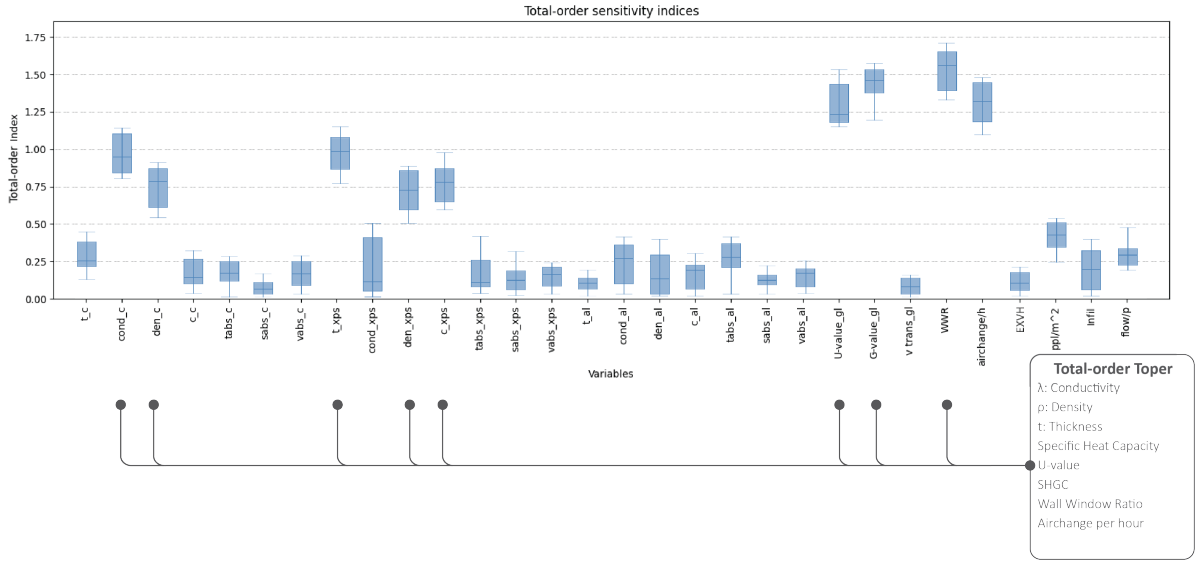

(a) Sobol' indices for operative Temperature.

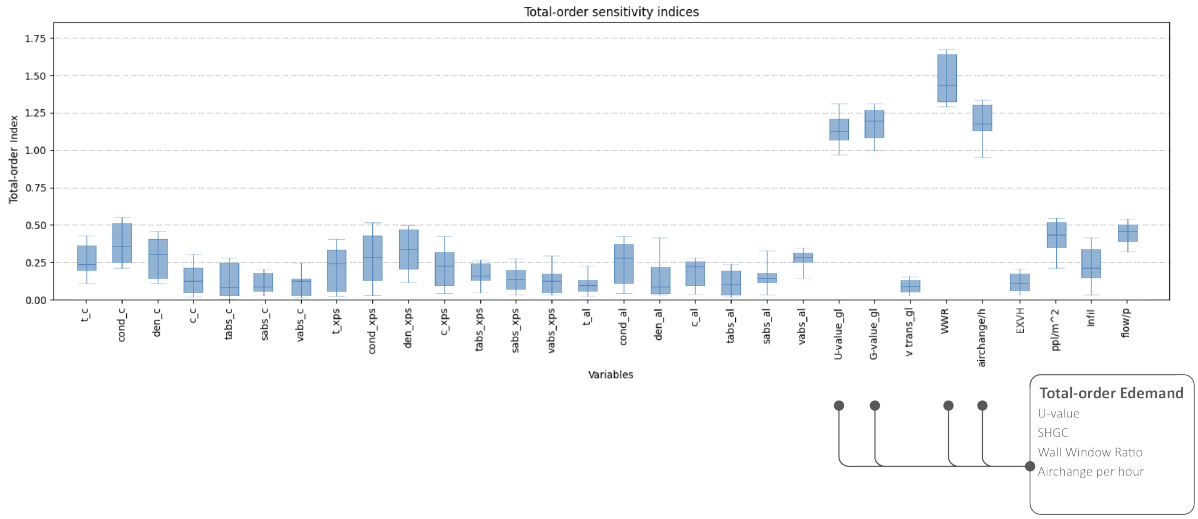

(b) Sobol' indices for total Energy demand.

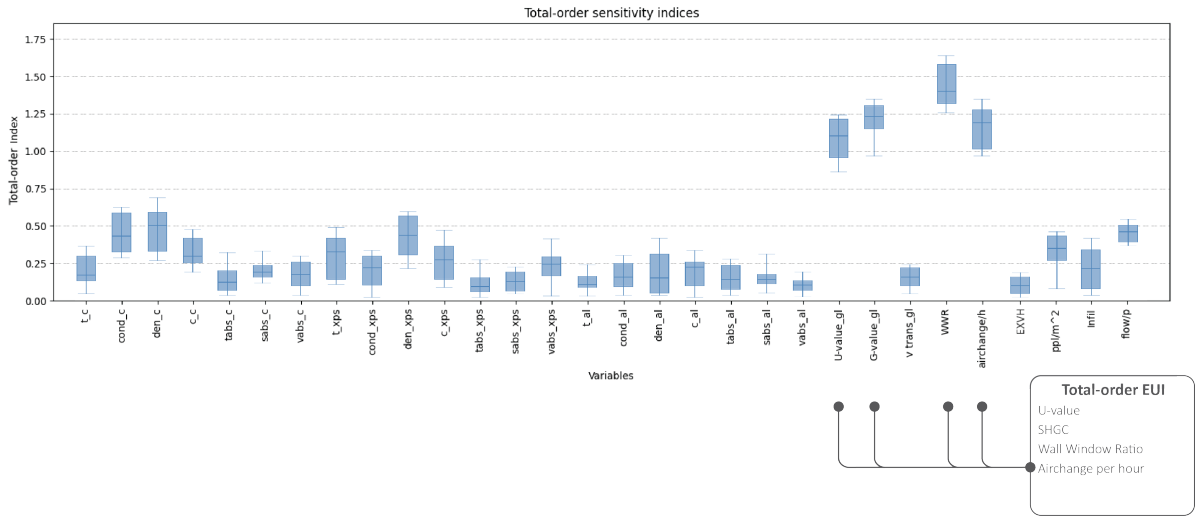

(c) Sobol' indices for EUI.

Figure 3.18: Sobol' Sensitivity Analysis results.

These research outcomes agree with the literature findings regarding the parameters that can influence thermal building simulations. According to Elhadad and Orban (2021) the variance of the thermal conductivity (λ) values affects the outcomes of the energy simulations, while the thickness of materials has the least impact. Moreover, the wall-window ratio is stated (Neale et al., 2022; Zeferina et al., 2019) as a parameter of significant influence on the results of an energy building simulation. Neale et al. (2022) adds to his findings the material property of thermal transmittance (U-value) of the exterior walls. Here, it is important to mention the definition of thermal transmittance and thermal mass, because they are depended on the variables of conductivity and density of this case study. The former is calculated by the fraction of thickness to conductivity and the latter is the multiplication of specific heat capacity with the density (ρ). Subsequently, the final simulations for the thermal resilience quantification are focused on the alternation of values of the variables with the most critical Sobol' indices.

3.5.3. Uncertainty Quantification

Uncertainty quantification (UQ) is the field of studying and analyzing the sources of uncertainty and variability in mathematical models and simulations. In building energy simulations, UQ involves quantifying the uncertainties in the inputs, parameters, and models that can affect the energy performance predictions of a building. UQ is becoming increasingly important in building design and energy retrofit projects as it helps to identify and reduce the risks of performance gaps between the predicted and actual energy performance of buildings. By reducing these uncertainties, UQ can improve the accuracy and reliability of energy performance predictions, reduce the risk of performance gaps, support decision-making, and optimize building performance. The sampling methods of MC and LHS can be used in the concept of probabilistic analysis. Monte Carlo and Latin Hypercube sampling are both widely used techniques for uncertainty quantification in thermal and energy dynamic building simulations (Sheikholeslami & Razavi, 2017). Monte Carlo simulation generates random samples from probability distributions, while Latin Hypercube sampling partitions the sample space into equally probable subregions, improving the representativeness of the sample (See section 2.3).

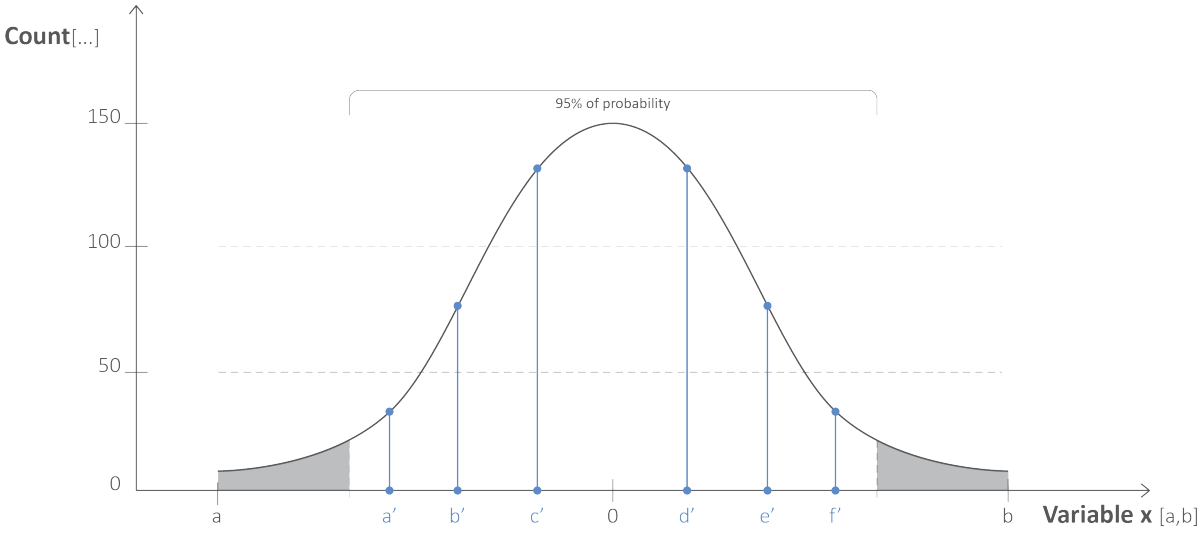

Figure 3.19: Concept diagram of probabilistic evaluation. The distribution curve presents the density of an input or output. Through this process samples can be extracted within a range of 95% of probability. Hereby, two samples are selected for each sub-region of the total count.

The process is implemented in the final simulation in order to map the whole spectrum of inputs and outputs and apply the sampling method in case of significant variance of the outputs. The density distribution curves most of the input variables are normal with a high density at their mean value. In the initial set-up of the simulation model, five values are assigned to each variable and 16250 outputs were scheduled to be generated, which is considered as an adequate amount of data for assessing the results. However, the distribution curves are not based on continuous data as the diagram 3.21 presents. The discrete numbers of inputs indicate that more values should be assigned but that was a decision that was made because of time limitations. Subsequently, the sampling methods of MC or LHS are skipped because the inputs have already a high density on a certain value.

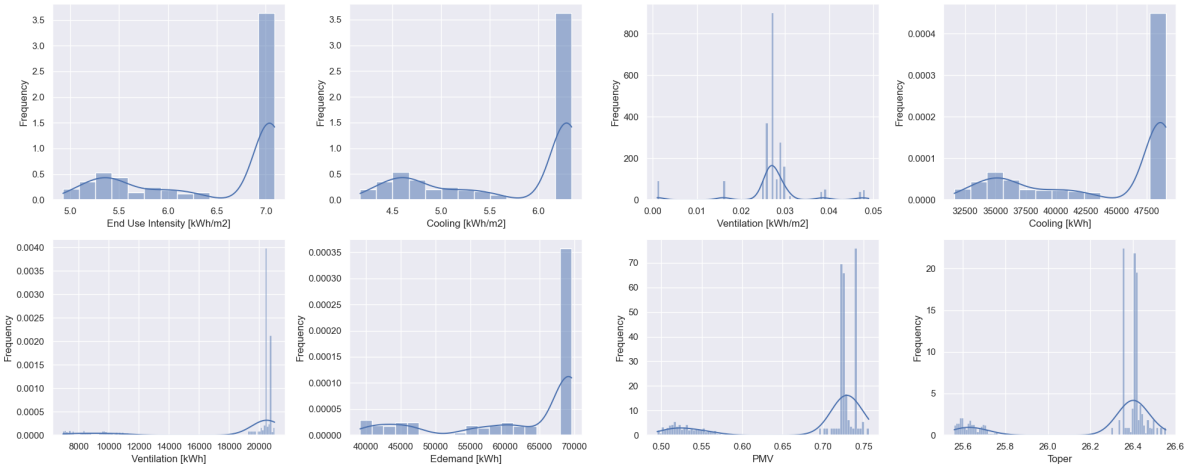

Figure 3.20: Frequency distribution curves of the output results.

The simulation outputs are mapped with distribution curves and hereby the frequency of the simulation outcomes can be depicted. The results of EUI and Cooling (per m^2) have a higher frequency at 7.0 kWh/m^2, while the Ventilation (per m^2) reaches the highest frequency at 0.027kWh/m^2. The

total Cooling demand has a peak at 47500kWh and the energy demand for Ventilation at 20000kWh hence the total energy demand reaches its highest frequency at 67500kWh for the whole duration of the heat-stress period (23-27 Jul). Regarding the metrics of thermal comfort, the PMV reaches a significant frequency at 0.725 and the operative temperature at 26.4°C. Overall, most of the distribution curves form a high peak at the right edge of the graph because of the total number of simulation results (3.20). As mentioned in section 3.3.2, the six simulation models run simultaneously in the computers of the VRlab, however, the whole process crashed and 3470 results were produced instead of the 16250 that were scheduled.

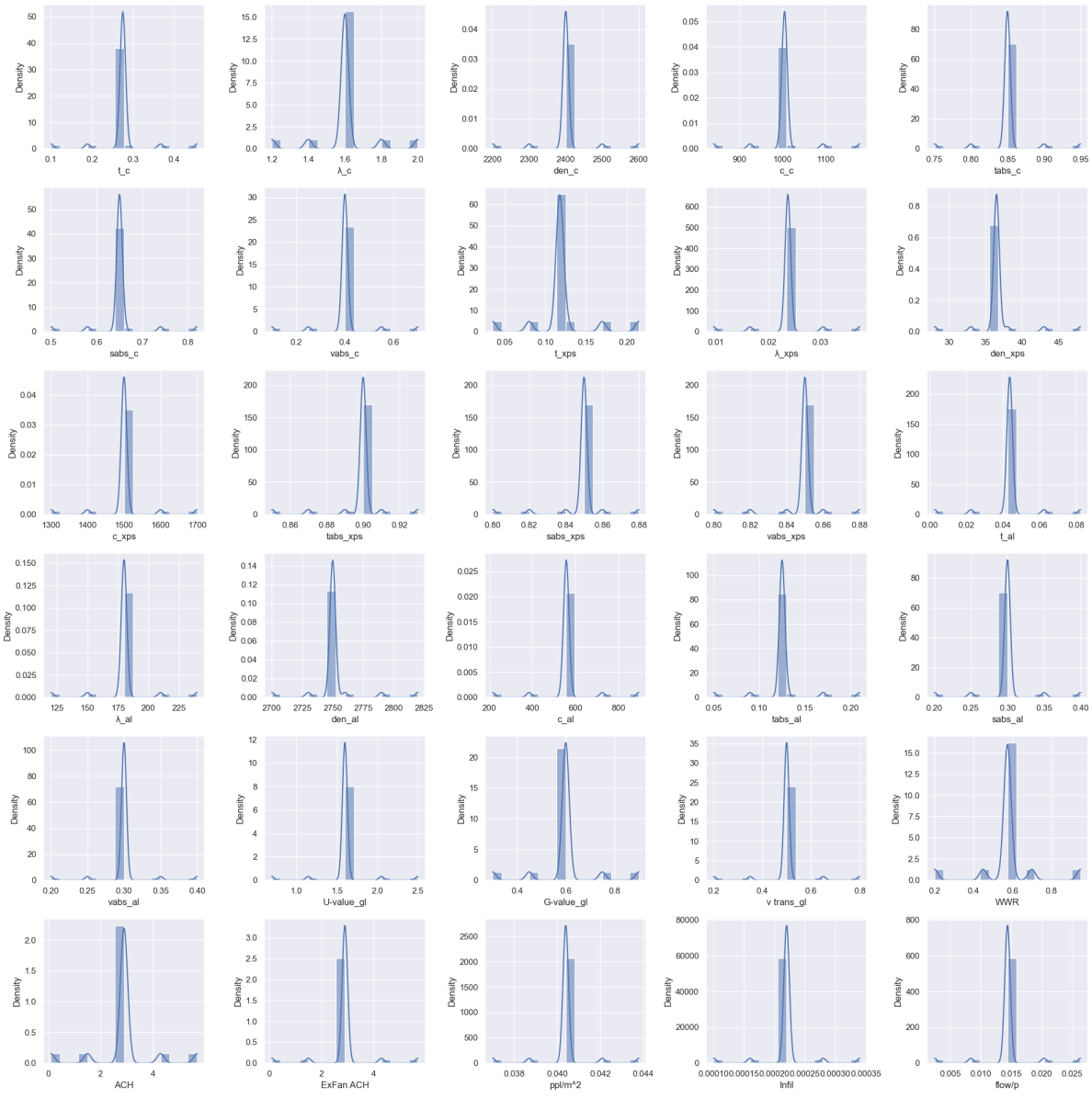

Figure 3.21: Density distribution curves of the input variables.

All in all, the distribution curves for both input variables and simulation outputs map the whole process and give valuable information for the probability of the results. Although the simulation results are incomplete, the frequency distribution curves formed their highest values and they started to decline

(right edge of the curves). Therefore, the workflow indicates the probability of the computed results since the rest of them, that are aborted, would have a lower probability.

3.6. Resilience Quantification

As mentioned in section 2.1, the thermal resilience indicators and their metrics must be clarified in order to quantify the thermal resilience in buildings against overheating stresses. In this thesis, the indicator of indoor operative temperature in relation to the energy demand for cooling and ventilation is calculated by generating hourly results from the simulation model that runs with the assigned EPW file of extreme outdoor temperatures. The whole calculation process is based on the concept of thermal resilience quantification as mentioned in chapter 2.1.3 in the literature review.

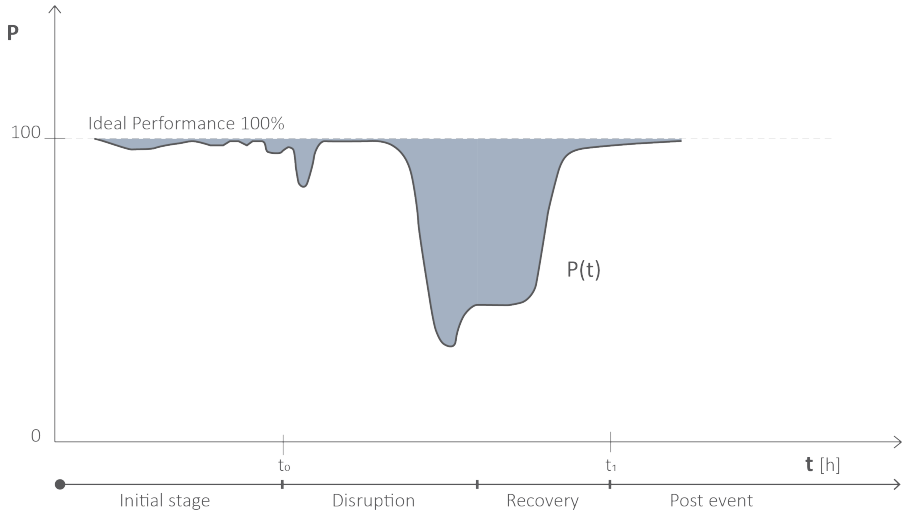

Figure 3.22: Main principle of resilience loss quantification, $R_{Loss} = \int_{t_0}^{t_1} [100 - P(t)]\, dt$.

To quantify the resilience of a system, one commonly used approach is to compare its performance during a hazard with its initial performance before the hazard occurred. However, this approach cannot be directly applied in the context of thermal resilience quantification. This is because simulations of the initial stage would be based on weather data that do not consider extreme temperatures. Using weather data from a typical meteorological year (TMY) is also not a viable option as it would involve comparing different cases. An assumption of ideal building performance is made to address this issue. However, achieving an ideal building performance can not be considered a realistic scenario. Instead, optimised building performance can be used as an ideal reference for quantifying thermal resilience as presented in the chart 3.23. Therefore the common equation for Resilience Loss quantification is adopted and adjusted as follows:

$$R_{Loss} = \int_{t_0}^{t_1} [p_{(t)}^{optimised} - p_{(t)}^{real}]\, dt \tag{3.2}$$

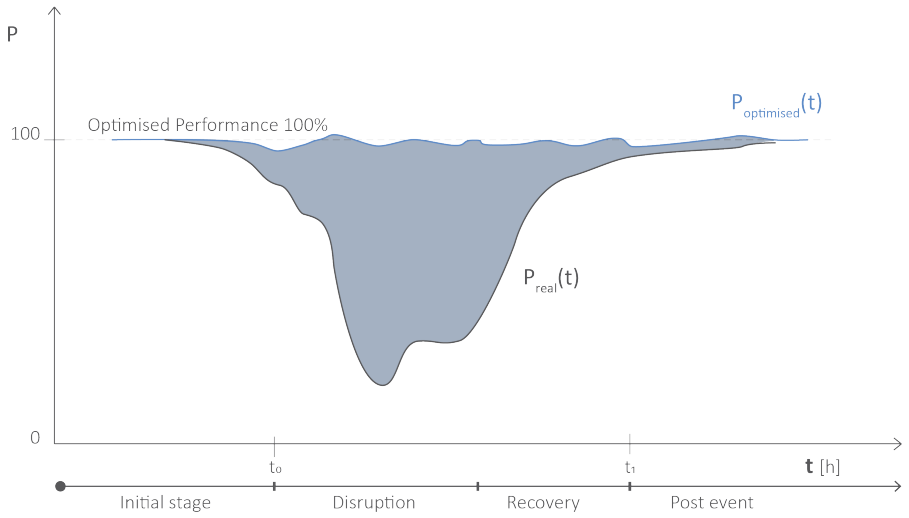

Figure 3.23: Thermal resilience quantification concept that is implemented in this case study.

As mentioned in the section 3.3.2, the calculation of the thermal resilience is based on hourly results of the indoor operative temperature and the energy demand for each thermal zone and hence the entire building can be computed. For the calculation, the temperature values are penalised by a weight factor according to the quantification method of Homaei Homaei $ Hamdy. In the stated manner, the temperature values over a certain comfort threshold are multiplied by a penalty factor. In the following example (3.24), the operative hourly temperatures of the 4th floor of the building are computed during the overheating event. The temperature values reach different levels of comfort. Thus, each value is multiplied with a penalty factor as shown in the table (3.2).

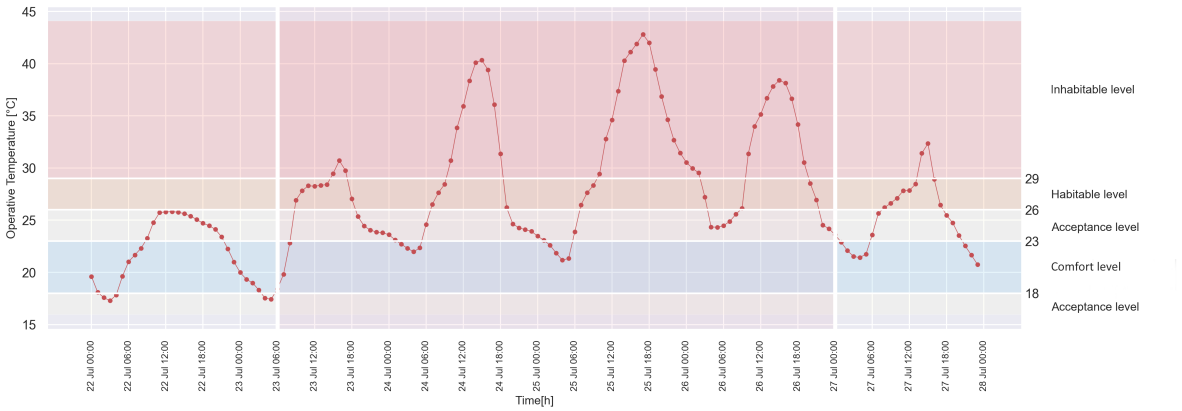

Figure 3.24: The temperature values in relation to the different levels of comfort. These are defined as Comfort, Acceptance, Habitable and Inhabitable

Levels of indoor comfort	Hazard penalty
Comfort	0.1
Acceptance	0.2
Habitable	0.5
Unhabitable	0.7

Table 3.2: Penalty factors that weighted the temperature values during the computing process.

The energy demand is represented by the sum of the energy for cooling and ventilation. Hereupon,

the hourly values of these two calculated metrics are multiplied in order to construct the thermal performance curve (3.3) of this particular building.

$$\mathrm{P}_{(t)} = p^{optimised}_{(t)} - p^{real}_{(t)} \tag{3.3}$$

Where:

$$p_{(t)} = E_{demand(t)} T_{w.oper(t)} \tag{3.4}$$

Optimisation

The simulation model uses the generative algorithm of the WallaceiX plugin that iterates the process until it generates the desired fitness with the result. In this case, the model ran 4970 iterations (15 hours) in order to specify the variables in order to minimise the difference of the hourly temperature values from the 21°C. The main fitness objective for this problem is to minimise the difference between the maximum and the minimum hourly operative temperature values from the indoor comfort threshold of 21°C. The variable values for the optimised case of this building are presented in detail in Appendix D.3. As a result, the hourly temperatures have an initial difference of 24 which is minimised to 10 (3.26) and hence the operative temperature fluctuates between 15°C and 25°C.

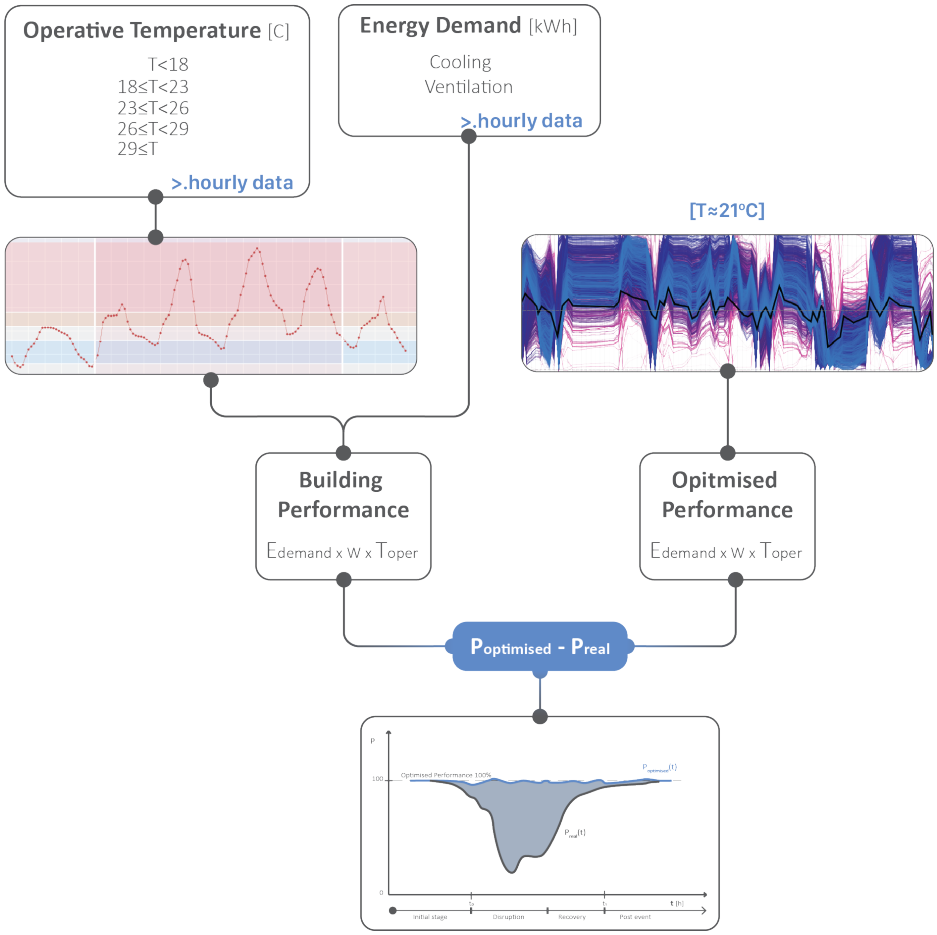

Figure 3.25: Thermal Resilience quantification workflow concept.

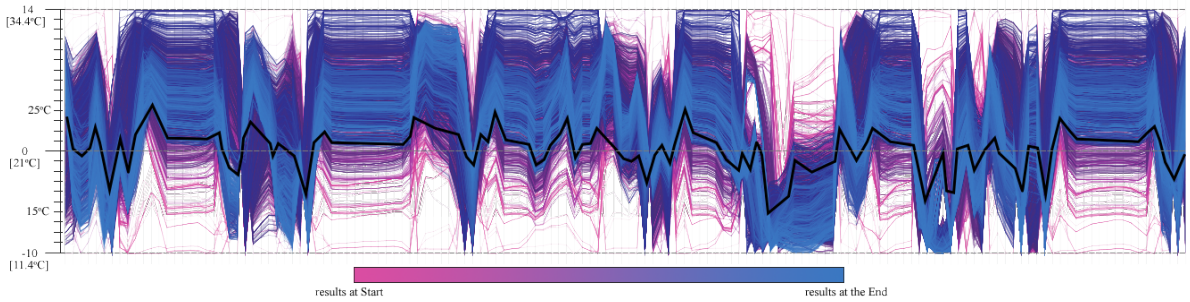

Figure 3.26: Achieved results from the optimisation process in relation to the simulation time. The optimised case was selected among 4970 results. The detailed optimisation process diagram is presented in Appendix C.6.

Overall, the process of resilience quantification for this case study requires a multiple GH component and optimisation engine such as WallaceiX. Moreover, the computed results are extracted from GH to CSV files and they are post-process in Python (See Appendix A.4). However, implementing the whole Python process is attended but compatibility errors occurred. The GH remote plug-in is still a work-in-progress level and it still needs improvement in order to load the required Py libraries for this particular task. However, these optimised results are used for defining the optimised thermal performance of the building and area compared with the actual hourly data for the quantification process. In the next section, the results are presented and comparisons are discussed.

3.6.1. Results Comparison and Discussion

In this section of the report the results are presented. As mentioned in the section 3.3.2 the simulation model is structured with respect to the building discrete thermal zones. Therefore, it is possible to extract values for both individual floors or rooms as well as for the entire building. At this stage of the workflow, the simulation model runs under certain numbers for the building and material parameters. Those were chosen by the outcomes of the SA analysis (see Section 3.5). Hence the effect of the WWR, SHGC, U-value, Visible transmittance, thermal conductivity, density and ACH over the thermal resilience Performance Indicator (PI) is presented hereby. The Resilience Loss is already computed in the results, so the PI indicates the actual resilience performance. The plots include the performance of the building before, during and after the disruption of the overheating event (23^{rd}-26^{th} July).

Results for the whole building

In the beginning, results for the whole building are presented. For this task, the performance curves consist of the average values of operative temperature and energy demand by each floor per hour. The fluctuation of the PI is significant when the WWR values change. As presented in the 3.27 the building performs better at 20% than a higher value of WWR. As the WWR increases, the PI decreases and hence the lowest PI score occurs when the WWR is at 90%.

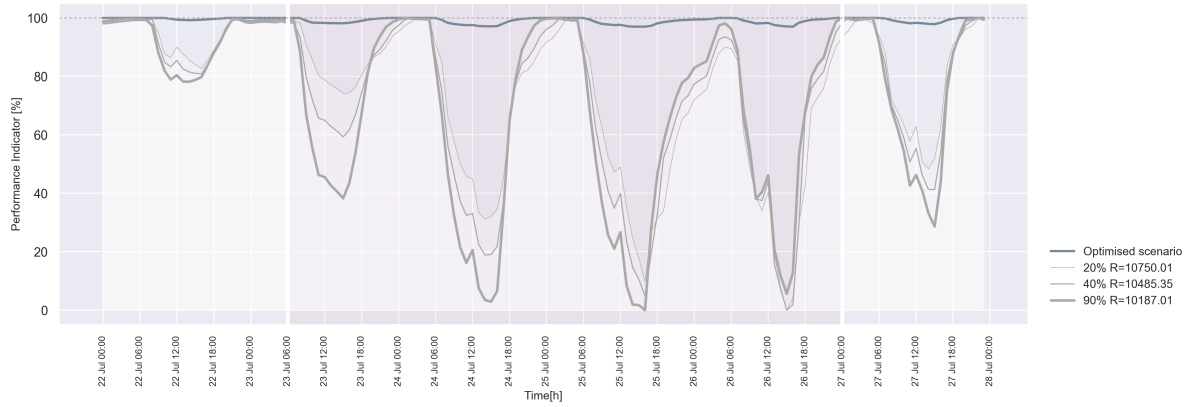

Figure 3.27: Comparison of thermal resilience performance for variant WWR.

The results are quite similar in the case of different SHGC values (3.28). For instance, the PI with an SHGC of 0.30 is higher (10804) than the PI with SHGC of 0.90.

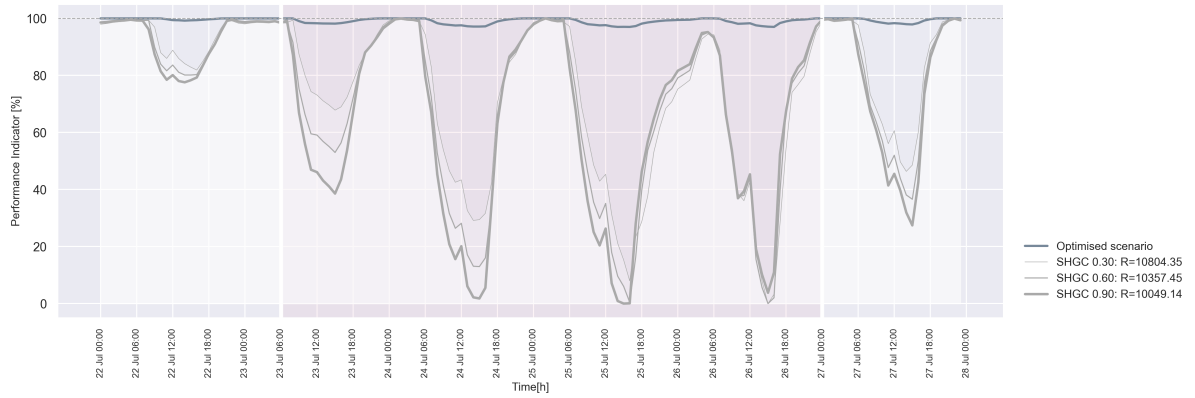

Figure 3.28: Comparison of thermal resilience performance for variant SHGC.

However, the PI changes slightly when the glass U-value changes. In the presented chart (3.29), the resilience performance of 10429 is achieved with a glass U-value of 2.40 (double glazing), while the performance with a glass of U-value of 0.70 (triple glazing) is lower (10278). This result is contradictory to the theoretical background of building physics. The U-value is a measure of how well the glass conducts heat. A lower U-value indicates better insulation properties, meaning less heat is transferred through the glass. Therefore, it is expected to achieve a higher score of PI when the U-value is lower.

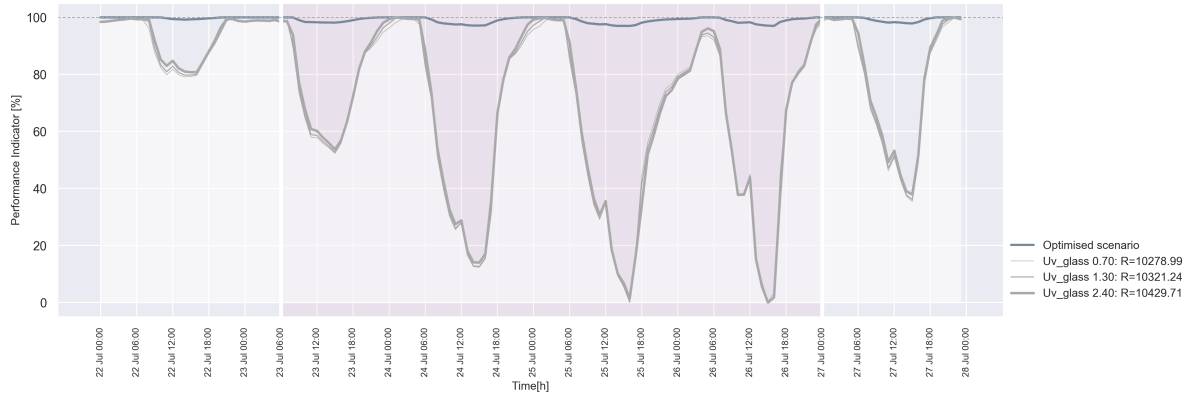

Figure 3.29: Comparison of thermal resilience performance for variant U-values.

Moreover, meaningful insights can be acquired in the case of modifying the air change per hour (ACH) parameter. The simulation run with ACH at 0.01, 1.50, 2.50 and 3.50, as a result, the resilience performance is noticeable. As presented in 3.30, the highest score of 11494 is achieved when the ACH is 3.50, while the lowest is when the ACH is 0.01. In general, the more the ACH increases, the higher the PI score is achieved. This statement holds true since increasing the rate at which indoor air circulates results in a more rapid cooling of the building's spaces. As a result, the indoor temperature is maintained at a more desirable and comfortable level.

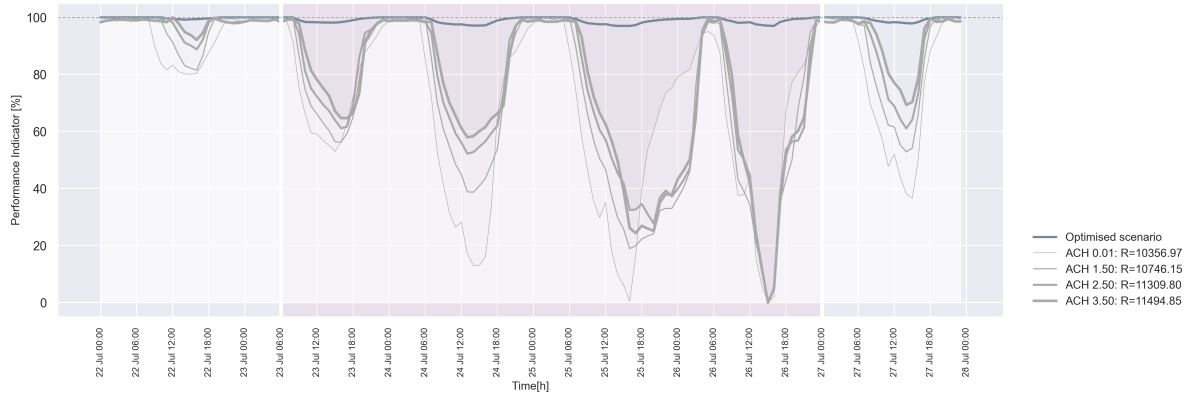

Figure 3.30: Comparison of thermal resilience performance for variant ACH.

Results for each thermal zone

As the whole building is simulated, the results of thermal resilience for each floor and the atrium can be compared to line charts in relation to the time. Valuable data can be extracted by comparing the performance of the ground and the top floor with different ACH values (3.31). In both cases, thermal resilience performance increases by increasing the value of ACH. This fact is reasonable since the higher the ACH value is, the faster the cooled air circulates over the indoor area.

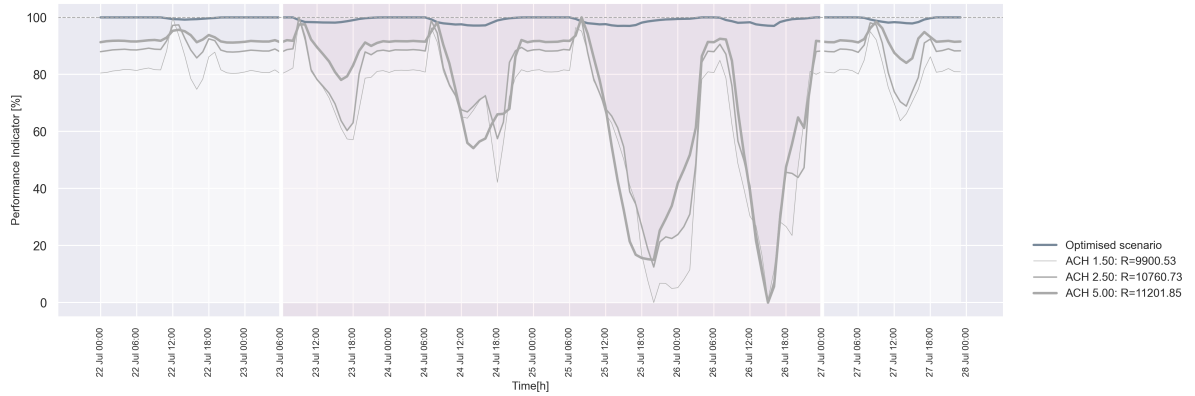

(a) Comparison of thermal resilience performance in the ground floor when the ACH changes.

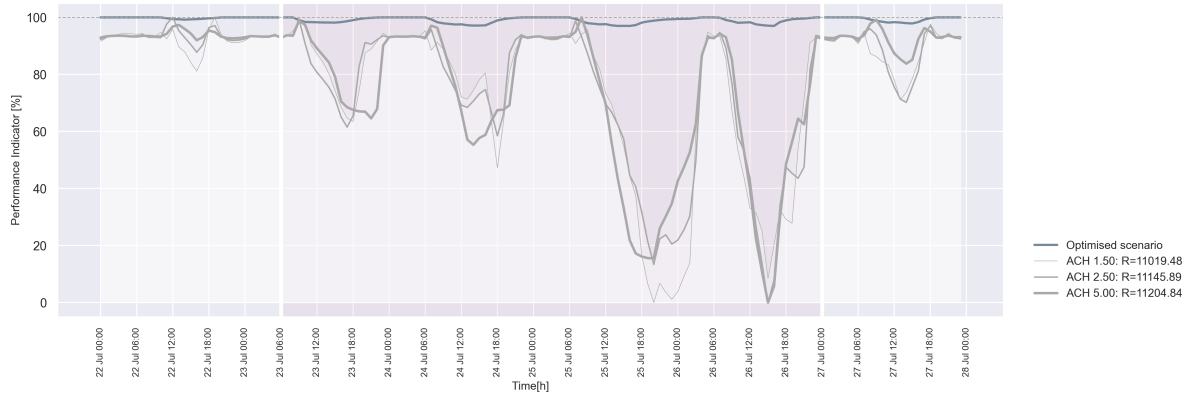

(b) Comparison of thermal resilience performance in the top floor when the ACH changes.

Figure 3.31: Comparison of thermal resilience performance between ground and top floors.

On the other hand, the exhaust fan ventilation parameter does not contribute to the building's performance. The chart 3.32 depicts inconsiderable differences in the performance when the performance of exhaust fan ventilation changes. Although the ventilation system helps the air to flow from indoors to outdoors and hence the passive cooling could be increased. However, the cooling performance and hence the indoor temperature remain the same. This argument is interpreted as right because the exhaust fan circulates the air from indoors to outdoors and it does not improve the cooling performance of the building.

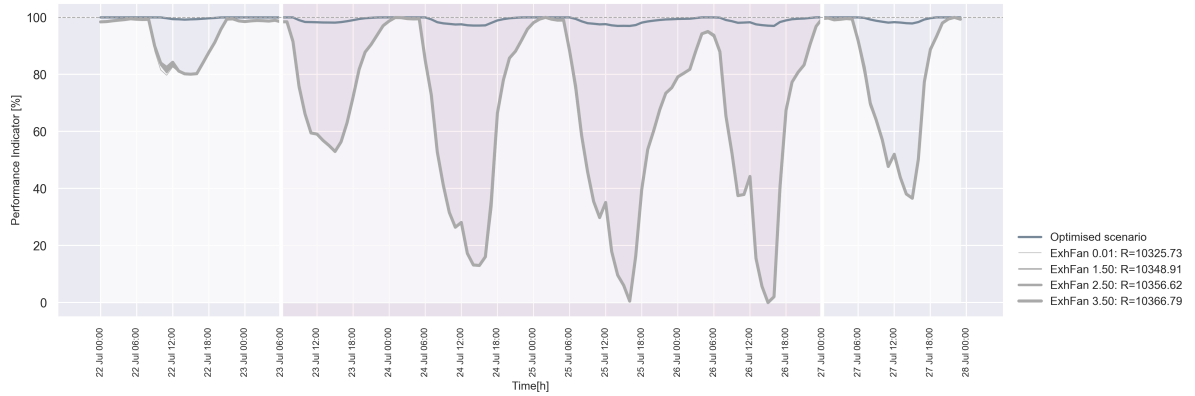

Figure 3.32: Comparison of thermal resilience performance for variant values of exhaust fan ventilation.

By setting all variables are set at their mean values, the performance of the ground floor is significantly higher than the performance of the floors above. More specifically in the chart 3.33 the sum of the Performance Indicator (PI) of the ground floor reaches a score of 9440 while PI of the other floors ranges between 7510 to 7798. However, the lower floors reach a lower PI score compared to the higher floors.

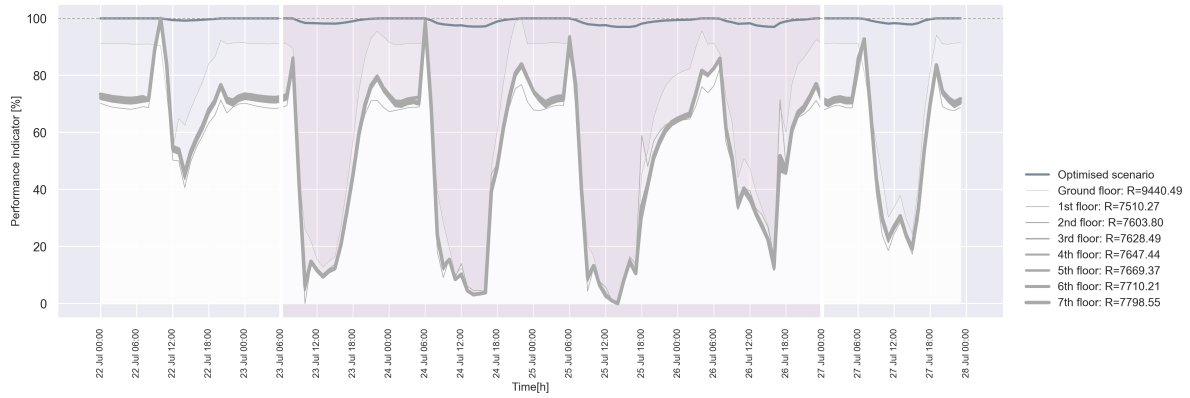

Figure 3.33: Comparison of thermal resilience performance in each floor.

By setting the WWR value to 50% (3.34) the PI is much higher for the ground floor in comparison to the 4^{th} and 8^{th}. The PI in the 4^{th} is lower than to 8^{th} as well.

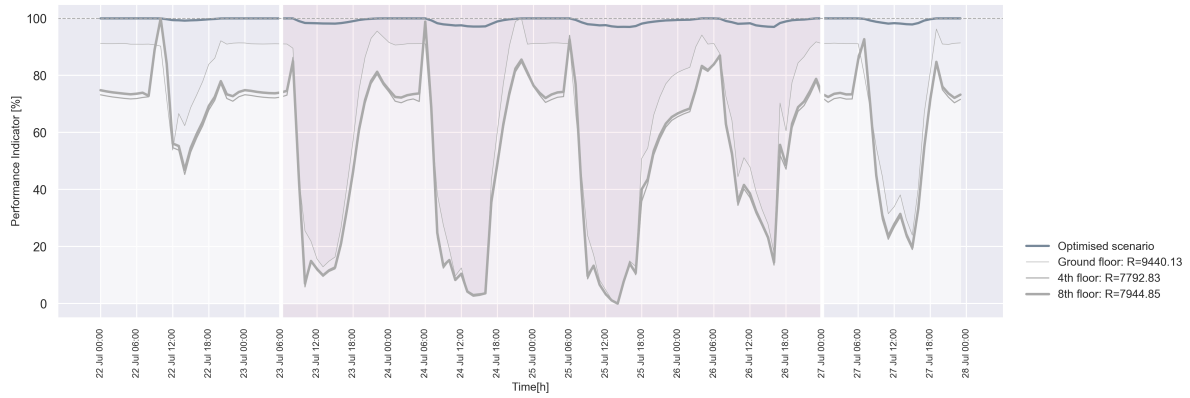

Figure 3.34: Comparison of thermal resilience performance when the wall-window ratio is 50%.

The results are quite similar by changing the values of thermal transmittance of glass (U-value) and solar heat gain coefficient (SHGC). Again the ground floor performs the best from the rest of the other floors and the floors in between score a lower PI in comparison with the roof.

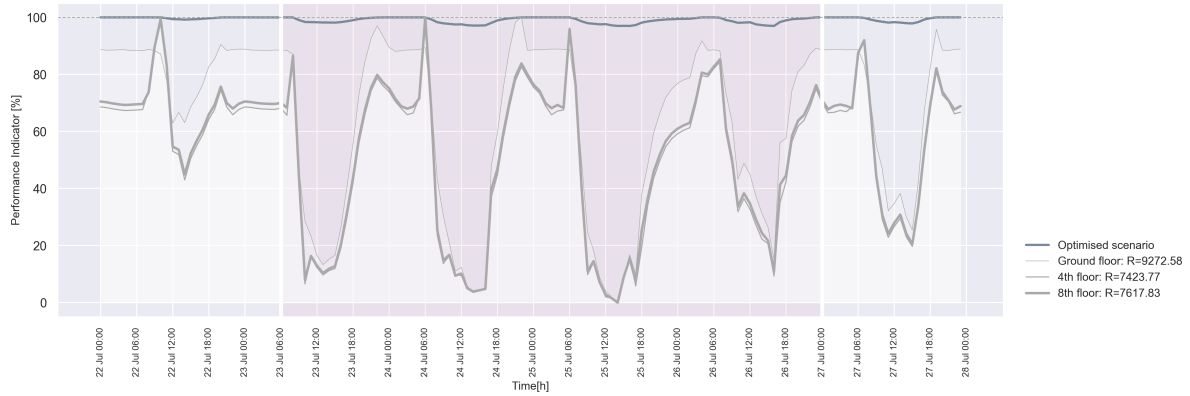

(a) Comparison of thermal resilience performance when the U-value of glass is 0.70.

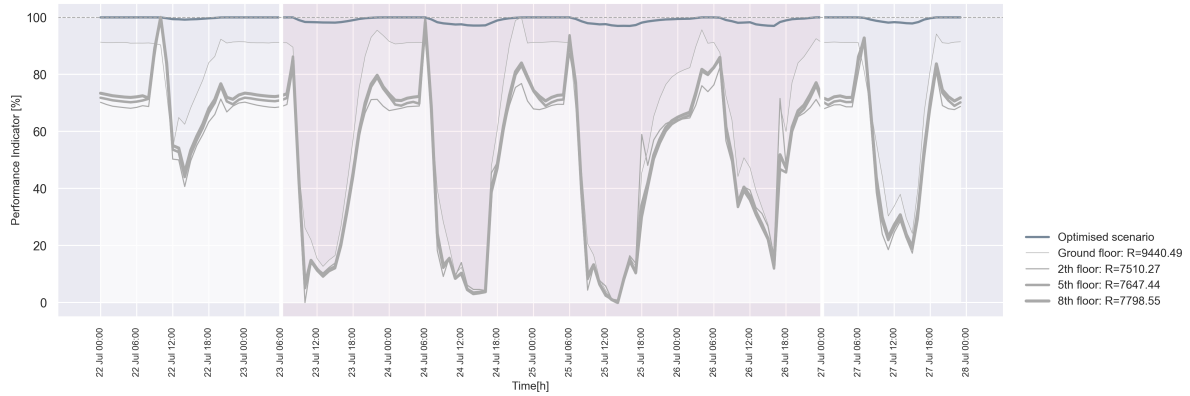

(b) Comparison of thermal resilience performance when the SHGC of glass is 0.60.

Figure 3.35: Comparison of thermal resilience performance between floors.

In the chart 3.36 the thermal resilience of the atrium with the ground floor, the 4^{th} and 8^{th} floors are compared. The difference in the atrium performance is significant in comparison with the others. While the office floors achieve higher PI value the performance of the atrium is almost half. Considering the size of these areas this argument is reasonable. The height of the atrium is equal to the building height and hence the air volume of this thermal zone is much larger. As a result, the air changes much slower than the regular office floors, thus the cooling system supports better smaller areas.

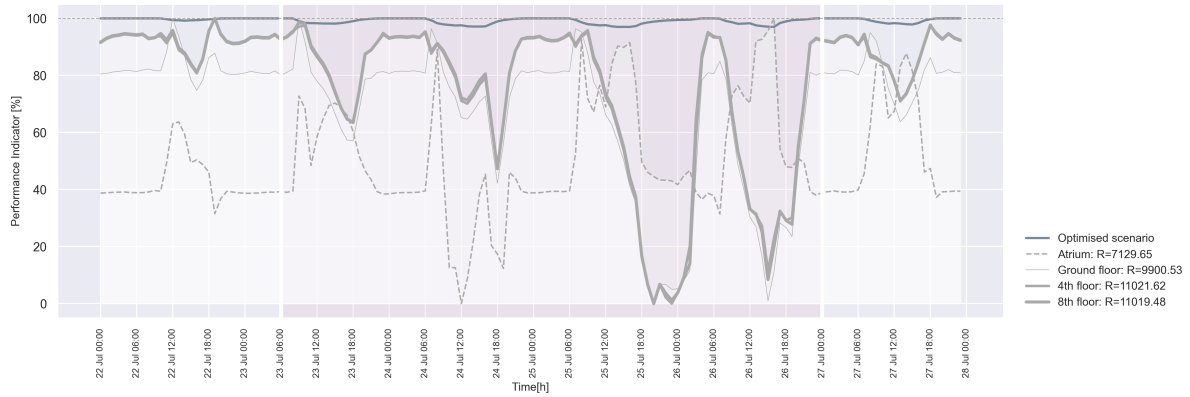

Figure 3.36: Comparison of thermal resilience performance in office floors and the atrium.

This fact can be clearly depicted in the chart 3.37. The PI of the atrium increases significantly

when a higher value is assigned to the ACH parameter. As a result, by doubling the ACH parameter the atrium reaches a noticeable performance of thermal resilience and recovers faster from the overheat stress.

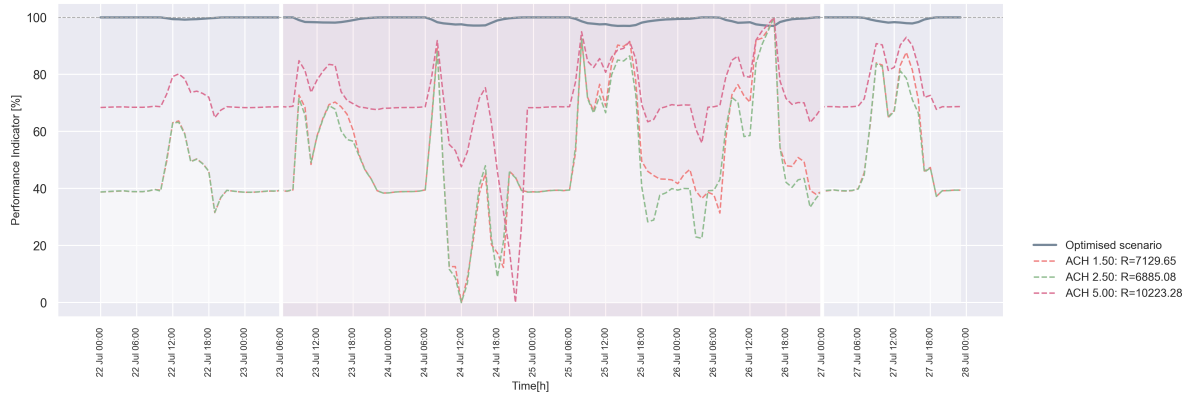

Figure 3.37: Comparison of thermal resilience performance in the atrium for variant ACH values.

Results Discussion

Overall, the building performance, in terms of thermal resilience, changes significantly when different values of ACH are applied. As presented in the bar chart below (3.38), the building performance reaches a peak at the higher value of ACH, while it fluctuates slightly when the WWR, the SHGC and the U-value change. In contrast, the building performance remains almost the same when the variables of ExFan, concrete conductivity, density, thickness and thermal insulation thickness and specific heat capacity change.

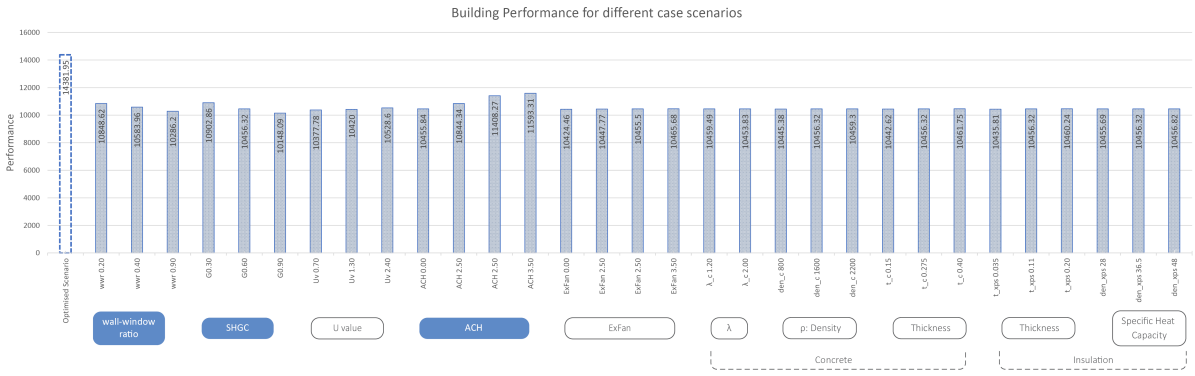

Figure 3.38: Overview comparison of thermal resilience performance for this case study.

Moreover, valuable insights can be obtained from the thermal resilience evaluation for each building's thermal zone. As indicated in the following chart (3.39), the ground floor achieves better performance in comparison with the rest of the floors. This is a reasonable result considering that the ground floor has a higher R-value and is protected by the floors above from extreme indoor temperatures. The performance of the top floor is slightly higher than the rest of the floors in between. However, the highest performance value is indicated in the thermal zone of the main cores of the building.

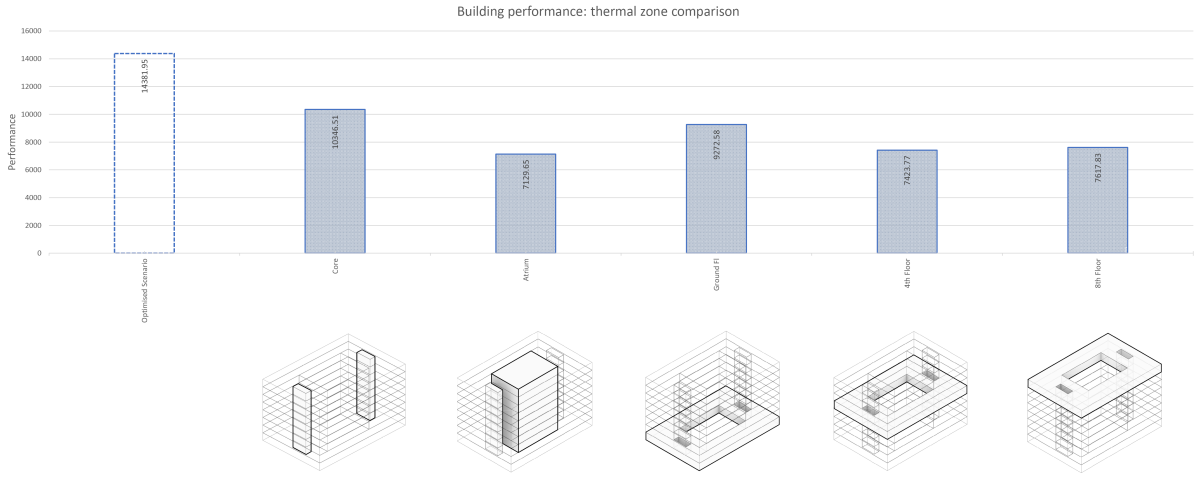

Figure 3.39: Overview comparison of thermal resilience performance among different thermal zones.

On the other hand, the central atrium performs worse than the rest thermal zones. This statement appears to be reasonable, given that the central atrium's volume is considerably larger than the other thermal zones. As a result, cooling the air in the central atrium becomes more challenging, leading to difficulties in reducing the hourly Operative Temperature values. Although this can be accomplished by increasing the ACH, the result would be to increase the hourly energy demand which affects the final thermal resilience result.

4

Conclusion & Discussion

Valuable insights about thermal resilience in buildings and concluding remarks about this research are presented in this chapter. Sub-questions and the main research question are answered and discussed below. Moreover, suggestions for further development are mentioned in the second part.

4.1. Introduction

This graduation project focused on developing a dynamic quantification framework and workflow for assessing the thermal resilience of buildings against extreme overheating case scenarios. The main fields of thermal resilience definition, weather data sets, early design support, dynamic modelling and uncertainty quantification formed the main core of the research and were explored extensively with the main goal to gain theoretical knowledge and implement it in practice.

Thermal resilience is a complex property that necessitates the involvement of multiple scientific fields to develop an effective quantification framework and obtain accurate results. The main core of a multidisciplinary team should include experts from building physics, climate science, and computational science. Furthermore, the field of material science and building systems can significantly enhance the overall work and yield high-quality outcomes.

In the context of extreme temperatures, weather data plays a vital role in this research. Historical heatwave data from Amsterdam was utilized in this case study; however, for a more comprehensive evaluation of thermal resilience in buildings, climate change scenarios should be considered. By incorporating potential future overheating scenarios, it becomes possible to predict building performance using more reliable data. This process involves weather data prediction, which necessitates deep knowledge of climate modelling and advanced skills in handling large datasets. Consequently, this process requires substantial computational resources.

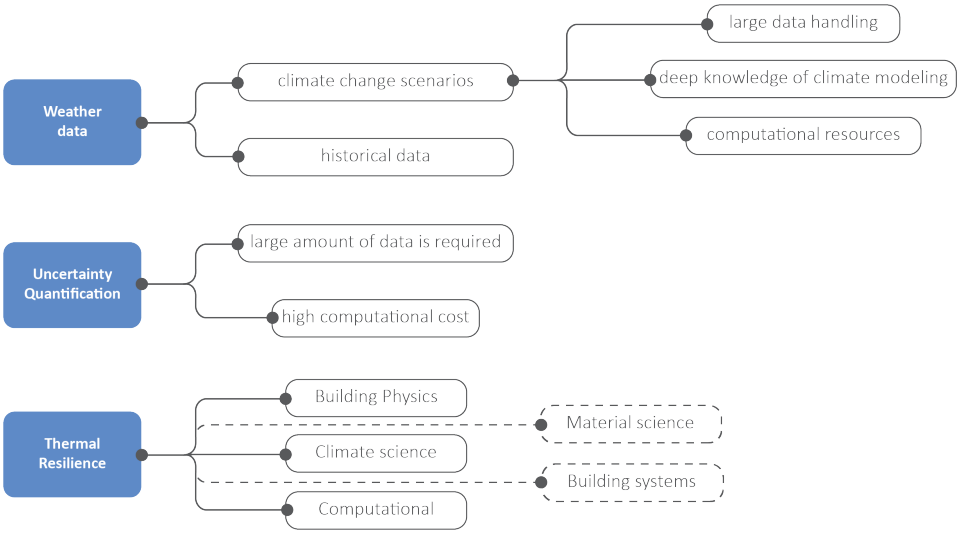

Figure 4.1: First concluding remarks about this research.

Since the early design stage involves varying material and building properties, and considering the variable scenarios associated with climate change, the field of uncertainty becomes closely intertwined with the main topic. It is crucial for assessing scenarios with higher probability and providing a comprehensive understanding of potential building performance. To achieve these results, a significant amount of data is required to encompass the entire range of possible scenarios. Consequently, the process demands substantial resources and incurs a high computational cost.

4.2. Sub-questions

What are the thermal resilience definition and its indicators?

The definition of thermal resilience lies in the performance of a building to be adequate enough against overheating hazards in order to overcome these hazards and mitigate the impact of extreme events. More specifically, thermal resilience is the capability of the building to absorb, adapt and recover from disruptive events. This assertion is based on the characteristics of a building's robustness, resistance, and recovery, which collectively define the primary phases involved in assessing the thermal resilience of a building. Robustness refers to the ability of a building to withstand various disturbances or stresses without suffering significant damage or performance degradation. Resistance, on the other hand, refers to the capacity of a building or its elements to resist the penetration of external factors (e.g. extreme heat) that may disrupt the desired thermal conditions. Recovery refers to the ability of a building to recover or restore thermal comfort and functionality after a disruption or disturbance. It is closely related to the concept of robustness but with a focus on the post-event response. In summary, robustness relates to the ability to withstand and adapt to disturbances, while resistance focuses on preventing or minimizing the impact of external factors on the thermal performance of the building, and recovery is the process of restoring normal thermal conditions after a disruption.

Assessing the thermal resilience of buildings requires the use of specific Key Performance Indicators (KPIs) that measure various aspects related to thermal performance and resilience. Indoor thermal comfort is considered as determinant KPI and is related to the levels of temperature, heat and humid-

ity indoors. Moreover, monitoring the energy demand for cooling or heating, in this case, cooling, is a crucial KPI for the evaluation framework. This KPI assesses the energy required for heating and cooling in the building. Lower demand indicates better thermal resilience, as it signifies the building's ability to maintain comfortable temperatures with minimal energy consumption. Nonetheless, it is important to differentiate between energy performance and the concept of energy efficiency. The former considers the overall energy performance of the building, while the latter aims to optimise the energy performance, reduce waste and achieve the desired outcome by using the least amount of energy.

Which metrics should be quantified in order to evaluate a building's thermal performance?

Metrics such as Heat Index (HI), Humidex (H), Standard Effective Temperature (SET), Predicted Mean Vote (PMV), Indoor Overheating Degree (IOD) and Weighted Unmet thermal Performance (WUMTP) are used for assessing the indoor comfort KPI mentioned above. However, each of them has advantages, handicaps and limitations that are presented extensively in the 2.1.3. The HI and the H are considered as applicable to the scope of this research because they neglect the impact of extreme temperatures and the performance of building systems. Moreover, metrics such as passive survivability and thermal autonomy are stated to be simplified because they are only focusing on the thermal performance during the disruptive event. PMV metric is based on heat balance equations and is used for assessing thermal comfort but several limitations are pointed out. Factors, such as local discomfort due to hot or cold surfaces and solar radiation variations. Moreover, this metric defines thermal comfort within a specific range between -3 and +3, which is considered as limited for evaluating thermal comfort. The IOD can be implemented in multi-zoning building studies for calculating the operative temperature but it gives unexpected results in case of extreme outdoor temperatures. The most representative metrics for calculating thermal comfort is the SET and the WUMTP and both of them can be used in whole-building studies by considering multiple parameters. The SET is a metric of human response to the thermal environment, hence personal factors of metabolic rate and clothing are incorporated. The WUMTP metric is based on the calculation of the operative temperature, in which the impact of air, radiant temperatures and the building elements and systems is incorporated. Moreover, its calculation method embeds the principles of thermal comfort levels and the duration time of stress stages since weighted penalty factors are applied. Therefore, this metric can be applied in order to evaluate the thermal comfort indoors before, during and after the disruptive event.

Quantification metrics such as the End Use Intensity (EUI), and the Total Energy Consumption are required for the evaluation of energy demand. The EUI measured the energy consumption per square meter of building area, as a result, comparisons between different buildings, designs and sizes can be made. The Total energy consumption represents the overall energy consumed by the building over a certain time period. It combines the energy usage for heating, cooling, lighting, equipment and other building systems. In this research, these metrics are adjusted in case of overheating stresses and focused on the cooling and ventilation demand for the whole building.

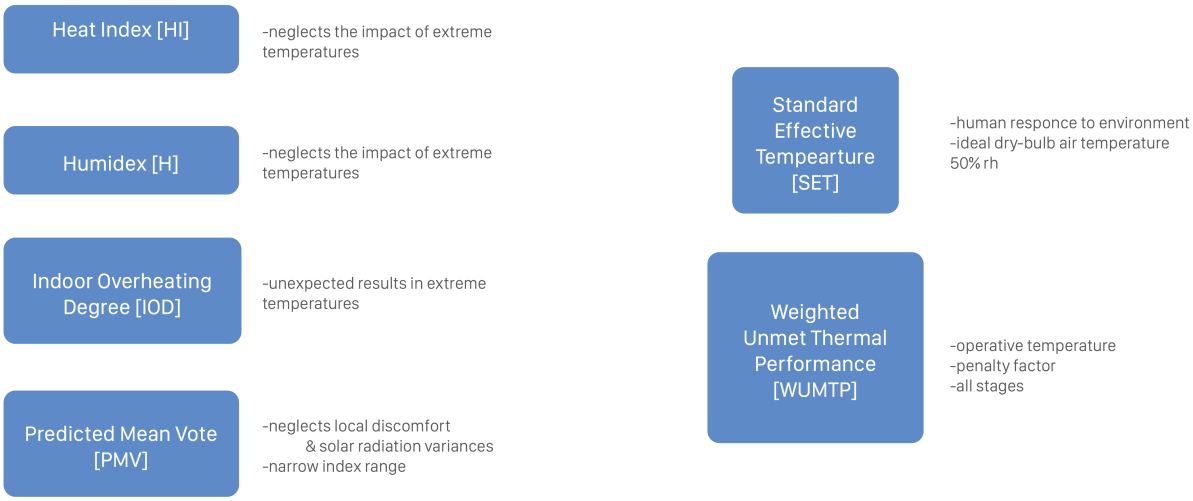

Figure 4.2: Comparison of different thermal metrics that have been researched in this thesis.

What kind of weather data sets are suitable for thermal resilience quantification against extreme overheating hazards?

Weather data that consider RCPs climate change scenarios and extreme values of temperatures can be used in order to assess the thermal resilience in buildings. The RCPs are climate scenarios that are based on the potential increase of temperature and Greenhouse Gas (GHG) emissions in the future. Subsequently, estimations for the building performance in future scenarios can be calculated. However, the computational process includes dynamic or statistical downscaling of Global Climate to Regional Climate models with respect to the RCPs. This process requires a large number of computational resources and high-skill knowledge in the field of climate modelling because of its complexity.

Alternatively, weather EPW files that are based on historical datasets can be used. In this approach, the historical data with extreme values of climate parameters, such as temperature and solar radiation, must be included in a common TMY file that is used as a basis. For this research historical data from extreme heat waves have occurred in Europe in 2003, 2019 and 2020 are obtained from KNMI and used for generating an EPW that includes the highest values of climate parameters.

How uncertainty quantification can be implemented in the computational workflow?

Implementing UQ in the computational workflow requires careful consideration of the specific problem, available data, and computational resources. It involves a combination of statistical techniques, sampling methods, model evaluations, and analysis to comprehensively capture and characterize the uncertainty in the computational model's predictions. The UQ can be implemented in the computational workflow through the techniques of problem formulation, uncertainty characterization, sensitivity analysis, sampling techniques, statistical analysis, and calibration of the model. Quantifying the uncertainty associated with the input parameters can be done with statistical analysis of the available data. In this manner, probability distributions are assigned to uncertain parameters in order to specify the range of data within a certain value of probability. Practically, density distribution curves are assigned to the size of each variable and hence the values that are used more times from the model are depicted. Similarly, frequency distribution curves are assigned to the results. Sampling techniques such as Monte Carlo (MC) and Latin hypercube sampling (LHS) can be utilized to generate samples from the input

parameter distributions. These are used for evaluating the simulation model under different scenarios. Sensitivity analysis is used to identify the parameters with the most significant influence on the results. As a result, this process helps to prioritize uncertainties for further analysis.

Which are the major influential parameters that affect the building's performance against extreme overheating?

The main influential parameters that affect the building's performance are building properties related to the building envelope and unitized systems. Sensitivity analysis reveals that parameters such as conductivity and density of concrete, thickness and specific heat capacity of thermal insulation have a relatively minor impact on the results. However, the final results of thermal resilience quantification revealed that the PI remained constant when these values change. Conversely, parameters related to glazing and cooling systems have a significant influence. Specifically, the percentage of glazing (WWR) on the facade and the thermal properties of the glass (U-value, SHGC, Visible transmittance) play a crucial role in determining the building's thermal performance. Additionally, the air change per hour (ACH) is also a critical factor for the building's overall performance.

4.3. Main research question

In what manner can a digital design workflow be devised to assess the thermal resilience of buildings against extreme heat wave stresses, and how can this workflow support designers and engineers during the initial stages of the design process in making informed decisions?

A digital workflow can be devised to assess the thermal resilience of buildings against extreme heat waves in the following manner:

Data Integration: Climate data including historical and extreme weather patterns should be integrated into the workflow. This provides valuable information about the climate challenges posed by the heat waves of the building's location. As a result, the user can identify the time period of the overheating stress by the indicative peaks of climate parameters (e.g. temperature). Therefore, specific time intervals are designated for running the simulation model.

Computational Modeling: Develop a computational model that simulates the thermal behaviour of buildings under extreme heat wave conditions. These models should consider factors such as building geometry, materials, insulation, glazing, ventilation, and cooling systems. They should accurately simulate energy consumption and indoor thermal comfort. In this thesis, the simulation model was developed in the GH environment where extreme weather patterns are linked with the simulation model. The aforementioned factors of building, material, insulation, glazing, ventilation and cooling systems and complementary Python scripts are incorporated into the model. Subsequently, hourly results were generated for energy consumption and indoor thermal comfort.

Early Design Support: All the factors initially should be defined by literature sources related to the building material properties and ventilation and cooling systems. Therefore, a range of values is assigned to these factors in order to include variant types of material, facade glazing percentage, ventilation and cooling systems.

Uncertainty quantification: UQ involves quantifying the design and/or climate uncertainties of problem inputs in order to indicate their probability to the results. The implementation of this aspect in the early design stage turns the deterministic calculation into a probabilistic way. By reducing these uncertainties, UQ can improve the accuracy and reliability of energy performance predictions, reduce the risk of performance gaps, and support decision-making.

Resilience Assessment - Optimisation: Define indicators and metrics that quantify the thermal resilience of buildings to extreme heat waves. These metrics (e.g. the operative temperature and the energy demand) include parameters like the performance of the cooling systems that should be monitored to evaluate building resilience. In this process, thresholds or performance targets that represent the desired level of resilience should be established. Additionally, implement optimization algorithms within the digital design workflow to identify optimal design solutions that maximize thermal resilience while considering other design constraints and objectives.

Visualization and Comparison: Visualize the simulation results in a user-friendly manner, allowing designers and engineers to comprehend and compare different design alternatives. This facilitates the evaluation of different strategies for enhancing thermal resilience, such as modifications to window-to-wall ratios, insulation thicknesses, shading configurations, and HVAC system specifications.

By following this digital design workflow, designers and engineers can effectively evaluate the thermal resilience of buildings against extreme heat wave stresses and make informed decisions early in the design process. This results in the development of more resilient buildings that can withstand and adapt to the challenges posed by heat waves.

4.4. Recommendations for further research

Based on the conducted research, the findings, and the conclusions presented in the current thesis, there are aspects yet to be determined.

Urban scale

The scope of this study is currently confined to building scale; however, the computational workflow employed can be expanded to encompass urban factors and parameters. These factors can be embedded in a dynamic computational workflow. Urban Heat Island (UHI) effect, refers to the phenomenon of higher temperatures due to human activities such as the high concentration of buildings, roads and infrastructure. Incorporating UHI data the potential impact on building thermal performance can be assessed. Additionally, surrounding Land Use and Urban Layout can affect the airflow patterns (Urban Canyon Effect), shading and the exposure of a building to Solar Radiation.

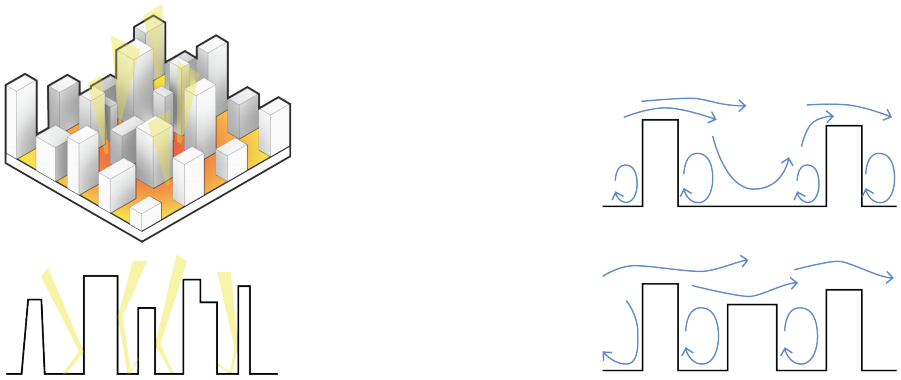

(a) Urban Heat Island effect. **(b)** Urban Canyon Effect

Figure 4.3: Urban factors that can affect thermal resilience of buildings.

Labeling

To further enhance the quantification framework, an additional development could involve the implementation of a labelling system. This system would allow for the classification of buildings based on their thermal resilience index, using distinct colours to differentiate between different levels of resilience. Consequently, buildings could be certified and benchmarked using a system similar to BREEAM and other environmental benchmarking systems. By introducing a labelling system, stakeholders such as building owners, occupants, and investors would have a clear understanding of a building's thermal resilience performance. The use of colours would provide a visual representation of the building's level of resilience, making it easily recognizable and comparable to other certified buildings. This would not only promote transparency and informed decision-making but also encourage the adoption of resilient building practices.

<3.6	RCI		Class A^+
<2.4	RCI	≤ 3.6	Class A
<1.5	RCI	≤ 2.4	Class B
<0.9	RCI	≤ 1.5	Class C
<0.6	RCI	≤ 0.9	Class E
	RCI	≤ 0.6	Class F

Figure 4.4: Classification of buildings according to their Resilience Class Index (Homaei & Hamdy, 2021b).

Alternative assessment method

The thermal resilience assessment for this thesis relies on explicit simulations conducted in Grasshopper and post-processing the results in Python. However, this approach is time-consuming due to complex data handling. An alternative workflow involves structuring the environmental model within a Python environment using the eppy library by EnergyPlus software. This eliminates the need for transferring data between different software. Additionally, implementing machine learning techniques brings significant advantages. By training energy models on historical data, machine learning algorithms can estimate the thermal resilience of buildings. These models learn the relationship between design parameters (e.g., insulation, glazing), weather parameters (e.g., solar radiation, dry-bulb temperature), and thermal performance indicators (e.g., indoor temperature, energy demand), enabling predictions of thermal resilience for different design options at the early stages of the design process, reducing the reliance on extensive simulations. This alternative approach improves efficiency, reduces the computa-

tional burden, and provides valuable insights during the early design stages.

Reinforcement learning (RL) algorithms can assess and enhance thermal resilience by guiding decision-making processes. RL agents interact with the environment (in this case building) over time steps, with defined states, actions, rewards, and goals. Weather data and occupant behaviour serve as initial variables (states), while actions involve adjusting temperature setpoints, shading devices, HVAC systems, and energy usage. The main goal of the agent can be stabilizing indoor temperature within a specific range. A reward function reflects the objective of thermal resilience, aiding the agent in improving thermal resilience indicators through its actions. RL enables the development of strategies that optimize thermal resilience by adapting to changing conditions, ultimately improving the building's ability to withstand temperature extremes (Wang & Hong, 2020).

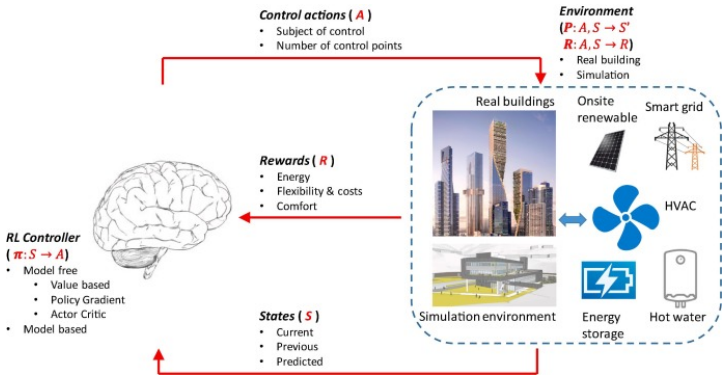

Figure 4.5: The RL agent interacts with the building and improves its performance.

In the case of existing buildings, Convolutional Neural Networks (CNNs) can be employed to analyze thermal images or other thermal data for evaluating thermal resilience (Tijskens et al., 2019). By training a CNN to identify patterns associated with effective shading, natural ventilation, or thermal insulation, valuable insights about thermal resilience can be derived. CNNs are commonly used for image analysis, allowing them to classify images into different categories based on their thermal characteristics. For example, a CNN can be trained to classify images as "comfortable," "moderately overheated," or "extremely overheated." This classification aids in identifying buildings or specific areas that are more susceptible to thermal stress. This approach, combined with the concept of building digital twins, enables real-time monitoring of a building's performance against heatwaves. Engineers can generate and classify thermal images instantly, facilitating ongoing assessment and intervention to improve thermal resilience.

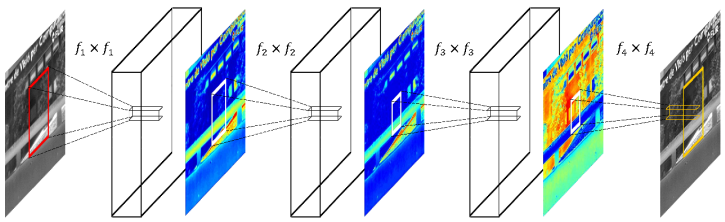

Figure 4.6: CNNs analyse thermal images.

5

Reflection

Graduation process

1. *What is the relation between your graduation project topic, your master track (Ar), and your master programme (MSc)?*

The thesis under discussion encompasses three research domains, primarily focusing on building environmental performance and computational intelligence. These fields form the core of the research, while the field of sustainable structures provides valuable supplementary information to enhance the background knowledge of resilience. Consequently, this research involves the collaboration of two chairs within the Building Technology track: Structural Design and Design Informatics. The thesis is guided by Simona Bianchi and Charalampos Andriotis. Within the chair of Structural Design, the research investigates the resilience of buildings in the face of climate change. Meanwhile, within the chair of Design Informatics, the exploration revolves around implementing resilience quantification in practical applications during the early design stage.

2. *How did your research influence your design/recommendations and how did the design/recommendations influence your research?*

The research initially established a strong theoretical foundation in resilience quantification, uncertainty quantification, and dynamic building simulation. This theoretical knowledge was subsequently applied in the practical implementation phase to bridge theory and practice. This integration of theory formed the basis of the computational workflow and early design support. Simultaneously, the practical implementation yielded valuable insights and information specifically related to the research's main focus on thermal resilience against overheating stresses. The research successfully clarified the significant building, design, and system parameters, and the visualization of simulation results facilitated the comparison of various design alternatives by designers. As a result, the study outcomes contribute to the advancement of research in the field of thermal resilience in buildings.

3. *How did the research approach work out (and why or why not)? And did it lead to the results you*

aimed for? (SWOT of the method).

The research encompassed several essential areas crucial for achieving the desired outcome. The primary objective of this research was to investigate the feasibility of implementing a computational workflow for quantifying thermal resilience against extreme heat events in practical applications. Consequently, a comprehensive analysis was undertaken, exploring five key areas throughout the project. These areas include resilience quantification in the built environment, weather data sets, uncertainty quantification, dynamic environmental building simulation, and statistical modeling. Each area presented its own challenges and complexities, but all were integral to the overarching goal of sustainable structures with computational tools, making each area a crucial component of this thesis project. While each area provided valuable insights, they also revealed numerous avenues for further research, some of which were simplified due to time constraints. The desired outcomes were successfully achieved, resulting in an improved understanding of the impact of extreme heatwaves on buildings. This research also lays the groundwork for enhancing the computational workflow by implementing more efficient tasks and expanding the scope of thermal resilience assessment to a larger scale.

Societal impact

1. *What is the impact of your project on sustainability (people, planet, profit/prosperity)?*

Sustainability was the key parameter that initiated this project's exploration. The topic addresses the problem of building performance during disruptive events posed by climate change. It explores the possibilities to design resilient and sustainable buildings to mitigate the vulnerability of the built environment. The research explores evaluation frameworks and assessment methodologies in order to develop more robust methods and tools to support the development of resilient and sustainable structures at the building level. Following this goal, this project investigates the climate adaptability of buildings through uncertainty-based risk analysis.

2. *What is the socio-cultural and ethical impact?*

The quantification of thermal resilience against extreme heat stresses in buildings has a direct relation to the wider social context. Here are a few key aspects of this relationship:

Human Health and Well-being: Extreme heat events can have severe consequences for human health, leading to heat-related illnesses and even fatalities. By quantifying thermal resilience, building designs can be enhanced to provide improved indoor comfort and mitigate the negative impact of extreme heat on occupants' health and well-being. This directly contributes to the social objective of safeguarding public health.

Climate Change Adaptation and Mitigation: Thermal resilience quantification aligns with the broader societal need for climate change adaptation and mitigation. By designing buildings that can withstand and adapt to extreme heat stresses, communities are better prepared for the changing climate. Additionally, resilient buildings with lower energy demands contribute to reducing greenhouse gas emissions and advancing sustainability goals.

3. *How does the project affect architecture / the built environment?*

Thermal resilience quantification against extreme heat stresses in buildings, utilizing a computational

workflow of dynamic environmental building simulations, has several effects on architecture and the built environment:

Design Optimization: The computational workflow allows architects and designers to evaluate various design alternatives and optimize building designs for thermal resilience. By simulating the thermal performance of different architectural configurations, materials, and systems, the workflow enables the identification of design strategies that enhance thermal comfort and mitigate the impact of extreme heat events. This leads to the creation of buildings that are better adapted to the local climate conditions.

Performance Prediction: The computational simulations provide insights into the thermal behaviour of buildings under extreme heat conditions. This helps architects and engineers understand how different design choices affect thermal performance and resilience. By accurately predicting the indoor temperatures, energy consumption, and thermal comfort levels, the simulations enable informed decision-making and facilitate the development of more effective design strategies.

Risk Mitigation: The simulations allow for the assessment of potential risks associated with extreme heat stresses. By quantifying the thermal resilience, the computational workflow helps identify areas of vulnerability within the building design. This information can be used to implement risk mitigation measures such as improved insulation, shading devices, natural ventilation strategies, or the integration of passive cooling techniques. These measures enhance the building's ability to withstand extreme heat events and protect the occupants.

Sustainability Integration: By incorporating thermal resilience quantification into the design process, the computational workflow promotes the integration of sustainability principles. Design choices that enhance thermal resilience often align with energy efficiency, reduced environmental impact, and enhanced occupant comfort. The workflow allows for the optimization of energy consumption and the development of environmentally responsible building solutions.

References

2022 european heat waves. (2023). https://en.wikipedia.org/wiki/2022_European_heat_waves

Abediniangerabi, B., Makhmalbaf, A., & Shahandashti, M. (2021). Deep learning for estimating energy savings of early-stage facade design decisions. *Energy and AI*, *5*, 100077. https://doi.org/10.1016/j.egyai.2021.100077

Abediniangerabi, B., Shahandashti, S. M., Bell, B., Chao, S. H., & Makhmalbaf, A. (2018). Building energy performance analysis of ultra-high-performance fiber-reinforced concrete (UHP-FRC) façade systems. *Energy and Buildings*, *174*, 262–275. https://doi.org/10.1016/J.ENBUILD.2018.06.027

Abediniangerabi, B., & Shahandashti, M. (2022). Machine Learning Methods for Estimating Energy Performance of Building Facade Systems. In *Handbook of smart energy systems* (pp. 1–31). Springer International Publishing. https://doi.org/10.1007/978-3-030-72322-4{_}112-1

Arup. (2012). *City Resilience Index | Understanding and Measuring City Resilience* (tech. rep.).

Arup. (2015). *Climate Action in Megacities 3.0* (tech. rep.). www.c40.org

ASHRAE, A. (2010). Ashrae standard 55–2010; thermal environmental conditions for human occupancy. *American Society of Heating: Refrigerating, and Airconditioning Engineers, Inc.: Atlanta, GA, USA*.

Attia, S., Holzer, P., Homaei, S., Kazanci, O. B., Zhang, C., & Heiselberg, P. (2022). Resilient Cooling in Buildings – A Review of definitions and evaluation methodologies. *CLIMA 2022 the 14th HVAC World Congress*. https://doi.org/10.34641/clima.2022.195

Attia, S., Levinson, R., Ndongo, E., Holzer, P., Berk Kazanci, O., Homaei, S., Zhang, C., Olesen, B. W., Qi, D., Hamdy, M., & Heiselberg, P. (2021). Resilient cooling of buildings to protect against heat waves and power outages: Key concepts and definition. *Energy and Buildings*, *239*, 110869. https://doi.org/10.1016/j.enbuild.2021.110869

Benardos, A., Athanasiadis, I., & Katsoulakos, N. (2014). Modern earth sheltered constructions: A paradigm of green engineering. *Tunnelling and Underground Space Technology*, *41*, 46–52. https://doi.org/https://doi.org/10.1016/j.tust.2013.11.008

Bennet, I. (2016). Simulation-based evaluation of high-rise residential building thermal resilience. *ASHRAE Transactions*, *122*.

Bianchi, S., Ciurlanti, J., Overend, M., & Pampanin, S. (2022). A probabilistic-based framework for the integrated assessment of seismic and energy economic losses of buildings. *Engineering Structures*, *269*, 114852. https://doi.org/10.1016/J.ENGSTRUCT.2022.114852

Bruneau, M., Chang, S. E., Eguchi, R. T., Lee, G. C., O'Rourke, T. D., Reinhorn, A. M., Shinozuka, M., Tierney, K., Wallace, W. A., & von Winterfeldt, D. (2003). A Framework to Quantitatively Assess and Enhance the Seismic Resilience of Communities. *Earthquake Spectra*, *19*(4), 733–752. https://doi.org/10.1193/1.1623497

C3s releases european state of the climate to reveal how 2019 compares to previous years. (n.d.). https://climate.copernicus.eu/c3s-releases-european-state-climate-reveal-how-2019-compares-previous-years

Cai, S., Zhang, B., & Cremaschi, L. (2017). Review of moisture behavior and thermal performance of polystyrene insulation in building applications. *Building and Environment*, *123*, 50–65. https://doi.org/https://doi.org/10.1016/j.buildenv.2017.06.034

Chan, A. (2011). Developing future hourly weather files for studying the impact of climate change on building energy performance in hong kong. *Energy and Buildings*, *43*(10), 2860–2868.

Chaoui, L. K., & Robert, A. (2009). Competitive cities and climate change. https://www.oecd.org/cfe/regionaldevelopment/44232251.pdf

Cheung, P. K., & Jim, C. (2019). Improved assessment of outdoor thermal comfort: 1-hour acceptable temperature range. *Building and Environment*, *151*, 303–317. https://doi.org/https://doi.org/10.1016/j.buildenv.2019.01.057

Cimellaro, G. P., Reinhorn, A. M., & Bruneau, M. (2010). Framework for analytical quantification of disaster resilience. *Engineering Structures*, *32*(11), 3639–3649. https://doi.org/10.1016/j.engstruct.2010.08.008

Corrado, V., & Mechri, H. E. (2009). Uncertainty and sensitivity analysis for building energy rating. *Journal of Building Physics*, *33*(2), 125–156. https://doi.org/10.1177/1744259109104884

Dhariwal, J., & Banerjee, R. (2015). Naturally ventilated building design under uncertainty using design of experiments. https://doi.org/10.26868/25222708.2015.2527

Dickinson, R., & Brannon, B. (2016). Generating future weather files for resilience. *Proceedings of the international conference on passive and low energy architecture, Los Angeles, CA, USA*, 11–13.

Ekström, T. (2021). *Predicting the energy performance of buildings : a method using probalistic risk analysis for data-driven decision-support.*

Ekström, T., Burke, S., Harderup, L. E., & Arfvidsson, J. (2020). Proposed method for probabilistic risk analysis using building performance simulations and stochastic parameters. *E3S Web of Conferences*, *172*. https://doi.org/10.1051/e3sconf/202017225005

Ekström, T., Sundling, R., Burke, S., & Harderup, L. E. (2021). Probabilistic risk analysis and building performance simulations – Building design optimisation and quantifying stakeholder consequences. *Energy and Buildings*, *252*, 111434. https://doi.org/10.1016/J.ENBUILD.2021.111434

Elhadad, S., & Orban, Z. (2021). A sensitivity analysis for thermal performance of building envelope design parameters. *Sustainability*, *13*(24). https://doi.org/10.3390/su132414018

Factor mapping and metamodelling. (2007). In *Global sensitivity analysis. the primer* (pp. 183–236). John Wiley & Sons, Ltd. https://doi.org/https://doi.org/10.1002/9780470725184.ch5

Favoino, F., Chalumeau, A., & Aquaronne, A. (2022). *Facade Resilience Evaluation Framework. A Qualitative Evaluation Tool To Support Resilient Facade Design Decision Making.* (tech. rep.). https://www.facadetectonics.org/papers/facade-resilience-evaluation-framework#!

Feehan, A., Nagpal, H., Marvuglia, A., & Gallagher, J. (2021). Adopting an integrated building energy simulation and life cycle assessment framework for the optimisation of facades and fenestration in building envelopes. *Journal of Building Engineering*, *43*, 103138. https://doi.org/10.1016/J.JOBE.2021.103138

Gaffen, D. J., & Ross, R. J. (1998). Increased summertime heat stress in the us. *Nature*, *396*(6711), 529–530.

Galanos, T., & Chronis, A. (2022). Time for Change – The InFraRed Revolution: How AI-driven Tools can Reinvent Design for Everyone. *Architectural Design*, *92*(3), 108–115. https://doi.org/10.1002/ad.2821

Giorgi, F. (2006). Regional climate modeling: Status and perspectives. *Journal de Physique IV (proceedings)*, *139*, 101–118.

Graham, L. T., Parkinson, T., & Schiavon, S. (2021). Lessons learned from 20 years of cbe's occupant surveys. *Buildings and Cities*, *2*(1).

Gregory, J., Stouffer, R. J., Molina, M., Chidthaisong, A., Solomon, S., Raga, G., Friedlingstein, P., Bindoff, N. L., Le Treut, H., Rusticucci, M., et al. (2007). Climate change 2007: The physical science basis.

Gueymard, C. A., & duPont, W. C. (2009). Spectral effects on the transmittance, solar heat gain, and performance rating of glazing systems. *Solar Energy*, *83*(6), 940–953. https://doi.org/https://doi.org/10.1016/j.solener.2008.12.012

Hamdy, M., Carlucci, S., Hoes, P. J., & Hensen, J. L. (2017). The impact of climate change on the overheating risk in dwellings—A Dutch case study. *Building and Environment*, *122*, 307–323. https://doi.org/10.1016/j.buildenv.2017.06.031

Heilig, G. K. (2012). World urbanization prospects: The 2011 revision. *United Nations, Department of Economic and Social Affairs (DESA), Population Division, Population Estimates and Projections Section, New York*, *14*, 555.

Homaei, S., & Hamdy, M. (2021a). Developing a test framework for assessing building thermal resilience. *Building Simulation 2021*, *17*, 1317–1324.

Homaei, S., & Hamdy, M. (2021b). Thermal resilient buildings: How to be quantified? a novel benchmarking framework and labelling metric. *Building and Environment*, *201*, 108022. https://doi.org/https://doi.org/10.1016/j.buildenv.2021.108022

Hopfe, C., Hensen, J., & Plokker, W. (2007). Uncertainty and sensitivity analysis for detailed design support [10th International IBPSA Building Simulation Conference (BS 2007), September 3-6, 2007, Beijing, China, BS 2007 ; Conference date: 03-09-2007 Through 06-09-2007]. In Y. Jiang (Ed.), *Proceedings of the 10th ibpsa building simulation conference, tsinghua university, beijing. september 2007* (pp. 1799–1804). International Building Performance Simulation Association (IBPSA).

Hosseini, S., Barker, K., & Ramirez-Marquez, J. E. (2016). A review of definitions and measures of system resilience. *Reliability Engineering & System Safety*, *145*, 47–61.

Howlader, M., Rashid, M., Mallick, D., & Haque, T. (2012). Effects of aggregate types on thermal properties of concrete. *ARPN Journal of Engineering and Applied Sciences*, *7*, 900–907.

Introduction to sensitivity analysis. (2007). In *Global sensitivity analysis. the primer* (pp. 1–15). John Wiley & Sons, Ltd. https://doi.org/https://doi.org/10.1002/9780470725184.ch1

Janssen, H. (2013). Monte-carlo based uncertainty analysis: Sampling efficiency and sampling convergence. *Reliability Engineering & System Safety*, *109*, 123–132. https://doi.org/https://doi.org/10.1016/j.ress.2012.08.003

Jenkins, L. T., Creed, M. J., Tarbali, K., Muthusamy, M., Trogrlić, R. Š., Phillips, J. C., Watson, C. S., Sinclair, H. D., Galasso, C., & McCloskey, J. (2023). Physics-based simulations of multiple natural hazards for risk-sensitive planning and decision making in expanding urban regions. *International Journal of Disaster Risk Reduction*, *84*, 103338.

Jentsch, M. F., Bahaj, A. S., & James, P. A. (2008). Climate change future proofing of buildings—generation and assessment of building simulation weather files. *Energy and Buildings*, *40*(12), 2148–2168.

Katal, A., Mortezazadeh, M., & Wang, L. L. (2019). Modeling building resilience against extreme weather by integrated cityffd and citybem simulations. *Applied Energy*, *250*, 1402–1417.

Kenward, A., & Raja, U. (2014). Blackout: Extreme weather, climate change and power outages. https://assets.climatecentral.org/pdfs/PowerOutages.pdf

KNMI. (2023). http://climexp.knmi.nl/start.cgi

Lovreglio, R., Spearpoint, M., & Girault, M. (2019). The impact of sampling methods on evacuation model convergence and egress time. *Reliability Engineering [?] System Safety*, *185*, 24–34. https://doi.org/10.1016/j.ress.2018.12.015

Manfren, M., James, P. A., & Tronchin, L. (2022). Data-driven building energy modelling–an analysis of the potential for generalisation through interpretable machine learning. *Renewable and Sustainable Energy Reviews*, *167*, 112686.

Marelli, S., Lamas, C., Konakli, K., Mylonas, C., Wiederkehr, P., & Sudret, B. (2022). *UQLab user manual – Sensitivity analysis* (tech. rep.) [Report UQLab-V2.0-106]. Chair of Risk, Safety and Uncertainty Quantification, ETH Zurich,Switzerland.

Marelli, S., Lüthen, N., & Sudret, B. (2022). *UQLab user manual – Polynomial chaos expansions* (tech. rep.) [Report UQLab-V2.0-104]. Chair of Risk, Safety and Uncertainty Quantification, ETH Zurich,Switzerland.

Mehta, P. K., & Monteiro, P. J. M. (2014). *Concrete: Microstructure, properties, and materials* (4th Edition). McGraw-Hill Education. https://www.accessengineeringlibrary.com/content/book/9780071797870

MIT. (2017). https://cshub.mit.edu/

Moazami, A., Nik, V. M., Carlucci, S., & Geving, S. (2019). Impacts of future weather data typology on building energy performance – Investigating long-term patterns of climate change and extreme weather conditions. *Applied Energy*, *238*, 696–720. https://doi.org/10.1016/j.apenergy.2019.01.085

Naboni, E., Natanian, J., Brizzi, G., Florio, P., Chokhachian, A., Galanos, T., & Rastogi, P. (2019). A digital workflow to quantify regenerative urban design in the context of a changing climate. *Renewable and Sustainable Energy Reviews*, *113*, 109255. https://doi.org/10.1016/j.rser.2019.109255

Neale, J., Shamsi, M. H., Mangina, E., Finn, D., & O'Donnell, J. (2022). Accurate identification of influential building parameters through an integration of global sensitivity and feature selection techniques. *Applied Energy*, *315*, 118956. https://doi.org/https://doi.org/10.1016/j.apenergy.2022.118956

Nik, V. M. (2016). Making energy simulation easier for future climate – Synthesizing typical and extreme weather data sets out of regional climate models (RCMs). *Applied Energy*, *177*, 204–226. https://doi.org/10.1016/J.APENERGY.2016.05.107

Nik, V. M., Coccolo, S., Kämpf, J., & Scartezzini, J.-L. (2017). Investigating the importance of future climate typology on estimating the energy performance of buildings in the epfl campus. *Energy Procedia*, *122*, 1087–1092.

Nik, V. M., Perera, A. T. D., & Chen, D. (2021). Towards climate resilient urban energy systems: a review. *National Science Review*, *8*(3), 2021. https://doi.org/10.1093/nsr/nwaa134

Nik, V. M., Perera, A., & Chen, D. (2021). Towards climate resilient urban energy systems: A review. *National Science Review*, *8*(3), nwaa134.

Olesen, B., Kurnitski, J., Moseley, P., Acchiardi, E., Novák, J., Lambert, Y., & Myrup, M. (2018). Aivc | air infiltration and ventilation centre. https://www.aivc.org/download/aivc2018-proceedings.pdf

Operative temperature. (2022). https://en.wikipedia.org/wiki/Operative_temperature

Pachauri, R., & Reisinger, A. (2007). Ipcc fourth assessment report. *IPCC, Geneva*, *2007*.

Panteli, M., Mancarella, P., Trakas, D. N., Kyriakides, E., & Hatziargyriou, N. D. (2017). Metrics and Quantification of Operational and Infrastructure Resilience in Power Systems. *IEEE Transactions on Power Systems*, *32*(6), 4732–4742. https://doi.org/10.1109/TPWRS.2017.2664141

Panteli, M., Trakas, D. N., Mancarella, P., & Hatziargyriou, N. D. (2017). Power Systems Resilience Assessment: Hardening and Smart Operational Enhancement Strategies. *Proceedings of the IEEE*, *105*(7), 1202–1213. https://doi.org/10.1109/JPROC.2017.2691357

Pörtner, H.-O., Roberts, D. C., Masson-Delmotte, V., Zhai, P., Tignor, M., Poloczanska, E., Mintenbeck, K., Alegría, A., Nicolai, M., Okem, A., et al. (2019). Technical summary. *IPCC special report on the ocean and cryosphere in a changing climate. Available: www. ipcc. ch/site/assets/uploads/sites/3/2019/11/04_SROCC_TS_FINAL. pdf.(July 2020)*, 61.

Punzo, V., Ciuffo, B., & Montanino, M. (2014). Sensitivity analysis. https://doi.org/10.1201/b17440

Resilience (engineering and construction). (2023).

Rummukainen, M. (2010). State-of-the-art with regional climate models. *Wiley Interdisciplinary Reviews: Climate Change*, *1*(1), 82–96.

Saltelli, A., Ratto, M., Andres, T., Campolongo, F., Cariboni, J., Gatelli, D., Saisana, M., & Tarantola, S. (2008). *Global sensitivity analysis: The primer*. John Wiley & Sons.

Selvakumar, M., Thangadurai, K., & James, D. (2021). A deep study on aluminum composite panel: Applications, merits, and demerits. https://kalaharijournals.com/resources/SP-Vol.6_55.pdf

Sensitivity analysis. (2023). https://en.wikipedia.org/wiki/Sensitivity_analysis

Sharifi, A., & Yamagata, Y. (2016). Urban Resilience Assessment: Multiple Dimensions, Criteria, and Indicators. *Advanced Sciences and Technologies for Security Applications*, 259–276. https://doi.org/10.1007/978-3-319-39812-9{_}13/TABLES/9

Sheikholeslami, R., & Razavi, S. (2017). Progressive latin hypercube sampling: An efficient approach for robust sampling-based analysis of environmental models. *Environmental Modelling & Software*, *93*, 109–126. https://doi.org/https://doi.org/10.1016/j.envsoft.2017.03.010

Standard deviation. (2023). https://en.wikipedia.org/wiki/Standard_deviation

Steadman, R. G. (1979). The assessment of sultriness. part i: A temperature-humidity index based on human physiology and clothing science. *Journal of Applied Meteorology and Climatology*, *18*(7), 861–873.

Sun, K., Specian, M., & Hong, T. (2020). Nexus of thermal resilience and energy efficiency in buildings: A case study of a nursing home. *Building and Environment*, *177*. https://doi.org/10.1016/j.buildenv.2020.106842

Taborianski, V. M., & Prado, R. T. (2012). Methodology of co2 emission evaluation in the life cycle of office building façades. *Environmental Impact Assessment Review*, *33*(1), 41–47.

Tavakoli, E., O'Donovan, A., Kolokotroni, M., & O'Sullivan, P. D. (2022). Evaluating the indoor thermal resilience of ventilative cooling in non-residential low energy buildings: A review. *Building and Environment*, *222*, 109376. https://doi.org/10.1016/J.BUILDENV.2022.109376

Theodosiou, T. G., Tsikaloudaki, A. G., Kontoleon, K. J., & Bikas, D. K. (2015). Thermal bridging analysis on cladding systems for building facades. *Energy and Buildings*, *109*, 377–384. https://doi.org/https://doi.org/10.1016/j.enbuild.2015.10.037

Tian, W., Heo, Y., Wilde, P., Li, Z., Yan, D., Park, C.-S., Feng, X., & Augenbroe, G. (2018). A review of uncertainty analysis in building energy assessment. *Renewable and Sustainable Energy Reviews*, *93*, 285–301. https://doi.org/10.1016/j.rser.2018.05.029

Tijskens, A., Janssen, H., & Roels, S. (2019). Optimising convolutional neural networks to predict the hygrothermal performance of building components. *Energies*, *12*(20). https://doi.org/10.3390/en12203966

A tool to improve climate resilience of facades. (n.d.). https://www.eocengineers.com/climate-friday-a-tool-to-improve-climate-resilience-of-facades/

U.s. doe. (2022). https://energyplus.net/assets/nrel_custom/pdfs/pdfs_v22.2.0/EngineeringReference.pdf

Vahid, N. M. (2012). Hygrothermal simulations of buildings concerning uncertainties of the future climate. https://publications.lib.chalmers.se/records/fulltext/159222.pdf

Van Steenkiste, T., van der Herten, J., Couckuyt, I., & Dhaene, T. (2018). Sequential sensitivity analysis of expensive black-box simulators with metamodelling. *Applied Mathematical Modelling*, *61*, 668–681. https://doi.org/https://doi.org/10.1016/j.apm.2018.05.023

Variance-based methods. (2007). In *Global sensitivity analysis. the primer* (pp. 155–182). John Wiley & Sons, Ltd. https://doi.org/https://doi.org/10.1002/9780470725184.ch4

Wang, Z., & Hong, T. (2020). Reinforcement learning for building controls: The opportunities and challenges. *Applied Energy*, *269*, 115036. https://doi.org/https://doi.org/10.1016/j.apenergy.2020.115036

Xiao, H., Pei, W., Deng, W., Kong, L., Sun, H., & Tang, C. (2020). A comparative study of deep neural network and meta-model techniques in behavior learning of microgrids. *IEEE Access*, *PP*, 1–1. https://doi.org/10.1109/ACCESS.2020.2972569

Yassaghi, H., & Hoque, S. (2019). An overview of climate change and building energy: Performance, responses and uncertainties. https://doi.org/10.3390/buildings9070166

Yücel, K., Basyigit, C., & Özel, C. (2003). Thermal insulation properties of expanded polystyrene as construction and insulating materials.

Zahra, S., Akbarnezhad, A., Javier, & Xiao, J. (2017). Multi-criteria selection of façade systems based on sustainability criteria. *Building and Environment*, *121*, 67–78. https://doi.org/https://doi.org/10.1016/j.buildenv.2017.05.016

Zeferina, V., Wood, R., Xia, J., & Edwards, R. (2019). Sensitivity analysis of a simplified office building. *Journal of Physics: Conference Series*, *1343*(1), 012129. https://doi.org/10.1088/1742-6596/1343/1/012129

Zhang, C., Kazanci, O. B., Levinson, R., Heiselberg, P., Olesen, B. W., Chiesa, G., Sodagar, B., Ai, Z., Selkowitz, S., Zinzi, M., Mahdavi, A., Teufl, H., Kolokotroni, M., Salvati, A., Bozonnet, E., Chtioui, F., Salagnac, P., Rahif, R., Attia, S., … Zhang, G. (2021). Resilient cooling strategies – A critical review and qualitative assessment. *Energy and Buildings*, *251*, 111312. https://doi.org/10.1016/j.enbuild.2021.111312

Zhou, Y. (2022). Climate change adaptation with energy resilience in energy districts—A state-of-the-art review. *Energy and Buildings*, *279*, 112649. https://doi.org/10.1016/j.enbuild.2022.112649

Zubrzycki, M. (2021). Ashrae handbook fundamentals si. https://www.academia.edu/45155353/ASHRAE_Handbook_Fundamentals_SI

A

Coding

Python and Grasshopper scripts that are used for this case study are presented.

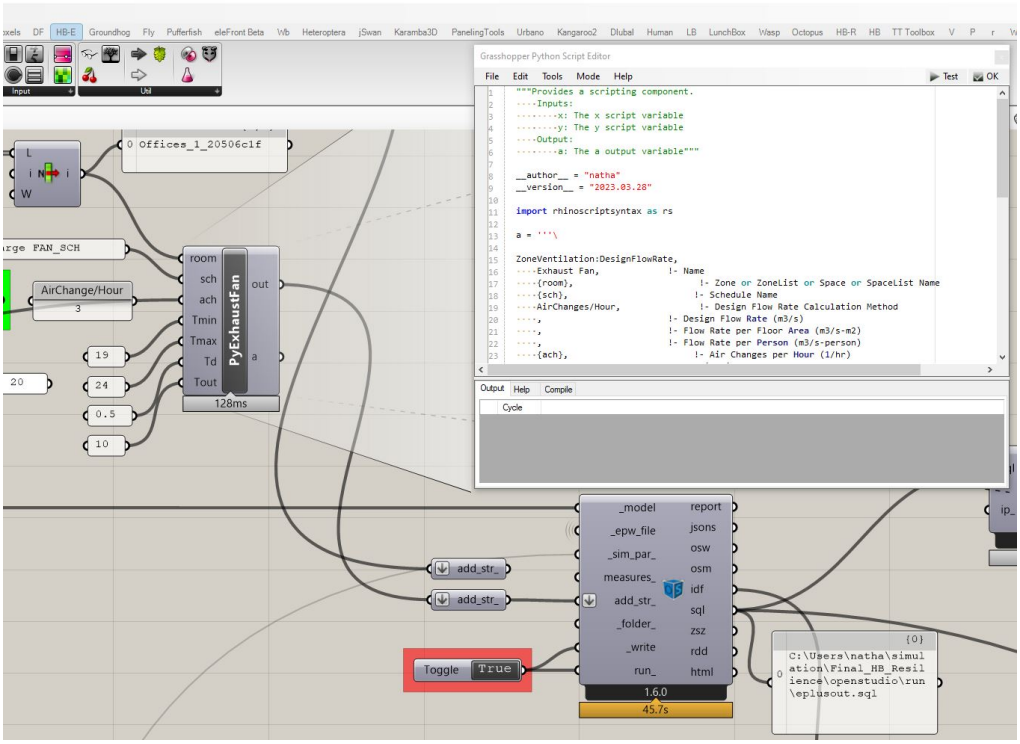

Figure A.1: Complementary Py script enriches the features of the environmental model.

Listing A.1: Add exhaust stystem in GH model.

```
"""Provides a scripting component.
    Inputs:
        x: The x script variable
        y: The y script variable
```

```
    Output:
        a: The a output variable"""
"""
An additional exhaust system in the GH script.
"""
__author__ = "nathanael"
__version__ = "2023.03.28"

import rhinoscriptsyntax as rs
a = '''\

ZoneVentilation:DesignFlowRate,
    Exhaust Fan,              !- Name
    {room},                        !- Zone or ZoneList or Space or SpaceList Name
    {sch},                        !- Schedule Name
    AirChanges/Hour,               !- Design Flow Rate Calculation Method
    ,                         !- Design Flow Rate (m3/s)
    ,                         !- Flow Rate per Floor Area (m3/s-m2)
    ,                         !- Flow Rate per Person (m3/s-person)
    {ach},                       !- Air Changes per Hour (1/hr)
    Exhaust,                  !- Ventilation Type
    650,                         !- Fan Pressure Rise (Pa)
    1,                        !- Fan Total Efficiency
    1,                        !- Constant Term Coefficient
    ,                         !- Temperature Term Coefficient
    ,                         !- Velocity Term Coefficient
    ,                         !- Velocity Squared Term Coefficient
    {Tmin},                     !- Minimum Indoor Temperature (C)
    ,                         !- Minimum Indoor Temperature Schedule Name
    {Tmax},                     !- Maximum Indoor Temperature (C)
    ,                         !- Maximum Indoor Temperature Schedule Name
    {Td},                     !- Delta Temperature (deltaC)
    ,                         !- Delta Temperature Schedule Name
    {Tout},                     !- Minimum Outdoor Temperature (C)
    ,                         !- Minimum Outdoor Temperature Schedule Name
    100,                      !- Maximum Outdoor Temperature (C)
    ,                         !- Maximum Outdoor Temperature Schedule Name
    40;                       !- Maximum Wind Speed (m/s)
    '''.format(room=room,sch=sch,ach=ach,Tmin=Tmin,Tmax=Tmax,Td=Td,Tout=Tout)
print(a)
```

Listing A.2: Sobol' sensitivity analysis with a mathematical model of building physics equations.

```
import pandas as pd
import numpy as np
import seaborn as sns
import scipy as sp
import scipy.stats as stats
from scipy.integrate import odeint
from scipy.integrate import solve_ivp
import matplotlib.pyplot as plt
from SALib.sample import saltelli
from SALib.sample import sobol_sequence
```

```
from SALib.analyze import sobol
import math

# defining a normal distribution given mean and standard deviation
def distribution(mu=0, sigma=1):
    distribution = stats.norm(mu, sigma)
    return distribution

# INDOOR TEMPERATURE CALCULATION
def calc_Tcomfort(X): # Calculate the indoor temperature
    return ((0.60*(((((((X[4]+X[5]+X[6])*X[1]*(0.13+X[7]+X[12]+X[17])+25*X[0]-0.13-X[7]-X
        [12]-X[17]+(X[0]+((X[22]+X[2]*Af*X[1]+X[24]*Qp)/(X[23]+X[2]*Af+X[8]*(Af-X[2]*Af)+X
        [13]*(Af-X[2]*Af)+X[18]*(Af-X[2]*Af)+1.2*1000*X[3]/3600))*(1-math.exp(-((X[23]*X[2]*(
        Af-X[2]*Af)+X[8]*(Af-X[2]*Af)+X[13]*(Af-X[2]*Af)+X[18]*(Af-X[2]*Af)+X
        [3]/3600*1.2*1000)/((Af-X[2]*Af)*(X[9]*X[10]*X[11]+X[14]*X[15]*X[16]+X[19]*X[20]*X
        [21])+Vair*1.2*1000))*t))))/(25*(-0.13-X[7]-X[12]-X[17])+1))-(X[0]+((X[22]+X[2]*Af*X
        [1]+X[24]*Qp)/(X[23]+X[2]*Af+X[8]*(Af-X[2]*Af)+X[13]*(Af-X[2]*Af)+X[18]*(Af-X[2]*Af)
        +1.2*1000*X[3]/3600))*(1-math.exp(-((X[23]*X[2]*(Af-X[2]*Af)+X[8]*(Af-X[2]*Af)+X
        [13]*(Af-X[2]*Af)+X[18]*(Af-X[2]*Af)+X[3]/3600*1.2*1000)/((Af-X[2]*Af)*(X[9]*X[10]*X
        [11]+X[14]*X[15]*X[16]+X[19]*X[20]*X[21])+Vair*1.2*1000))*t))))*0.13))/(0.13+X[8]+X
        [13]+X[18]))+(X[0]+((X[22]+X[2]*Af*X[1]+X[24]*Qp)/(X[23]+X[2]*Af+X[8]*(Af-X[2]*Af)+X
        [13]*(Af-X[2]*Af)+X[18]*(Af-X[2]*Af)+1.2*1000*X[3]/3600))*(1-math.exp(-((X[23]*X[2]*(
        Af-X[2]*Af)+X[8]*(Af-X[2]*Af)+X[13]*(Af-X[2]*Af)+X[18]*(Af-X[2]*Af)+X
        [3]/3600*1.2*1000)/((Af-X[2]*Af)*(X[9]*X[10]*X[11]+X[14]*X[15]*X[16]+X[19]*X[20]*X
        [21])+Vair*1.2*1000))*t))))+(X[8]+X[13]+X[18])*(X[0]+((X[22]+X[2]*Af*X[1]+X[24]*Qp)/(
        X[23]+X[2]*Af+X[8]*(Af-X[2]*Af)+X[13]*(Af-X[2]*Af)+X[18]*(Af-X[2]*Af)+1.2*1000*X[3]))
        *(1-math.exp(-((X[23]*X[2]*(Af-X[2]*Af)+X[8]*(Af-X[2]*Af)+X[13]*(Af-X[2]*Af)+X[18]*(
        Af-X[2]*Af)+X[3]/3600*1.2*1000)/((Af-X[2]*Af)*(X[9]*X[10]*X[11]+X[14]*X[15]*X[16]+X
        [19]*X[20]*X[21])+Vair*1.2*1000))*t)))/(0.60+X[8]+X[13]+X[18])-X[0])

# INDOOR TEMPERATURE CALCULATION BACK-UP
# def calc_Tcomfort(X): # Calculate the indoor temperature
    # return ((0.60*(((((((Aabs_c+Aabs_x+Aabs_al)*SOLrad*(0.13+Rc+Rx+Ral)+25*Te-0.13-Rc-Rx-
        Ral+(Te+((Gg+WWR*Af*SOLrad+ppl*Qp)/(Ug+WWR*Af+Uc*(Af-WWR*Af)+Ux*(Af-WWR*Af)+Ual*(Af-
        WWR*Af)+1.2*1000*n))*(1-math.exp(-((Ug*WWR*(Af-WWR*Af)+Uc*(Af-WWR*Af)+Ux*(Af-WWR*Af)+
        Ual*(Af-WWR*Af)+n*1.2*1000)/((Af-WWR*Af)*(dc*denc*cc+dx*denx*cx+dal*denal*cal)+Vair
        *1.2*1000))*t))))/(25*(-0.13-Rc-Rx-Ral)+1))-(Te+((Gg+WWR*Af*SOLrad+ppl*Qp)/(Ug+WWR*Af
        +Uc*(Af-WWR*Af)+Ux*(Af-WWR*Af)+Ual*(Af-WWR*Af)+1.2*1000*n))*(1-math.exp(-((Ug*WWR*(Af
        -WWR*Af)+Uc*(Af-WWR*Af)+Ux*(Af-WWR*Af)+Ual*(Af-WWR*Af)+n*1.2*1000)/((Af-WWR*Af)*(dc*
        denc*cc+dx*denx*cx+dal*denal*cal)+Vair*1.2*1000))*t))))*0.13))/(0.13+Uc+Ux+Ual))+(Te
        +((Gg+WWR*Af*SOLrad+ppl*Qp)/(Ug+WWR*Af+Uc*(Af-WWR*Af)+Ux*(Af-WWR*Af)+Ual*(Af-WWR*Af)
        +1.2*1000*n))*(1-math.exp(-((Ug*WWR*(Af-WWR*Af)+Uc*(Af-WWR*Af)+Ux*(Af-WWR*Af)+Ual*(Af
        -WWR*Af)+n*1.2*1000)/((Af-WWR*Af)*(dc*denc*cc+dx*denx*cx+dal*denal*cal)+Vair
        *1.2*1000))*t))))+(Uc+Ux+Ual)*(Te+((Gg+WWR*Af*SOLrad+ppl*Qp)/(Ug+WWR*Af+Uc*(Af-WWR*Af
        )+Ux*(Af-WWR*Af)+Ual*(Af-WWR*Af)+1.2*1000*n))*(1-math.exp(-((Ug*WWR*(Af-WWR*Af)+Uc*(
        Af-WWR*Af)+Ux*(Af-WWR*Af)+Ual*(Af-WWR*Af)+n*1.2*1000)/((Af-WWR*Af)*(dc*denc*cc+dx*
        denx*cx+dal*denal*cal)+Vair*1.2*1000))*t)))/(0.60+Uc+Ux+Ual)-Te)


Af = 504 # The total facade surface [m2]
Qp = 105 # exposed energy/person [W]
t = 3600*1 # duraction of calculation [s]
```

```
Vair = 4158 # Volume of the room [m3]

# BUILDING - WEATHER VARIABLES
X[0] : Te # initial outdoor temperature of the problem [C]
X[1] : SOLrad # solar radiation [W/m2K]
X[2] : WWR # wall-window ration of the facade [%]
X[3] : n # airchange rate [m3/s]

# OCCUPANCY VARIABLE
X[24] : ppl # number of people using the building

# MATERIAL VARIABLES
X[4] : Aabs_c # absorbance coefficient concrete
X[5] : Aabs_x # absorbance coefficient XPS insulation
X[6] : Aabs_al # absorbance coefficient aluminum cladding

X[7] : Rc # R-value concrete [m2·K/W]
X[8] : Uc # U-value of concrete [W/m2K]
X[9] : dc # thickness of conrete [m]
X[10] : denc # density of concrete [kg/m3]
X[11] : cc # specific heat of conrete [J/(kg K)]

X[12] : Rx # R-value XPS insulation [m2·K/W]
X[13] : Ux # U-value XPS insulation [W/m2K]
X[14] : dx # thickness of XPS insulation [m]
X[15] : denx # density of XPS insulation [kg/m3]
X[16] : cx # specific heat of XPS insulation [J/(kg K)]

X[17] : Ral # R-value aluminum cladding [m2·K/W]
X[18] : Ual # U-value aluminum cladding [W/m2K]
X[19] : dal # thickness of aluminum cladding [m]
X[20] : denal # density of aluminum cladding [kg/m3]
X[21] : cal # specific heat of aluminum cladding [J/(kg K)]

X[22] : Gg # G-value of glass [W/m2K]
X[23] : Ug # U-value of glass [W/m2K]

print(X[:])

# define the mean and the standard deviation of the variables

Te=distribution (28.769,5.306725827*28.769)
SOLrad=distribution (190.72,298.5882476*190.72)
WWR=distribution(0.57125,0.216495525*0.57125)
n=distribution(2.975,1.443303502*2.975)
Aabs_c=distribution(0.83375,0.072165175*0.83375)
Aabs_x=distribution(0.8995,0.02886607*0.8995)
Aabs_al=distribution(0.12425,0.043299105*0.12425)
Rc=distribution(0.14435,0.037525891*0.14435)
Uc=distribution(7.46253438,2.122795083*7.46253438)
dc=distribution(0.249,0.05773214*0.249)
denc=distribution(2398,115.4642802*2398)
```

```
cc=distribution(988.5,86.59821014*988.5)
Rx=distribution(4.16725,0.447424086*4.16725)
Ux=distribution(0.2427915,0.026436792*0.2427915)
dx=distribution(0.0944,0.034639284*0.0944)
denx=distribution(36.91,5.195892609*36.91)
cx=distribution(1498,115.4642802*1498)
Ral=distribution(0.02485,0.008659821*0.02485)
Ual=distribution(46.58715558,19.41659173*46.58715558)
dal=distribution(0.00496,0.002309286*0.00496)
denal=distribution(2749.5,28.86607005*2749.5)
cal=distribution(561.5,202.0624903*561.5)
Gg=distribution(0.498,0.11546428*0.498)
Ug=distribution(1.5415,0.490723191*1.5415)
ppl=distribution(299.5,28.86607005*299.5)

fig, axes = plt.subplots(nrows=5, ncols=5, figsize=(20, 20))

sns.histplot(data=[np.random.normal(28.769,5.306725827*28.769) for _ in range(2000)], label="
    Dry-bulb Temperature", ax=axes[0, 0])
axes[0, 0].legend(loc='lower center',bbox_to_anchor=(0.5, -0.25), frameon=False, handlelength
    =0)
sns.histplot(data=[np.random.normal(190.72,298.5882476*190.72) for _ in range(2000)], label="
    Solar Radiation", ax=axes[0, 1])
axes[0, 1].legend(loc='lower center',bbox_to_anchor=(0.5, -0.25), frameon=False, handlelength
    =0)
sns.histplot(data=[np.random.normal(0.57125,0.216495525*0.57125) for _ in range(2000)], label
    ="Wall Window Ratio", ax=axes[0, 2])
axes[0, 2].legend(loc='lower center',bbox_to_anchor=(0.5, -0.25), frameon=False, handlelength
    =0)
sns.histplot(data=[np.random.normal(2.975,1.443303502*2.975) for _ in range(2000)], label="
    Airchange / h", ax=axes[0, 3])
axes[0, 3].legend(loc='lower center',bbox_to_anchor=(0.5, -0.25), frameon=False, handlelength
    =0)
sns.histplot(data=[np.random.normal(0.83375,0.072165175*0.83375) for _ in range(2000)], label
    ="Thermal Absorbance C", ax=axes[0, 4])
axes[0, 4].legend(loc='lower center',bbox_to_anchor=(0.5, -0.25), frameon=False, handlelength
    =0)
sns.histplot(data=[np.random.normal(0.8995,0.02886607*0.8995) for _ in range(2000)], label="
    Thermal Absorbance XPS", ax=axes[1, 0])
axes[1, 0].legend(loc='lower center',bbox_to_anchor=(0.5, -0.25), frameon=False, handlelength
    =0)
sns.histplot(data=[np.random.normal(0.12425,0.043299105*0.12425) for _ in range(2000)], label
    ="Thermal Absorbance AL", ax=axes[1, 1])
axes[1, 1].legend(loc='lower center',bbox_to_anchor=(0.5, -0.25), frameon=False, handlelength
    =0)

sns.histplot(data=[np.random.normal(0.14435,0.037525891*0.14435) for _ in range(2000)], label
    ="R-value C", ax=axes[1, 2])
axes[1, 2].legend(loc='lower center',bbox_to_anchor=(0.5, -0.25), frameon=False, handlelength
    =0)
sns.histplot(data=[np.random.normal(7.46253438,2.122795083*7.46253438) for _ in range(2000)],
     label="U-value C", ax=axes[1, 3])
```

```
axes[1, 3].legend(loc='lower center',bbox_to_anchor=(0.5, -0.25), frameon=False, handlelength=0)
sns.histplot(data=[np.random.normal(0.249,0.05773214*0.249) for _ in range(2000)], label="Thickness C", ax=axes[1, 4])
axes[1, 4].legend(loc='lower center',bbox_to_anchor=(0.5, -0.25), frameon=False, handlelength=0)
sns.histplot(data=[np.random.normal(2398,115.4642802*2398) for _ in range(2000)], label="Density C", ax=axes[2, 0])
axes[2, 0].legend(loc='lower center',bbox_to_anchor=(0.5, -0.25), frameon=False, handlelength=0)
sns.histplot(data=[np.random.normal(988.5,86.59821014*988.5) for _ in range(2000)], label="Specific Heat C", ax=axes[2, 1])
axes[2, 1].legend(loc='lower center',bbox_to_anchor=(0.5, -0.25), frameon=False, handlelength=0)

sns.histplot(data=[np.random.normal(4.16725,0.447424086*4.16725) for _ in range(2000)], label="R-value XPS", ax=axes[2, 2])
axes[2, 2].legend(loc='lower center',bbox_to_anchor=(0.5, -0.25), frameon=False, handlelength=0)
sns.histplot(data=[np.random.normal(0.2427915,0.026436792*0.2427915) for _ in range(2000)], label="U-value XPS", ax=axes[2, 3])
axes[2, 3].legend(loc='lower center',bbox_to_anchor=(0.5, -0.25), frameon=False, handlelength=0)
sns.histplot(data=[np.random.normal(0.0944,0.034639284*0.0944) for _ in range(2000)], label="Thickness XPS", ax=axes[2, 4])
axes[2, 4].legend(loc='lower center',bbox_to_anchor=(0.5, -0.25), frameon=False, handlelength=0)
sns.histplot(data=[np.random.normal(36.91,5.195892609*36.91) for _ in range(2000)], label="Density XPS", ax=axes[3, 0])
axes[3, 0].legend(loc='lower center',bbox_to_anchor=(0.5, -0.25), frameon=False, handlelength=0)
sns.histplot(data=[np.random.normal(1498,115.4642802*1498) for _ in range(2000)], label="Specific Heat XPS", ax=axes[3, 1])
axes[3, 1].legend(loc='lower center',bbox_to_anchor=(0.5, -0.25), frameon=False, handlelength=0)

sns.histplot(data=[np.random.normal(0.02485,0.008659821*0.02485) for _ in range(2000)], label="R-value AL", ax=axes[3, 2])
axes[3, 2].legend(loc='lower center',bbox_to_anchor=(0.5, -0.25), frameon=False, handlelength=0)
sns.histplot(data=[np.random.normal(46.58715558,19.41659173*46.58715558) for _ in range(2000)], label="U-value AL", ax=axes[3, 3])
axes[3, 3].legend(loc='lower center',bbox_to_anchor=(0.5, -0.25), frameon=False, handlelength=0)
sns.histplot(data=[np.random.normal(0.00496,0.002309286*0.00496) for _ in range(2000)], label="Thickness AL", ax=axes[3, 4])
axes[3, 4].legend(loc='lower center',bbox_to_anchor=(0.5, -0.25), frameon=False, handlelength=0)
sns.histplot(data=[np.random.normal(2749.5,28.86607005*2749.5) for _ in range(2000)], label="Density AL", ax=axes[4, 0])
axes[4, 0].legend(loc='lower center',bbox_to_anchor=(0.5, -0.25), frameon=False, handlelength=0)
```

```
sns.histplot(data=[np.random.normal(561.5,202.0624903*561.5) for _ in range(2000)], label="
    Specific Heat AL", ax=axes[4, 1])
axes[4, 1].legend(loc='lower center',bbox_to_anchor=(0.5, -0.25), frameon=False, handlelength
    =0)

sns.histplot(data=[np.random.normal(0.498,0.11546428*0.498) for _ in range(2000)], label="G-
    value Glass", ax=axes[4, 2])
axes[4, 2].legend(loc='lower center',bbox_to_anchor=(0.5, -0.25), frameon=False, handlelength
    =0)
sns.histplot(data=[np.random.normal(1.5415,0.490723191*1.5415) for _ in range(2000)], label="
    U-value Glass", ax=axes[4, 3])
axes[4, 3].legend(loc='lower center',bbox_to_anchor=(0.5, -0.25), frameon=False, handlelength
    =0)
sns.histplot(data=[np.random.normal(299.5,28.86607005*299.5) for _ in range(2000)], label="
    Occupancy", ax=axes[4, 4])
axes[4, 4].legend(loc='lower center',bbox_to_anchor=(0.5, -0.25), frameon=False, handlelength
    =0)

fig.subplots_adjust(wspace=0.5, hspace=0.5)
@
```

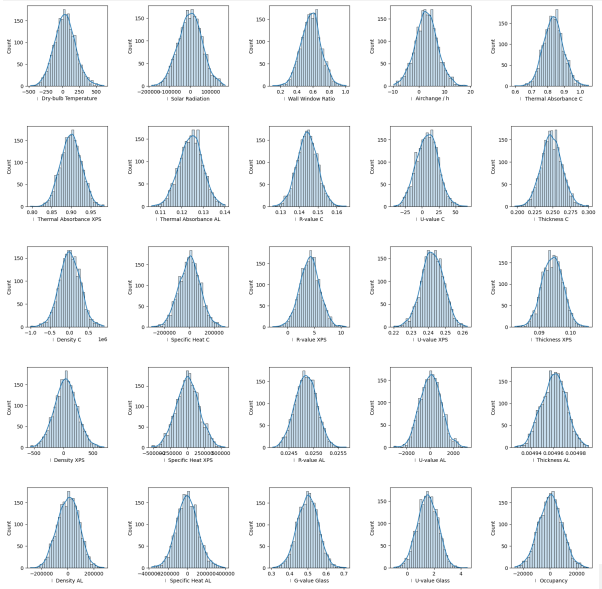


```


"""""""""""""""""""""""
Sensitivity Analysis
"""""""""""""""""""""""

# defining the problem
problem = {
    'names': ['Dry-bulb Temperature', 'Solar radiation', 'Wall Window Ratio','Airchange/hour'
        ,'Thermal Absorbance C','Thermal Absorbance XPS','Thermal Absorbance Al','R-avlue C',
        'U-value C','Thickness C','Density C','Specific Heat C','R-value XPS','U-Value XPS','
        Thickness XPS','Density XPS','Specific Heat XPS','R-value AL','U-value AL','Thickness
         AL','Density AL','Specific Heat AL','G-value Glass','U-value Glass','Occupancy'],
    'num_vars': 25,
    'bounds': [[28.769,5.306725827*28.769], [190.72,298.5882476*190.72],
        [0.57125,0.216495525*0.57125], [2.975,1.443303502*2.975],
```

```
        [0.83375,0.072165175*0.83375], [0.8995,0.02886607*0.8995],
        [0.12425,0.043299105*0.12425], [0.14435,0.037525891*0.14435],
        [7.46253438,2.122795083*7.46253438], [0.249,0.05773214*0.249],
        [2398,115.4642802*2398], [988.5,86.59821014*988.5], [4.16725,0.447424086*4.16725],
        [0.2427915,0.026436792*0.2427915], [0.0944,0.034639284*0.0944],
        [36.91,5.195892609*36.91], [1498,115.4642802*1498], [0.02485,0.008659821*0.02485],
        [46.58715558,19.41659173*46.58715558], [0.00496,0.002309286*0.00496],
        [2749.5,28.86607005*2749.5], [561.5,202.0624903*561.5], [0.498,0.11546428*0.498],
        [1.5415,0.490723191*1.5415], [299.5,28.86607005*299.5]],
    'dists': ['norm', 'norm', 'norm','norm','norm', 'norm', 'norm','norm','norm', 'norm', '
        norm','norm','norm', 'norm', 'norm','norm','norm', 'norm', 'norm','norm','norm', '
        norm', 'norm','norm','norm']
}
param_values = saltelli.sample(problem, 100)
Y = np.zeros(len(param_values))
for i in range(len(param_values)):
  Y[i] = calc_Tcomfort(param_values[i][:])

# Plot the results
fig, ax = plt.subplots(figsize=(20, 5))

ax.bar(range(len(Si['ST'])), Si['ST'], yerr=Si['ST_conf'], align='center', alpha=0.5, ecolor=
    'black', capsize=10)
ax.set_xticks(range(len(Si['ST'])))
ax.set_xticklabels(problem['names'],rotation=90)
ax.set_ylabel('Global Sobol Index')
ax.set_xlabel('Variables')
ax.set_title(' Total-order sensitivity results')

plt.show()
```

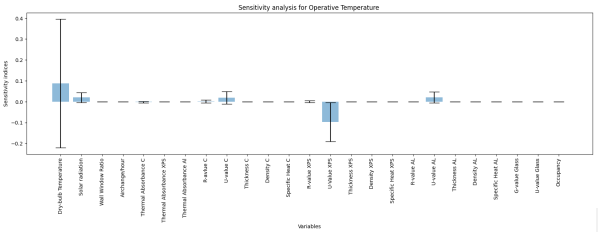

Listing A.3: Sobol' sensitivity analysis with final simulation outcomes.

```
"""""""""""""""""""""""
Import Libraries
"""""""""""""""""""""""
import pandas as pd
import numpy as np
import matplotlib.pyplot as plt
import seaborn as sns
from scipy.stats import uniform
from sklearn.gaussian_process import GaussianProcessRegressor
from sklearn.gaussian_process.kernels import RBF
from SALib.sample import saltelli
from SALib.analyze import sobol
```

```
"""""""""""""""""""""""""
Import Simulation Outcomes
"""""""""""""""""""""""""
# Load input and output data from CSV file
data = pd.read_csv(r'C:\Users\natha\OneDrive - Delft University of Technology/01_THESIS/02_WORKING/21_VRLab/Results3.csv')
data
```

	t_c	λ_c	den_c	c_c	tabs_c	sabs_c	wabs_c	t_xps	λ_xps	den_xps	...	Infil	flow/p	End Use Intensity (kWh/m2)	Cooling (kWh/m2)	Ventilation (kWh/m2)	Cooling [kWh]	Mechanical [kWh]	Edemand [kWh]	PMV	Toper
0	0.100	1.2	2200	840	0.75	0.65	0.40	0.1175	0.03375	36.5	...	0.00022	0.0144	10.889	10.135	0.027	79840.57991	57034.57237	136675.1523	1.260994	28.199019
1	0.189	1.2	2200	840	0.75	0.65	0.40	0.1175	0.03375	36.5	...	0.00022	0.0144	10.889	10.135	0.027	79835.21164	56979.46071	136814.6724	1.259878	28.195119
2	0.278	1.2	2200	840	0.75	0.65	0.40	0.1175	0.03375	36.5	...	0.00022	0.0144	10.884	10.130	0.027	79599.29831	57013.58454	136612.6828	1.260348	28.195853
3	0.367	1.2	2200	840	0.75	0.65	0.40	0.1175	0.03375	36.5	...	0.00022	0.0144	10.881	10.127	0.026	79579.49526	57010.61519	136588.1105	1.259407	28.193293
4	0.456	1.2	2200	840	0.75	0.65	0.40	0.1175	0.03375	36.5	...	0.00022	0.0144	10.882	10.128	0.026	79596.35478	57071.93968	136658.2845	1.259038	28.192572
...	...	...	...	...	...	...	...	...	...	...	...	...	...	...	...	...	...	...	...	...	...
3465	0.275	1.6	2400	1005	0.85	0.50	0.55	0.1700	0.02350	28.0	...	0.00022	0.0144	10.876	10.122	0.027	79538.31881	57013.28073	136551.5995	1.258306	28.188996
3466	0.275	1.6	2400	1005	0.85	0.58	0.55	0.1700	0.02350	28.0	...	0.00022	0.0144	10.879	10.125	0.027	79557.47641	56974.97147	136532.4479	1.258969	28.190890
3467	0.275	1.6	2400	1005	0.85	0.66	0.55	0.1700	0.02350	28.0	...	0.00022	0.0144	10.881	10.127	0.026	79575.16312	56972.58248	136547.7656	1.259454	28.192630
3468	0.275	1.6	2400	1005	0.85	0.74	0.55	0.1700	0.02350	28.0	...	0.00022	0.0144	10.887	10.133	0.026	79625.31190	56953.37516	136578.6871	1.259813	28.193857
3469	0.275	1.6	2400	1005	0.85	0.82	0.55	0.1700	0.02350	28.0	...	0.00022	0.0144	10.891	10.137	0.027	79654.34828	56940.53750	136594.8858	1.260325	28.195523

3470 rows × 38 columns

```
# Get input names from the first row of the data DataFrame
input_names = list(data.columns[:30])
output_names = list(data.columns[30:31])

inputs = data.iloc[:, :30].values
outputs = data.iloc[:, 30].values

# Create a separate list of (min, max) tuples for each input variable
bounds = [(inputs[:, i].min(), inputs[:, i].max()) for i in range(inputs.shape[1])]

# Create an empty list to store the distribution curves
distribution_curves = []

# Plot histograms with density in Y axis for each input variable
fig, axs = plt.subplots(nrows=len(input_names), figsize=(5, 25))

for i, name in enumerate(input_names):
    # Plot the histogram with density curve
    sns.histplot(data=data, x=name, kde=True, stat='density', ax=axs[i], color='green',
        line_kws={'color': 'blue'})
    axs[i].set_ylabel('Density')
    axs[i].set_xlabel(name)

    # Get the distribution curve from the plot
    distribution_curve = axs[i].lines[0]
    # Add the distribution curve to the list
    distribution_curves.append(distribution_curve)

plt.tight_layout()
plt.show()
```

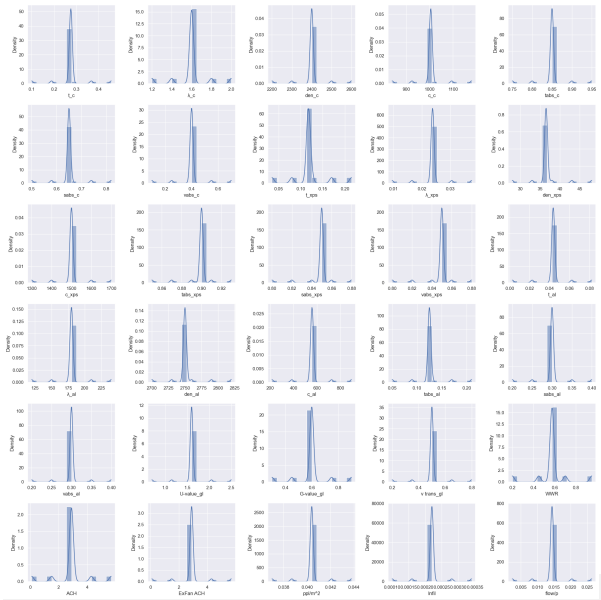

```
"""""""""""""""""""""""""
Train Model
"""""""""""""""""""""""""
# Separate the input data and output variable
X = data.iloc[:, :30].values
y = data.iloc[:, 30].values

# Create the Gaussian regression model
kernel = RBF(length_scale=1.0)
model = GaussianProcessRegressor(kernel=kernel)

# Fit the model to the data
model.fit(X, y)

"""""""""""""""""""""""""
Check Error and accuracy
"""""""""""""""""""""""""
from sklearn.metrics import mean_squared_error, r2_score

# Make predictions on the training data
y_pred = model.predict(X)

# Calculate mean squared error (MSE)
mse = mean_squared_error(y, y_pred)

# Calculate root mean squared error (RMSE)
rmse = np.sqrt(mse)

# Calculate R-squared (coefficient of determination)
r2 = r2_score(y, y_pred)

print("Mean Squared Error (MSE):", mse)
print("Root Mean Squared Error (RMSE):", rmse)
print("R-squared (Coefficient of Determination):", r2)

```

```
Mean Squared Error (MSE): 3.1843427918102322e-18
Root Mean Squared Error (RMSE): 1.0882751452689858e-09
R-squared (Coefficient of Determination): 0.9999999999999472

# Create a scatter plot of predicted vs. actual values
sns.set_theme(style="darkgrid")
plt.scatter(y, y_pred)
plt.plot([y.min(), y.max()], [y.min(), y.max()], 'w--', lw=1)  # Plotting the ideal line
plt.xlabel('Actual Values')
plt.ylabel('Predicted Values')
plt.title('Accuracy of Gaussian Regression Model')
plt.show()
```

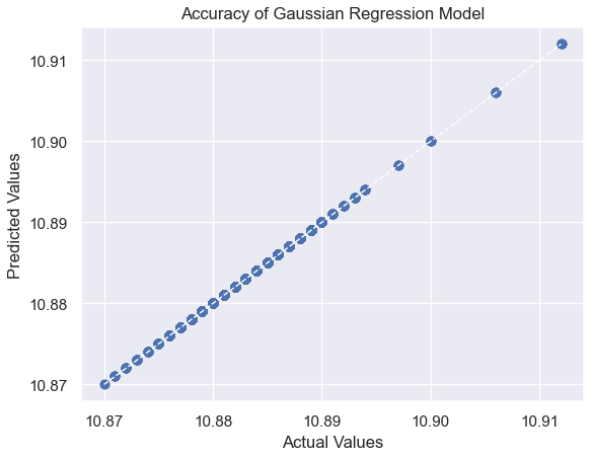


```

"""""""""""""""""""""""""
Check Fitting
"""""""""""""""""""""""""
# Generate test points for prediction
X_test = data.iloc[:, :30].values

# Predict the mean and standard deviation of the output at test points
y_mean, y_std = model.predict(X_test, return_std=True)

# Plot the predicted mean with uncertainty
plt.figure(figsize=(20, 6))
plt.plot(y_mean, color='blue', lw=0.1, label='Predicted Mean')
plt.xlabel('Sample Index')
plt.ylabel('Output')
plt.title('Fitting of the Gaussian Regression Model')
plt.legend()
plt.show()
```


```


# Define the range of the graph to show
start_index = 35
```

```
end_index = 65  # Adjust the end index as needed

# Plot the predicted mean with uncertainty for the specified range
plt.figure(figsize=(20, 6))  # Adjust the figure size as needed
plt.plot(y_mean[start_index:end_index], color='darkgrey', lw=0.25, label='Fitting Curve')
plt.scatter(range(start_index, end_index), y_train[start_index:end_index], label='Training Points', s=100, edgecolor='blue', facecolor='none')
plt.scatter(range(start_index, end_index), y_mean[start_index:end_index], color='red', label='Test Points', s=20 )
plt.fill_between(range(start_index, end_index), (y_mean[start_index:end_index] - 2 * y_std[start_index:end_index]), (y_mean[start_index:end_index] + 2 * y_std[start_index:end_index]),
                 color='lightgray', alpha=0.6, label='Uncertainty (2 std)')
plt.xlabel('Sample Index')
plt.ylabel('Output')
plt.title('Fitting of the Gaussian Regression Model')
plt.legend()
plt.xlim(start_index, end_index)  # Set the x-axis limits
plt.show()
```


```
"""""""""""""""""""""""""
Compute Sensitivity Indices
"""""""""""""""""""""""""
# Define the problem definition for sensitivity analysis
problem = {
    'num_vars': X.shape[1],
    'names': ['Input {}'.format(i+1) for i in range(X.shape[1])],
    'bounds': [(X[:, i].min(), X[:, i].max()) for i in range(X.shape[1])]
}
param_values = saltelli.sample(problem, 3470)

# Perform sensitivity analysis using Sobol indices
Y = model.predict(param_values)
Si = sobol.analyze(problem, Y)


# Extract the first-order indices
first_order_indices = Si['S1']

# Extract the total indices
total_order_indices = Si['ST']

# Print the first-order and total sensitivity indices
print("First-Order Indices:", Si['S1'])
print("Total-Order Indices:", Si['ST'])

Total-Order Indices: [0.05243534, 0.22456776, 0.245687, 0.15885685, 0.0356890, 0.0921525,
```

```
    0.0156948, 0.1723466, 0.022436, 0.244797, 0.141234, 0.0293735, 0.016438, 0.0126347,
    0.036438, 0.013688, 0.011235, 0.0174945, 0.0125724, 0.01245745, 0.002478653, 0.652442,
    0.731215, 0.5436586, 0.847649, 0.7236738, 0.123687, 0.183165, 0.112546, 0.141534]

# Total_order_indices are arrays containing the indices data
fig, axs = plt.subplots(nrows=2, figsize=(8, 6))

# Create boxplot for total-order indices
axs[1].boxplot(total_order_indices)
axs[1].set_xticks(range(1, len(problem['names']) + 1))  # Set x-axis tick positions
axs[1].set_xticklabels(problem['names'], rotation=90, ha='right')  # Set x-axis tick labels
axs[1].set_ylabel('Total-Order Index')
axs[1].set_xlabel('Variables')
axs[1].set_title('Total-Order sensitivity indices')
# Adjust layout and spacing
plt.tight_layout()

# Display the plot
plt.show()
```

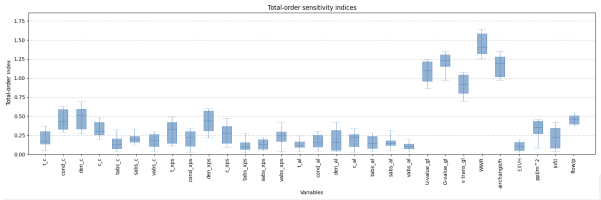

Listing A.4: Calculation of Resilience Loss.

```
"""""""""""""""""""""""
Import Libraries
"""""""""""""""""""""""
import pandas as pd
import numpy as np
import matplotlib.pyplot as plt
import seaborn as sns
import os
"""""""""""""""""""""""""""""""""""""""""""""""""""""""""""""""""""""""""""""""
For this example the results of variant WWR values are presented
"""""""""""""""""""""""""""""""""""""""""""""""""""""""""""""""""""""""""""""""
# Load input and output data from CSV file
data = pd.read_csv('WWR-comparison.csv')

date=data.iloc[:,1]
# sns.set_palette("pastel")
# sns.set_theme(style="ticks")
sns.set_theme(style="darkgrid")
fig, ax = plt.subplots(figsize=(15,5))

"""""""""""""""""""""""""""""""""""
Area calculation - Resilience Loss
"""""""""""""""""""""""""""""""""""
# Get the y-values of the curves for the optimized scenario and wall-window ratio scenarios
y_optimized = data.iloc[:, 3].values
```

```
y_0_20 = data.iloc[:, 5].values
y_0_40 = data.iloc[:, 6].values
# y_0_60 = data.iloc[:, 4].values
y_0_90 = data.iloc[:, 7].values
# Calculate the area between y_optimized and y=0
R_100 = np.trapz(np.abs(y_optimized), dx=1)
# Calculate the area between the curves using numerical integration
area_0_20 = np.trapz(y_optimized - y_0_20, dx=1)  # dx is the spacing between x-values (assumed as 1 here)
area_0_40 = np.trapz(y_optimized - y_0_40, dx=1)
# area_0_60 = np.trapz(y_optimized - y_0_60, dx=1)
area_0_90 = np.trapz(y_optimized - y_0_90, dx=1)
R_0_20=R_100-area_0_20
R_0_40=R_100-area_0_40
# R_0_60=R_100-area_0_60
R_0_90=R_100-area_0_90

# 'steelblue'
sns.lineplot(x=date, y=data.iloc[:, 3],alpha=1,color='lightslategrey', linewidth=2,label='Optimised scenario')
sns.lineplot(x=date, y=data.iloc[:, 5],alpha=1,color='darkgrey', linewidth=0.5,label=f'20% R={R_0_20:.2f}')
sns.lineplot(x=date, y=data.iloc[:, 6],alpha=1,color='darkgrey', linewidth=1,label=f'40% R={R_0_40:.2f}')
# sns.lineplot(x=date, y=data.iloc[:, 4],alpha=1,color='darkgrey', linewidth=1.5,label='60%')
sns.lineplot(x=date, y=data.iloc[:, 7],alpha=1,color='darkgrey', linewidth=2.2,label=f'90% R={R_0_90:.2f}')


# add labels in X and Y axes
plt.xlabel('Time[h]',fontdict={'fontsize':10})
plt.ylabel('Performance Indicator [%]',fontdict={'fontsize':10})

# # Find the index of the x-axis tick with the desired label
# heatstress_start = '23 Jul 06:00'
# # # Find the index of the desired x-axis tick label, if it exists
# # desired_index = np.where(date == heatstress_start)[0]
# # # Add a white vertical line at the desired x-axis tick index
# # plt.axvline(x=desired_index[0], color='white', linestyle='-')

# Add a white vertical line at the desired x tick index
plt.axvline(x='23 Jul 06:00', color='white',linewidth=3.5, linestyle='-')
plt.axvline(x='27 Jul 00:00', color='white',linewidth=3.5, linestyle='-')

# Specify the desired x-axis tick labels
heatstress_start = '23 Jul 06:00'
heatstress_end = '27 Jul 00:00'

# Find the indices of the desired x-axis tick labels, if they exist
start_index = np.where(date == heatstress_start)[0]
end_index = np.where(date == heatstress_end)[0]
if start_index.size > 0 and end_index.size > 0:
```

```
    # Set the background color before the start date to white
    # ax.axvspan(date.iloc[0], date.iloc[start_index[0]], facecolor='lightblue')

    # Set the background color between the start and end dates to red
    ax.axvspan(date.iloc[start_index[0]], date.iloc[end_index[0]], facecolor='palevioletred',
    alpha=0.08)

    # Set the background color after the end date to white
    # ax.axvspan(date.iloc[end_index[0]], date.iloc[-1], facecolor='white')

# Fill the area between the curves with a color
plt.fill_between(date, y_0_20, color='white',alpha=0.25)
plt.fill_between(date, y_0_40, color='white',alpha=0.25)
# plt.fill_between(date, y_0_60, color='white',alpha=0.25)
plt.fill_between(date, y_0_90, color='white',alpha=0.25)

# Reduce the frequency of the x axis ticks
# ax.set_xticks(ax.get_xticks()[::12])
plt.xticks(date[::6].tolist()+['28 Jul 00:00'],rotation = 90, fontsize=8)
plt.axhline(100, color='darkgrey', linestyle='--',linewidth=0.8)
plt.legend(loc='right', bbox_to_anchor=(1.17,0.15),
           ncol=1,fontsize=10,frameon=False)

```

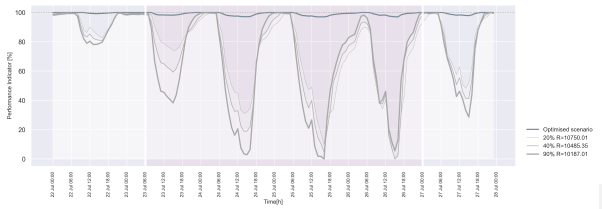


```
"""""""""""
Save Figure
"""""""""""
# save the plot as a PNG file in the same folder as the script
fig.savefig('WWRcomparison.png', bbox_inches='tight',dpi=300)
```

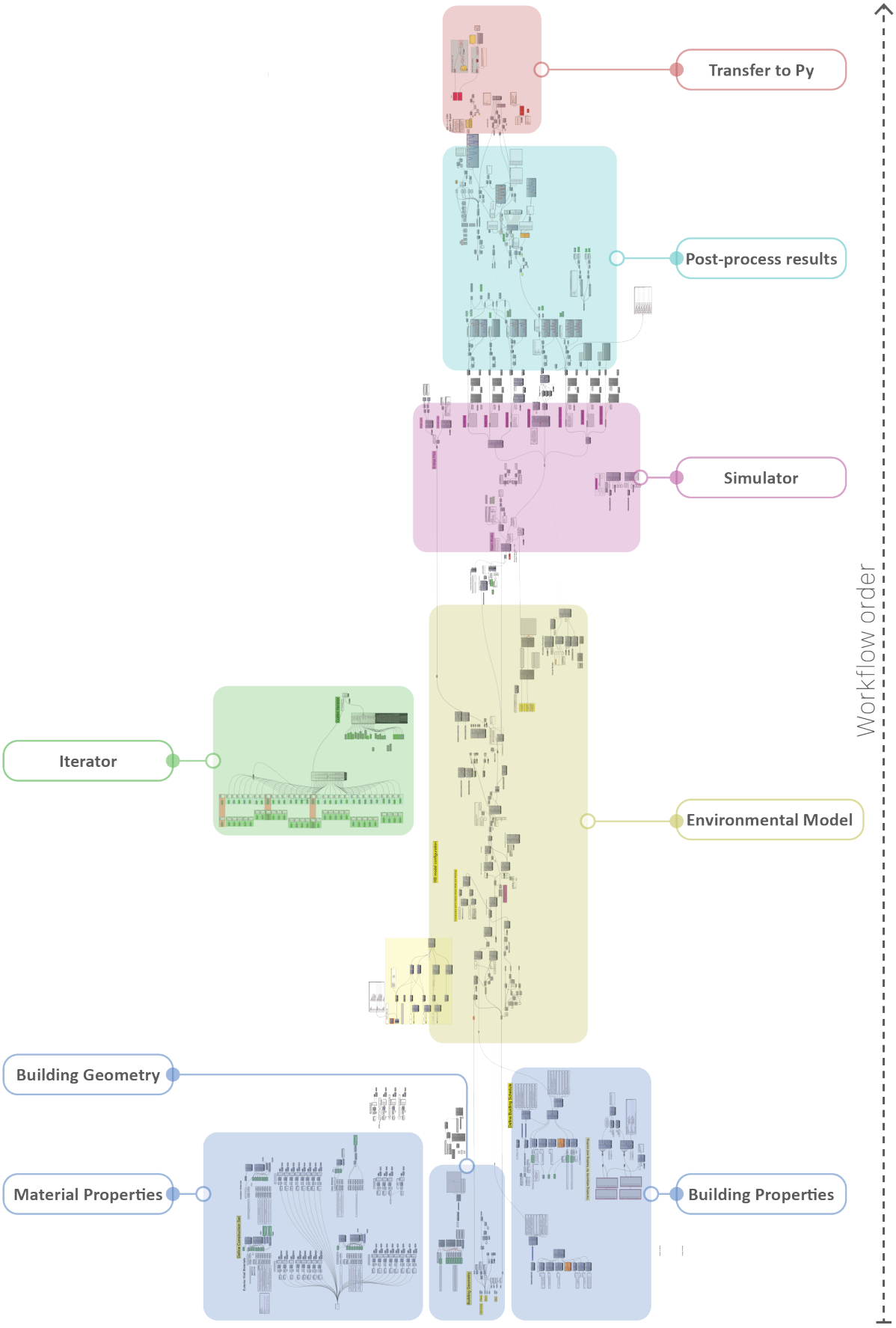

Figure A.2: Core Grasshopper script used for this case study.

B

Weather Data-sets

Visualization charts of weather data that were generated are presented. Moreover, Grasshopper and Python scripts are included.

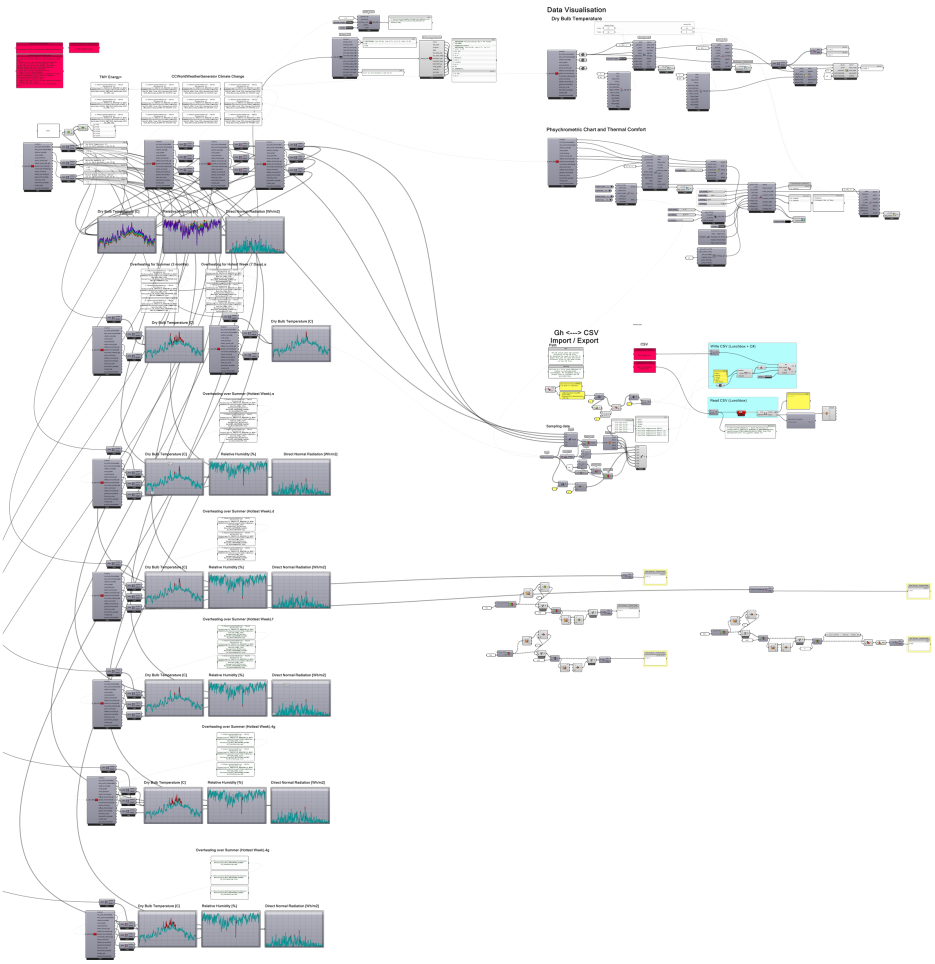

Figure B.1: Grasshopper script for visualising weather data.

```
import matplotlib.pyplot as plt
import numpy as np
import pandas as pd
import csv
import os

# read the csv file
df = pd.read_csv('test file_3.csv')

"""
Find the highest temperatures among the three files of heatwave data.
"""

# select the columns to compare
cols_to_compare = ['Temp TMY[C]', 'Temp 03', 'Temp 19', 'Temp 22']

# loop through each row of the dataframe
for index, row in df.iterrows():

    # find the maximum value among the selected columns
    max_val = max(row[cols_to_compare])

    # compare the maximum value with the value in the first column
    if max_val > row['Temp TMY[C]']:
        # if max value is greater, add it in the fourth column
        df.loc[index, 'Temp OH[C]'] = max_val
    else:
        # if not, add the value in the first column in the fourth column
        df.loc[index, 'Temp OH[C]'] = row['Temp TMY[C]']

# save the modified dataframe to a new csv file
df.to_csv('test file_3_modified.csv', index=False)

# convert the 'date' column to datetime format
df_3['Date'] = pd.to_datetime(df_3['Date'], format='%m/%d/%Y %H:%M')

# format the 'date' column to the desired format
df_3['Date'] = df_3['Date'].dt.strftime('%d %b %H:%M')

# print the updated dataframe
print(df_3['Date'])

date=df_3['Date']
month=df_3['Month']
index=df_3['Index']
hour=df_3['Hour']
tempTMY_3=df_3['Temp TMY[C]']
temp03_3=df_3['Temp 03']
temp19_3=df_3['Temp 19']
temp22_3=df_3['Temp 22']
tempOH_3=df_3['Temp OH[C]']

```

```
# Filter the data for the summer months of the year.
df_filtered_s_3 = df_3.loc[3624:5831]

sns.set_theme(style="darkgrid")
# creating the bar plot
fig  = plt.figure(figsize=(25,5))
plt.grid(True)

plt.bar(date, tempTMY_3, color ='grey', #edgecolor='black',linewidth=0.01,
        width = 0.5 ,alpha=1, label='TMY')

plt.plot(date, temp03_3, '-', markersize=1, linewidth=0.65,alpha=0.8, label='heatwave 2003')
plt.plot(date, temp19_3, '-', markersize=1, linewidth=0.65,alpha=0.8, label='heatwave 2019')
plt.plot(date, temp22_3, '-', markersize=1, linewidth=0.65,alpha=0.8, label='heatwave 2022')
# plt.plot(date, tempOH_3, 'r-', markersize=1, linewidth=0.8, label='Overheat Temperatures')

# heat wave threshold and maximum temperatures for each scenario
th=28

# plt.axhline(th, color='r',lw=1, linestyle='-', label='Threshold of 28\u00B0C')

# plt.fill_between(date,tempOH_3, th, color="r",
                  # where=(tempOH_3> th), interpolate=True, alpha=0.7)

plt.xticks(date[::371].tolist()+['31 Aug 23:00'], fontsize=8)
plt.yticks(fontsize=8)

# add labels in X and Y axes
plt.xlabel('Time[h]',fontdict={'fontsize':10})
plt.ylabel('Dry Bulb Temperature [\u00B0C]',fontdict={'fontsize':10})
plt.title('Heatwaves occured in Amsterdam',fontdict={'fontweight':'medium','fontsize':12})

plt.legend(loc='lower center', bbox_to_anchor=(0.5, -0.2),
           labels=['heatwave 2003','heatwave 2019','heatwave 2022'],
           ncol=4,fontsize=10,frameon=False)
# plt.legend(loc='lower center', bbox_to_anchor=(0.5, -0.3),
#            labels=['Temp 2003','Temp 2019','Temp 2022','Extreme Temp','TMY'],
#            ncol=5,fontsize=8,frameon=False)

plt.show()

"""
Compute the extreme temperatures during July.
"""

sns.set_theme(style="darkgrid")
# creating the bar plot
fig, ax = plt.subplots(figsize=(25,5))
plt.grid(True)
# plt.grid(which='major', axis='x', linestyle='-',color='white')
plt.plot(date, temp03_3, '-', markersize=1, linewidth=0.65,alpha=0.8, label='heatwave 2003')
plt.plot(date, temp19_3, '-', markersize=1, linewidth=0.65,alpha=0.8, label='heatwave 2019')
```

```
plt.plot(date, temp22_3, '-', markersize=1, linewidth=0.65,alpha=0.8, label='heatwave 2022')
plt.plot(date, tempOH_3, 'r-', markersize=1, linewidth=2, label='Maximum Temperatures')

# # heat wave threshold and maximum temperatures for each scenario
th=29
# max_TMY= max(tempTMY)
# max_HS=max(temp)

plt.axhline(th, color='r',lw=1, linestyle='--', label='threshold')

plt.fill_between(date,tempOH_3, th, color="r",
                  where=(tempOH_3> th), interpolate=True, alpha=0.5)

plt.xticks(date[::12].tolist(), fontsize=8)
plt.yticks(fontsize=8)

# Specify the desired x-axis tick labels
heatstress_start = '23 Jul 14:00'
heatstress_end = '26 Jul 19:00'

# Add a white vertical line at the desired x tick index
plt.axvline(x='23 Jul 14:00', color='white',linewidth=3.5, linestyle='-')
plt.axvline(x='26 Jul 19:00', color='white',linewidth=3.5, linestyle='-')

# Find the indices of the desired x-axis tick labels, if they exist
start_index = np.where(date == heatstress_start)[0]
end_index = np.where(date == heatstress_end)[0]
if start_index.size > 0 and end_index.size > 0:
    # Set the background color before the start date to white
    # ax.axvspan(date.iloc[0], date.iloc[start_index[0]], facecolor='lightblue')

    # Set the background color between the start and end dates to red
    ax.axvspan(date.iloc[start_index[0]], date.iloc[end_index[0]], facecolor='palevioletred',
        alpha=0.08)

    # Set the background color after the end date to white
    # ax.axvspan(date.iloc[end_index[0]], date.iloc[-1], facecolor='white')

plt.bar(date, tempTMY_3, color ='white', alpha=1, edgecolor='black', linewidth=0.15,
        width = 1, label='TMY')

# add labels in X and Y axes
plt.xlabel('Time[h]',fontdict={'fontsize':10})
plt.ylabel('Dry Bulb Temperature [\u00B0C]',fontdict={'fontsize':10})
plt.title('Overheat period',fontdict={'fontweight':'medium','fontsize':10})
plt.legend(loc='lower center', bbox_to_anchor=(0.5, -0.2),
           labels=['Heatwave 2003','Heatwave 2019','Heatwave 2022','Generated Data','
               Threshold of 29\u00B0C'],
           ncol=6,fontsize=10,frameon=False)
plt.show()
```

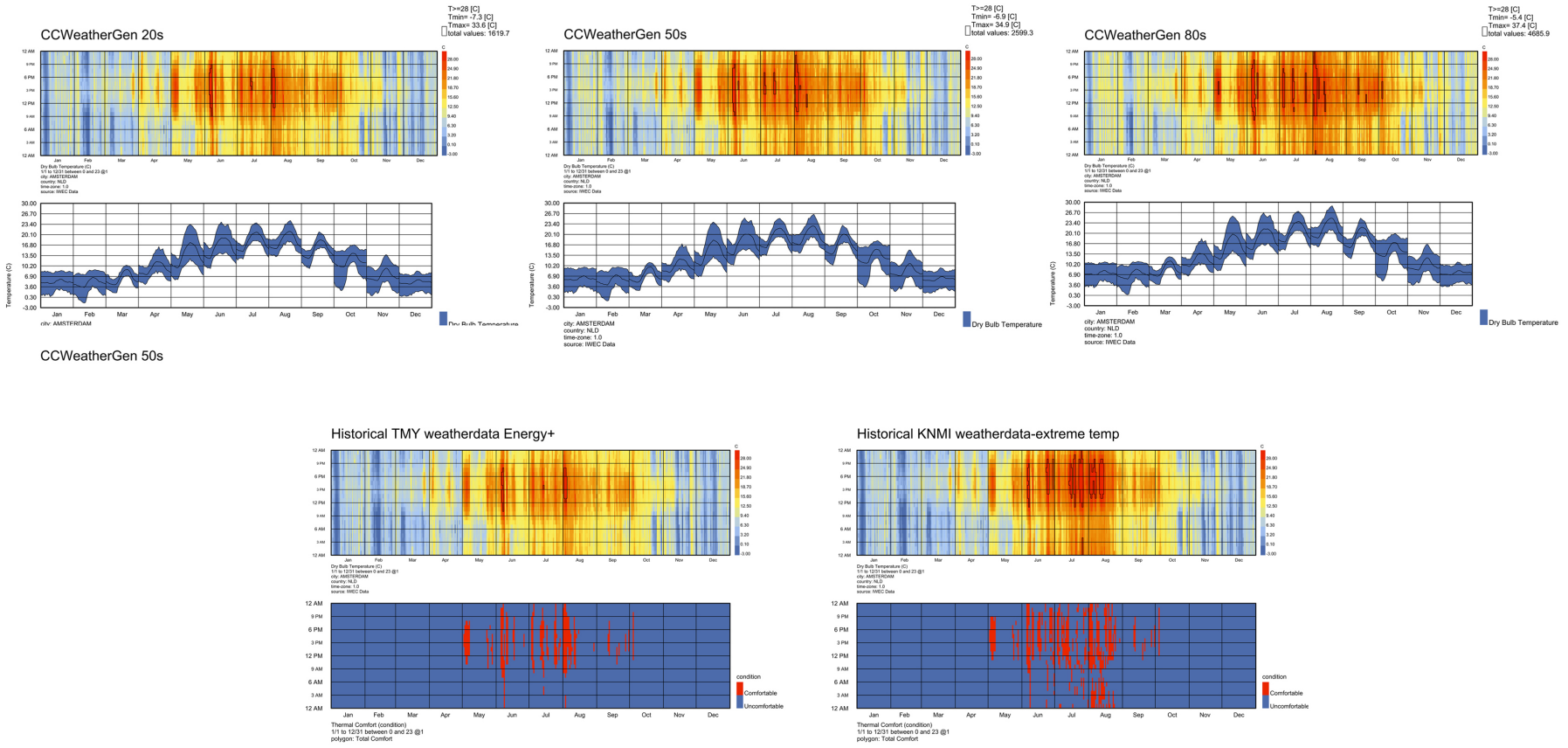

Figure B.2: Weather Charts in Grasshopper environment.

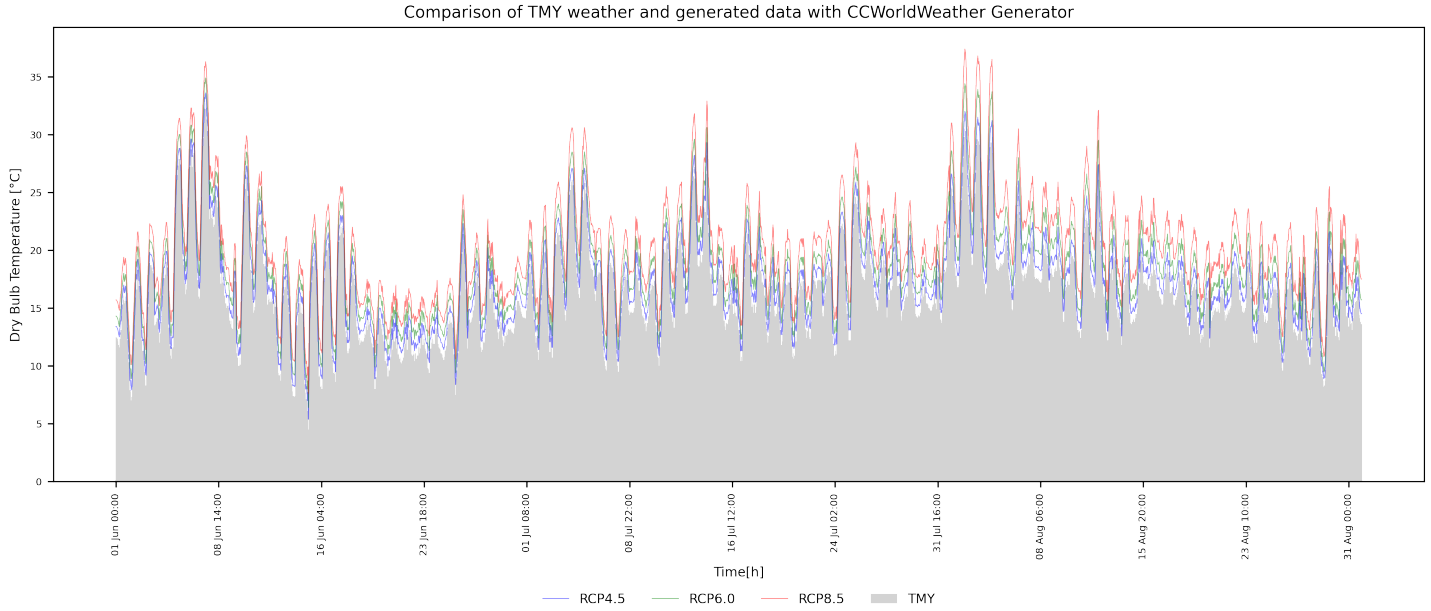

(a) Chart of weather data during summer.

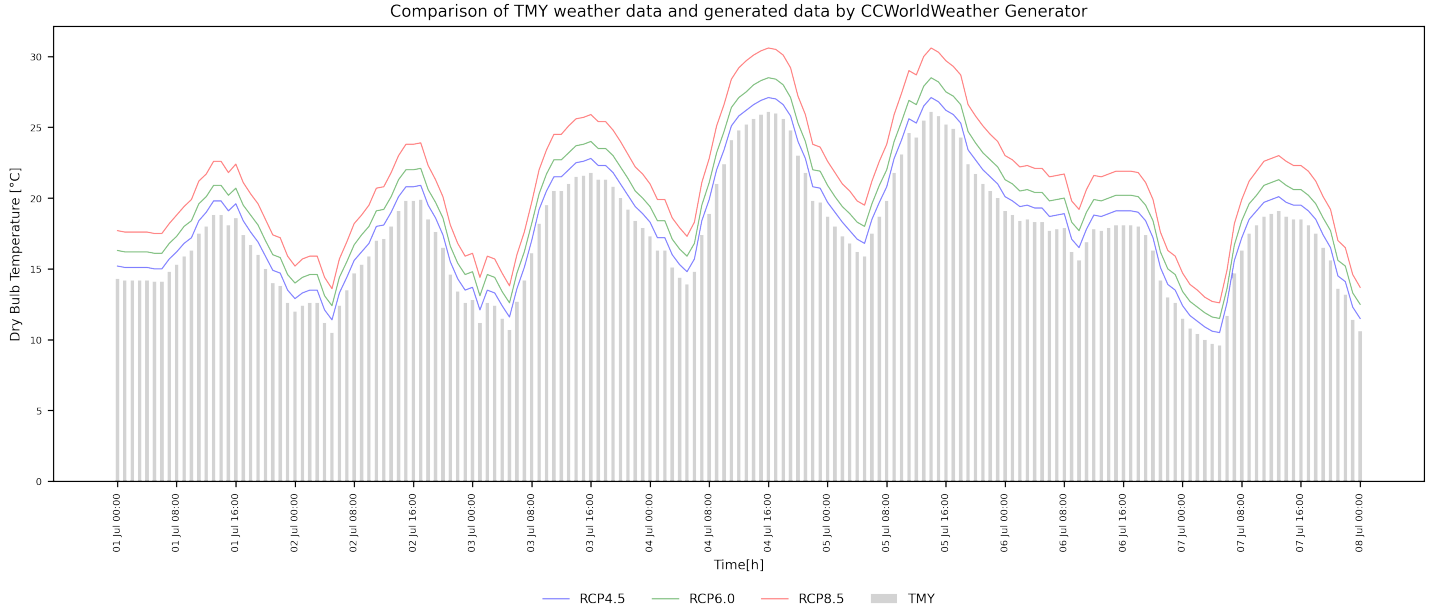

(b) Chart of weather data during a summer week.

Figure B.3: Weather data of extreme temperatures generated with CCWorldWeather Generator.

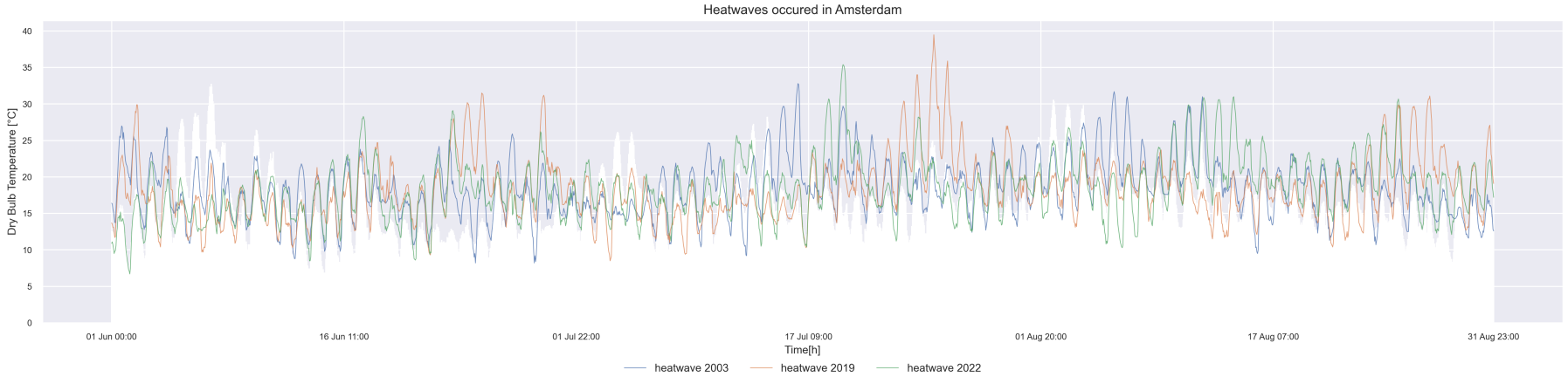

(a) Heatwaves that occurred in Amsterdam.

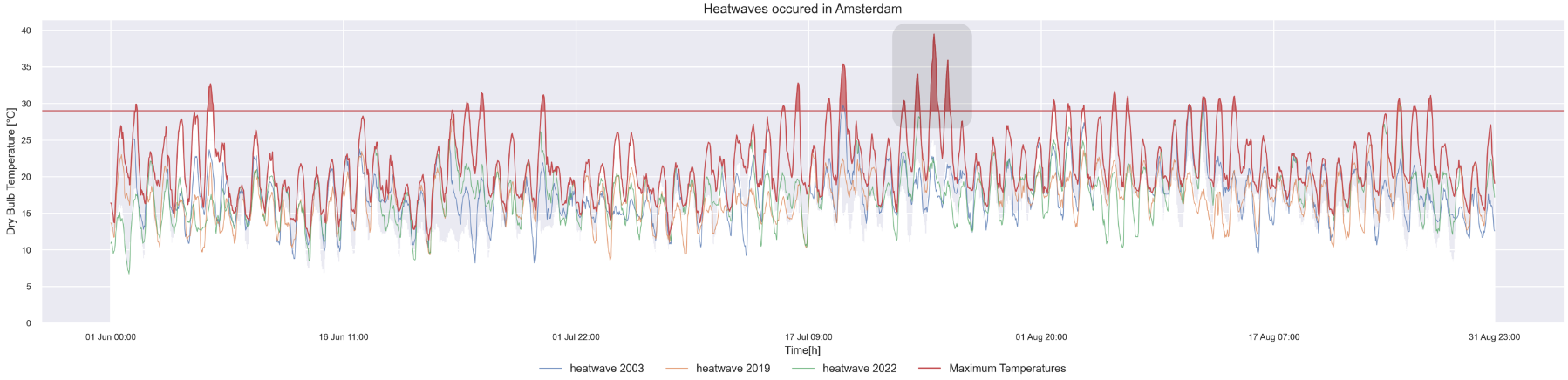

(b) Extreme temperatures beyond the threshold of 29°C are pointed out.

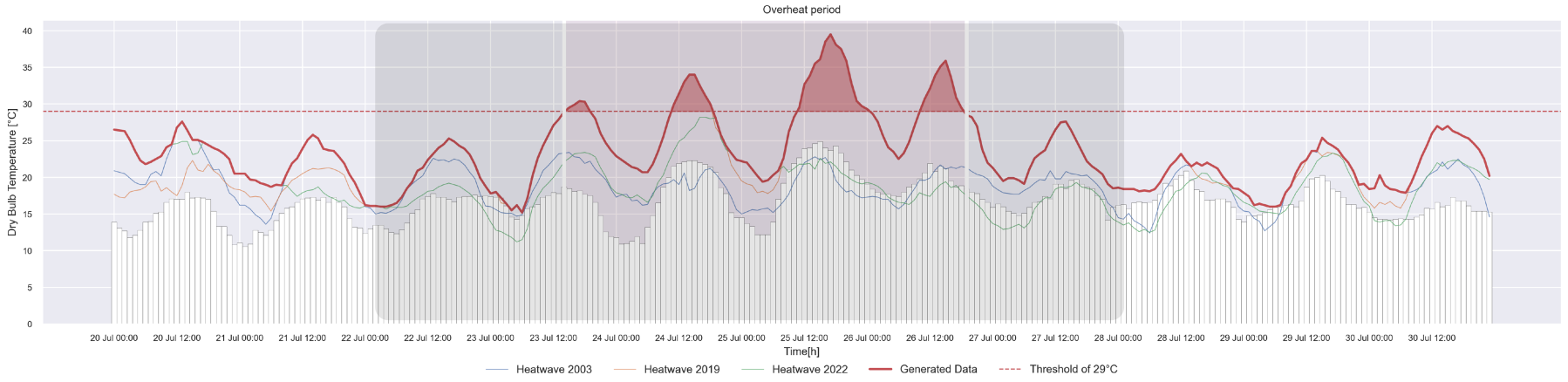

(c) Zoom-in to the overheat-stress period.

C

Diagrams and Charts

Detailed workflow diagrams and explanatory chats are presented in this section.

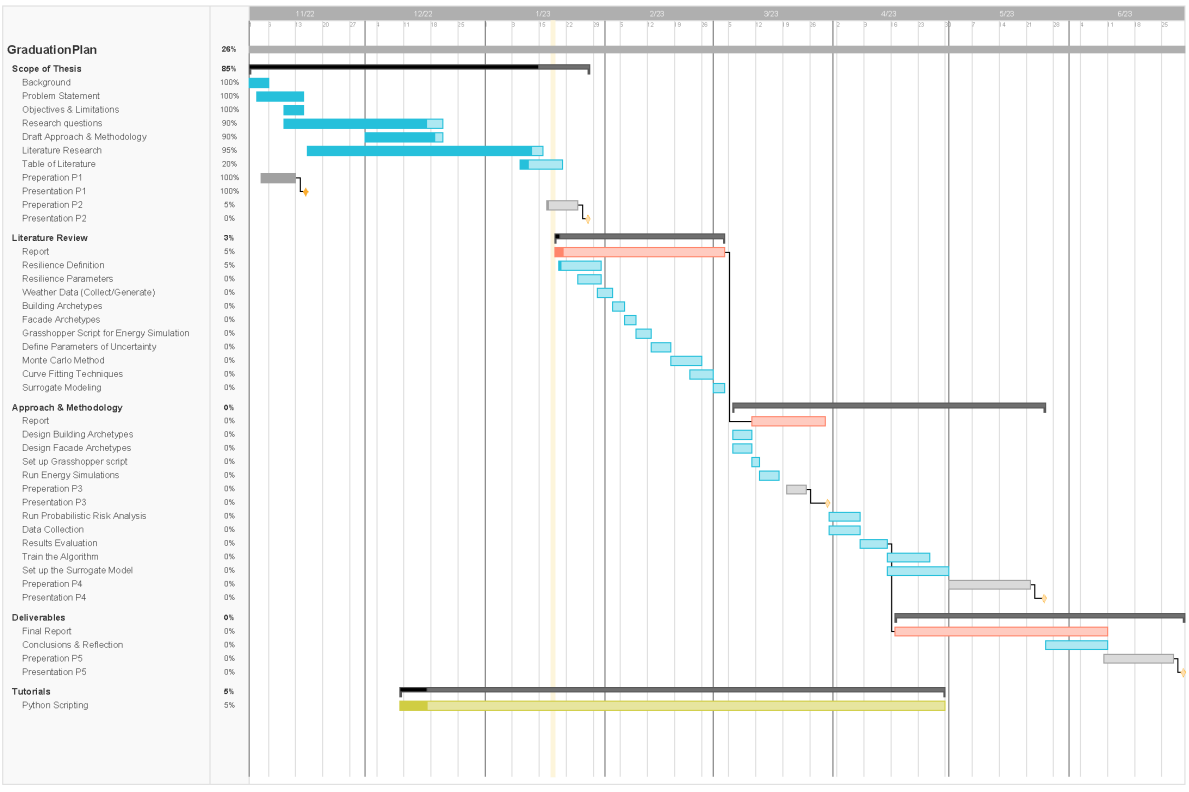

Figure C.1: Graduation Plan.

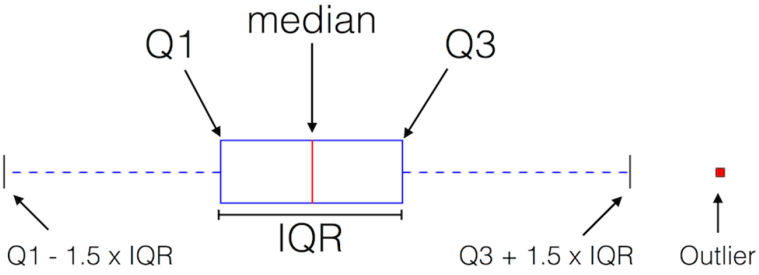

Q1: *Quartile 1*, or median of the *left* data subset
after dividing the original data set into 2 subsets via the median
(25% of the data points fall below this threshold)

Q3: *Quartile 3*, median of the *right* data subset
(75% of the data points fall below this threshold)

IQR: *Interquartile-range*, Q3 - Q1

Outliers: Data points are considered to be outliers if
value < *Q1 - 1.5 x IQR* or
value > Q3 + 1.5 x IQR

(a) Whiskers represent the entire population sample values.

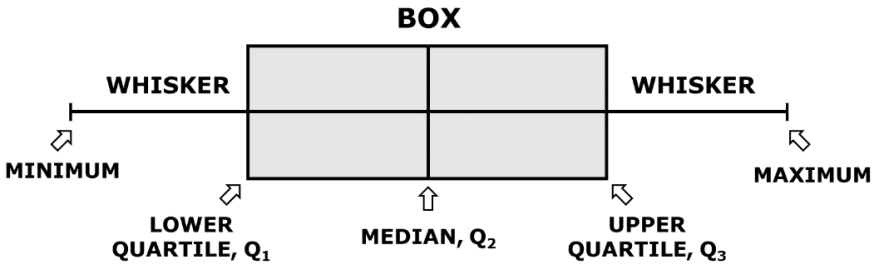

(b) Quartiles represent a part of the population sample size.

Figure C.2: Boxplot explanation (https://www150.statcan.gc.ca/n1/edu/power-pouvoir/ch12/5214889-eng.htm).

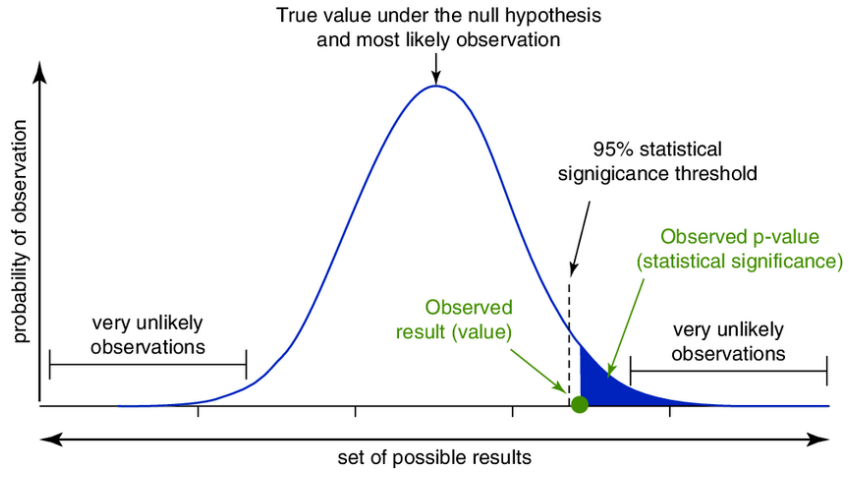

Figure C.3: Probabilistic distribution of results.
(https://productstar.ru/tpost/pgj7dzbkr1-statistical-significance-in-ab-testing-a).

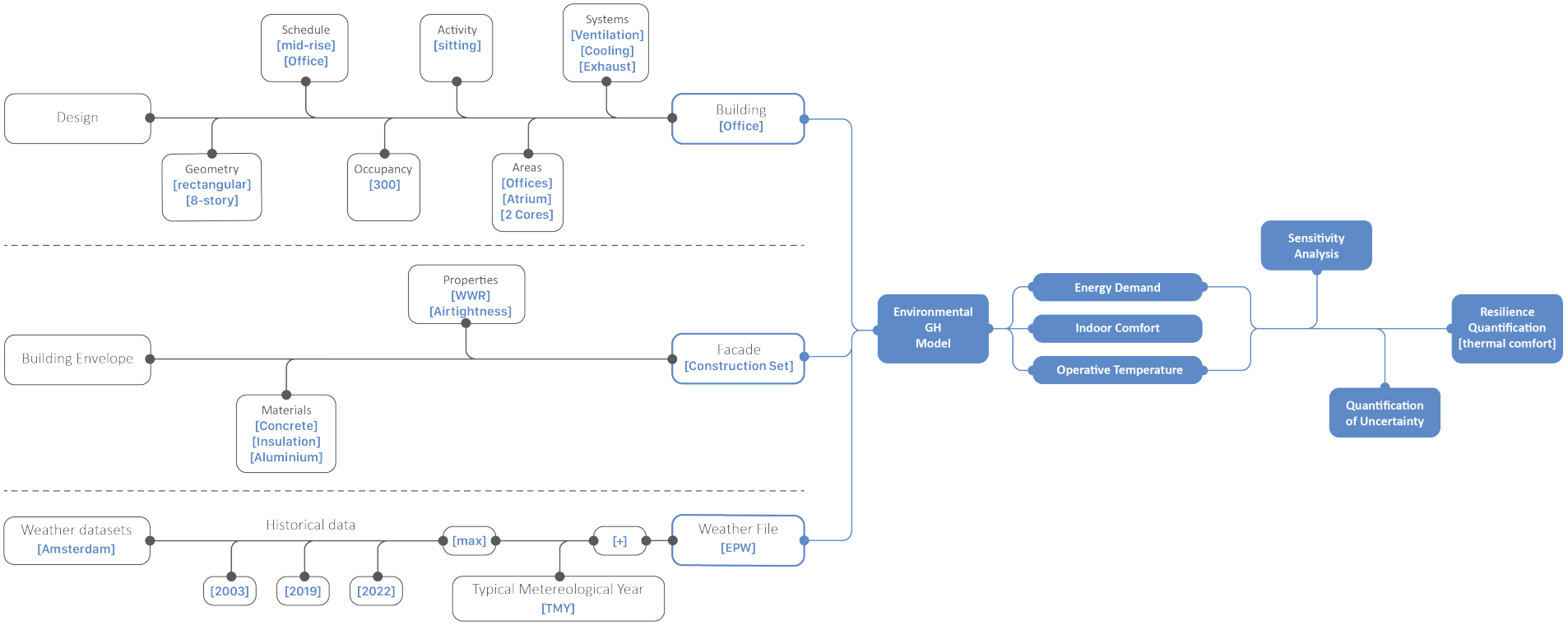

Figure C.4: Case study workflow detailed diagram.

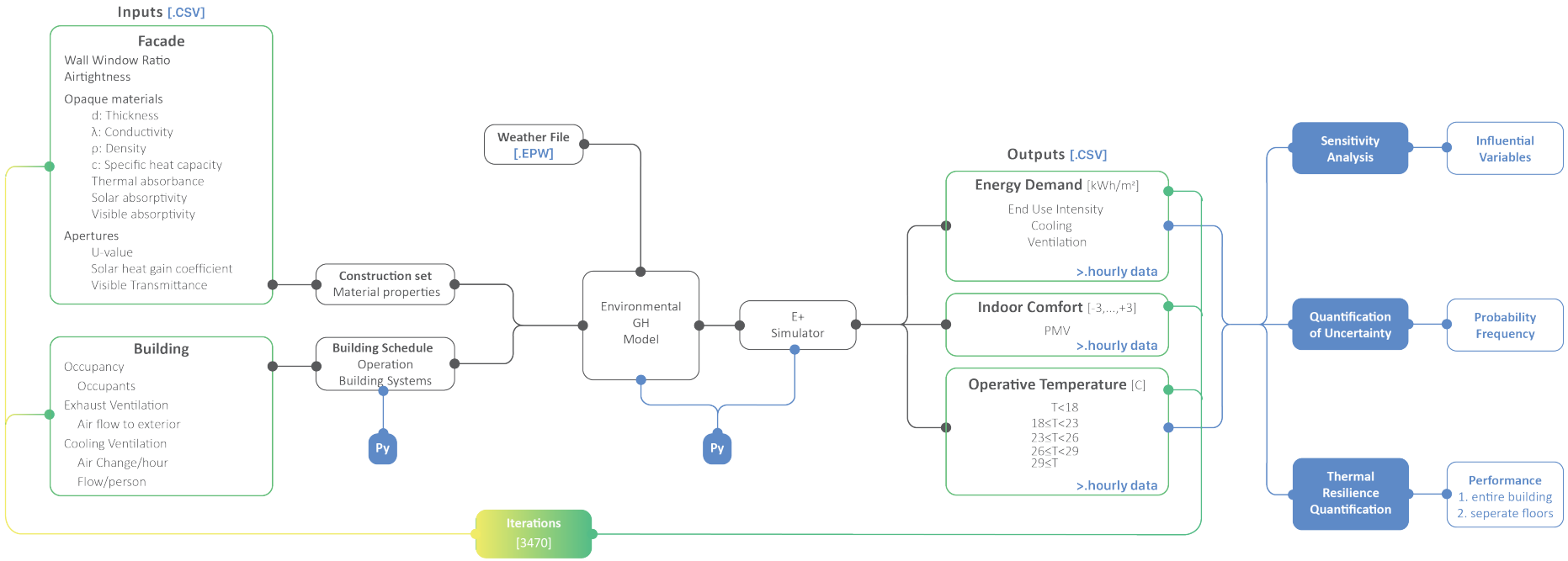

Figure C.5: Computational workflow detailed diagram.

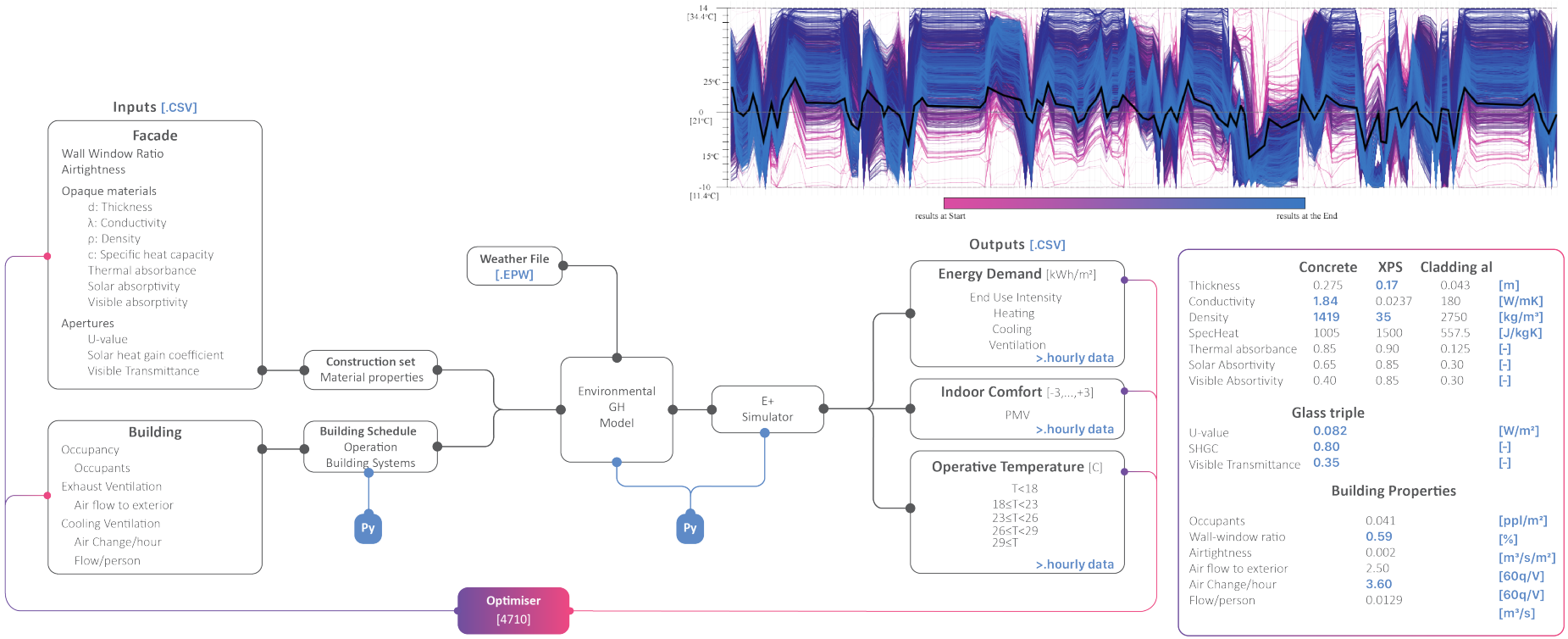

Figure C.6: Optimization detailed diagram.

D

Tables

Tables with detailed description of the building and facade properties are presented in this part.

Standardised design options

	General Dimensions	**Unit**	**GFA total**	**Unit**	**Volume total**	**Unit**
Building	45 x 30	[m]	8280	[m^2]	45360	[m^3]
Atrium	22 x 15		360		12096	
Offices	-		7920		33264	
			GFA ground floor			
Atrium			360			
Offices			990			
			1350			
			GFA/floor			
Offices			990			
Floor height	4.2					
Building height	33.6					
			Surface			
Façade			5040			

Table D.1: General building design dimensions.

Assigned value range to simulation variables

Material Properties	**Concrete**	**Reference**	**XPS insulation**	**Reference**	**Aluminum**	**Reference**	**Unit**
Thickness	0.15-0.35		0.035-0.15		0.001-0.0085		[m]
Conductivity	1.2-2.0	(Zubrzycki, 2021)	0.024-0.038		120-240		[W/mK]
Density	800-2100	(Howlader et al., 2012)	28-45	(Cai et al., 2017)	2700-2800	(Zubrzycki, 2021)	[kg/m^3]
SpecHeat	840-1170	(Olesen et al., 2018)	1300-1700	(Yücel et al., 2003)	215-900	(Selvakumar et al., 2021)	[J/kgK]
Thermal absorbance	0.75-0.95	(Mehta & Monteiro, 2014)	0.85-0.95		0.05-0.20	(Theodosiou et al., 2015)	-
Solar Absortivity	0.50-0.80		0.80-0.90		0.20-0.40		-
Visible Absortivity	0.10-0.70		0.80-0.90		0.20-0.40		-
	Glass						
U value	0.70-2.40	(Zubrzycki, 2021)					[W/m^{2}K]
SHGC	0.30-0.90	(Gueymard & duPont, 2009)					-
Visible Transmittance	0.20-0.80						-
Building Properties	**Occupancy**						
Occupants	0.0370-0.0435						[ppl/m^2]
	Façade						
Infiltration	0.0001-0.0003	("U.S. DoE", 2022)					[m^3/s / m^2]
Wall-window ratio	0.20-0.95						[%]
	Ventilation						
Flow / person	0.0024-0.0235	(Olesen et al., 2018)					[m^3/person]
AirChange/Hour	0.01-5.00	("U.S. DoE", 2022)					[60q/V]

Table D.2: The simulation model variables are defined within a certain range of values as they are presented above. These and the simulation results were used as inputs for the final variance-based sensitivity analysis.

Parameters of the optimised building case

Material Properties	**Concrete**	**XPS insulation**	**Aluminum**	**Unit**
Thickness	0.275	**0.17**	0.04375	[m]
Conductivity	**1.84**	0.02375	180	[W/mK]
Density	**1419**	**35**	2750	[kg/m^3]
SpecHeat	1005	1500	557.5	[J/kgK]
Thermal absorbance	0.85	0.9	0.125	-
Solar Absortivity	0.65	0.85	0.30	-
Visible Absortivity	0.4	0.85	0.30	-
	Glass			
U value	**0.82**			[W/m^2]
SHGC	**0.80**			-
Visible Transmittance	**0.35**			-
Building Properties	**Occupancy**			
Occupants	0.04025 (305ppl)			[ppl/m^2]
	Façade			
Infiltration	0.0002			[m^3/s / m^2]
Wall-window ratio	**0.59**			[%]
	Ventilation			
Flow / person	0.01295			[m^3/person]
AirChange/Hour	**3.6**			[60q/V]

Table D.3: Optimised parameters for stabilising the operative temperature around 21°C.

Values of variables of one-at-a-time sensitivity analysis.

			Parameters				
		Standard	**Variables**				
			Min	Max	Mean	COV	SD
Concrete	R value		0.08	0.2	0.14	0.8571429	0.06
	Thermal absorbance		0.75	0.95	0.8	0.25	0.111803399
	Solar Absortivity		0.5	0.8	0.7	0.4285714	0.158113883
	Visible Absortivity		0.1	0.7	0.5	1.2	0.316227766
XPS insulation	R value		3.6	5	4	0.35	0.761577311
	Thermal absorbance		0.85	0.95	0.9	0.1111111	0.05
	Solar Absortivity		0.8	0.9	0.85	0.1176471	0.05
	Visible Absortivity		0.8	0.9	0.85	0.1176471	0.05
Aluminum	R value		0.01	0.03	0.02	1	0.01
	Thermal absorbance		0.05	0.2	0.1	1.5	0.079056942
	Solar Absortivity		0.2	0.4	0.3	0.6666667	0.1
	Visible Absortivity		0.2	0.4	0.3	0.6666667	0.1
Glass	U value		0.5	1.7	0.7	1.7142857	0.721110255
	SHGC		0.3	0.7	0.5	0.8	0.2
	Visible Transmittance		0.2	0.8	0.5	1.2	0.3
Occupancy	ppl/area		0.025	0.284	0.057	4.5438596	0.162100278
Infiltration	Flow to exterior		0.0001	0.0003	0.000227	0.8810573	0.000103581
Ventilation	Flow / person		0.0024	0.0235	0.0167	1.2634731	0.011196651
	AirChange/Hour		0.01	3	1	2.99	1.577989227
Building	Wall Window Ratio		35	90	55	1	28.50438563
	Façade surface	504					
	Volume	4158					
Cooling	Setpoint		21	26	24	0.2083333	2.549509757

Table D.4: Values of one-at-a-time sensitive analysis.B.(26variables)

			Parameters				
		Standard	**Variables**				
			Min	Max	Mean	COV	SD
Concrete	Thickness		0.15	0.35	0.25	0.8	0.1
	Conductivity		0.1	0.3	0.2	1	0.1
	Density		2200	2600	2400	0.166666667	200
	SpecHeat		840	1170	970	0.340206186	168.6712779
	Thermal absorbance		0.75	0.95	0.8	0.25	0.111803399
	Solar Absortivity		0.5	0.8	0.7	0.428571429	0.158113883
	Visible Absortivity		0.1	0.7	0.5	1.2	0.316227766
XPS insulation	Thickness		0.035	0.15	0.085	1.352941176	0.057987068
	Conductivity		0.024	0.038	0.03	0.466666667	0.007071068
	Density		28	45	32	0.53125	9.617692031
	SpecHeat		1300	1700	1500	0.266666667	200
	Thermal absorbance		0.85	0.95	0.9	0.111111111	0.05
	Solar Absortivity		0.8	0.9	0.85	0.117647059	0.05
	Visible Absortivity		0.8	0.9	0.85	0.117647059	0.05
Aluminum	Thickness		0.001	0.0085	0.0035	2.142857143	0.003952847
	Conductivity		120	240	180	0.666666667	60
	Density		2700	2800	2750	0.036363636	50
	SpecHeat		215	900	600	1.141666667	345.1267883
	Thermal absorbance		0.05	0.2	0.1	1.5	0.079056942
	Solar Absortivity		0.2	0.4	0.3	0.666666667	0.1
	Visible Absortivity		0.2	0.4	0.3	0.666666667	0.1
Glass	Thickness		0.003	0.018	0.12	0.125	0.109756549
	Conductivity		0.7	1.4	1.1	0.636363636	0.353553391
	Visible Transmittance		0.4	0.8	0.6	0.666666667	0.2
	Visible Reflectance		0.05	0.15	0.1	1	0.05
	Long-wave transmittance		0.65	0.75	0.7	0.142857143	0.05
	Infrared emissivity F		0.02	0.05	0.03	1	0.015811388
	Infrared emissivity B		0.04	0.08	0.06	0.666666667	0.02
Occupancy	ppl/area		0.025	0.284	0.057	4.543859649	0.162100278
Infiltration	Flow to exterior		0.0001	0.0003	0.000227	0.881057269	0.000103581
Ventilation	Flow / person		0.0024	0.0235	0.0167	1.263473054	0.011196651
	AirChange/Hour		0.01	3	1	2.99	1.577989227
Building	Wall Window Ratio		35	90	55	1	28.50438563
	Façade surface	504					
	Volume	4158					
Cooling	Setpoint		21	26	24	0.208333333	2.549509757

Table D.5: Values of one-at-a-time sensitive analysis.A.(34variables)

Values of variables of sensitivity analysis with the building physics equation.

		Standard	Variables		References
			Mean(mu)	SD(sigma)	
Concrete	R value		0.14435	0.03752589	
	U value		7.46253438	2.122795083	
	Thickness		0.249	0.05773214	
	Density		2398	415.4642802	
	SpecHeat		928.5	56.59821014	
	Thermal absorbance		0.83375	0.072165175	
XPS insulation	R value		4.16725	0.447424086	(Abediniangerabi et al., 2021)
	U value		0.2427915	0.026436792	(Abediniangerabi et al., 2018)
	Thickness		0.0944	0.034639284	(Dhariwal & Banerjee, 2015)
	Density		32.91	5.195892609	(Corrado & Mechri, 2009)
	SpecHeat		1498	115.4642802	(Bianchi et al., 2022)
	Thermal absorbance		0.8995	0.02886607	(Hopfe et al., 2007)
Aluminum	R value		0.02485	0.008659821	
	U value		46.58715558	19.41659173	
	Thickness		0.00496	0.002309286	
	Density		2749.5	28.86607005	
	SpecHeat		561.5	202.0624903	
	Thermal absorbance		0.12425	0.043299105	
Glass	G value		0.498	0.11546428	
	U value		1.5415	0.490723191	
Weather	Te dry-bulb Temperature		28.769	5.306725827	
	Solar Radiation		190.72	298.5882476	
Building	Wall Window Ratio		0.57125	0.216495525	
	Façade surface	504			
	Volume	4158			
Occupancy	Number of people		299.5	28.86607005	
	Energy / person	105			
Duraction	Time	3600			
Ventilation	Air change / hour		2.975	1.443303502	

Table D.6: Mean and standard deviation values that are assigned to the calculation for operative temperature.

Literature Review			Thesis Structure															
Authors in APA 7	Title	Publication year	Problem Statement	Resilience Definition	Resilience Parameters	Resilience Metrics	Weather Data	Building Archetypes	Façade Archetypes	Simulation Model	Data collection	Parameters of Uncertainty	Probabilistic Risk Assessment	Monte Carlo Method	Curve fitting techniques	Surrogate Modeling	Deep Learning	Linear Regression	Bayesian Method
Abadinangarshi et al. 2018	Energy Performance Analysis of Ultra-High-Performance Fiber-Reinforced Concrete (UHP-FRC) Façade Systems	2018							X	X									
Abadinangarshi et al. 2021	Deep learning for estimating energy savings at early-stage façade design decisions	2021						X	X	X		X					X	X	
Abadinangarshi et al. 2019	Accuracy-Scale and Whole-Energy Performance Analysis of Ultra-High-Performance Fiber-Reinforced Concrete (UHP-FRC) Façade Systems	2019							X	X									
Abadinangarshi et al. 2022	Machine Learning Methods for Estimating Energy Performance of Building Façade Systems	2022							X	X									
Abadinangarshi et al. 2018	Building energy performance analysis of ultra-high-performance fiber-reinforced concrete (UHP-FRC) façade systems	2018						X	X	X	X	X							
Abadinangarshi et al. 2020	A data-driven framework for energy-conscious design of building façade systems	2020						X	X	X	X	X							
Al-Humaiqani et al. 2022	The built environment resilience qualities to climate change impact: Concepts, frameworks, and directions for future research	2022		X	X														
Argyroudis et al. 2020	Resilience assessment framework for critical infrastructure in a multi-hazard environment: Case study on transport assets	2020																	
Arup et al. 2012	City Resilience Index | Understanding and Measuring City Resilience	2012		X															
Arup et al. 2014	City Resilience Index | Research Report Volume II Urban Measurement Report Acknowledgements	2014		X															
Arup et al. 2015	Climate Action in Megacities 3.0	2015		X															
Arup et al. 2014	City Resilience Index | Research Report Volume 1 Desk Study	2014		X															
Arup et al. 2017	Future-proofing energy systems: The Energy Resilience Framework	2017		X															
Arup et al. 2014	City Resilience Index | Research Report Volume 2 Fieldwork Data Analysis Acknowledgements	2014		X															
Arup,Glass et al. 2021	Carbon footprint of façades: significance of glass Findings from the life cycle assessment of 16 façade typologies & 18,000 design simulations	2021		X					X	X									
Aisla et al. 2022	Resilient Cooling in Buildings—A Review of definitions and evaluation methodologies	2022		X	X	X				X									
Aisla et al. 2021	Resilient cooling of buildings to protect against heat waves and power outages: Key concepts and definition	2021		X	X	X			X										
Asaria et al. 2014	Integrated energy and environmental life cycle assessment of office building envelopes	2014			X				X										
Bianchi et al. 2022	A probabilistic-based framework for the integrated assessment of seismic and energy economic losses of buildings	2022		X				X		X	X	X	X		X				
Bruneau et al. 2003	A Framework to Quantitatively Assess and Enhance the Seismic Resilience of Communities	2003		X	X														
Ceven et al. 2012	Development of a climate change risk and vulnerability assessment tool for urban areas	2012																	
Cellura et al. 2019	Multi-Objective Building Envelope Optimization through a Life Cycle Assessment Approach	2019		X	X	X													
Charrenski et al. 2014	Environmental sustainability assessment tools for low-carbon and climate resilient, low income housing: resilience	2014		X		X													
Ciancio et al. 2019	Resilience of a building in future climate conditions in three European cities	2019	X				X			X	X								
Cimellaro et al. 2010	Framework for analytical quantification of disaster resilience	2010	X	X	X	X													
Dicorinno et al. 2020	Proposed method for probabilistic risk analysis using building performance simulations and stochastic parameters	2020										X	X		X				
Dicorinno et al. 2021	Predicting the energy performance of buildings : a method using probabilistic risk analysis for data-driven decision-support	2021	X			X		X		X	X	X	X	X	X				
Dicorinno et al. 2021	Probabilistic risk analysis and building performance simulations – Building design optimisation and quantifying stakeholder consequences	2021				X		X		X	X	X	X	X	X				
El-Zein et al. 2015	Assessment of vulnerability to climate change using a multi-criteria outranking approach with application to heat stress in Sydney	2015										X	X						
Fakhruddin et al. 2020	Assessing vulnerability and risk of climate change	2020	X									X	X						
Favorino et al. 2022	Façade Resilience Evaluation Framework: A Qualitative Evaluation Tool To Support Resilient Façade Design Decision Making	2022		X	X	X			X										
Feehan et al. 2021	Adopting an integrated building energy simulation and life cycle assessment framework for the optimisation of façades and fenestration in building envelopes	2021						X	X	X		X							
Facilleve et al. 2021	Dynamic assessment of urban resilience to natural hazards	2021	X										X	X					
Figliola et al. 2022	Digital workflow for climate resilient building façade generation	2022			X				X	X									
Galanos et al. 2021	The Routledge Companion to Artificial Intelligence in Architecture	2021								X							X		
Galanos et al. 2022	Time for Change – The InFraRed Revolution: How AI-driven Tools can Reinvent Design for Everyone	2022								X							X		
Gaillon et al. 2019	Realizing resilience for decision-making	2019																	
Hagenlocl et al. 2017	Reliability of energy efficient building retrofitting – probability assessment of performance and cost (Annex 55, RAP-RETRO)	2017	X							X	X	X	X	X					
Henry et al. 2012	Generic metrics and quantitative approaches for system resilience as a function of time	2012																	
Hosseini et al. 2021	Metrics and enhancement strategies for grid resilience and reliability during natural disasters	2021				X								X			X		
Hou et al. 2020	Efficient, probabilistic assessment of hygrothermal performance: sequential Monte Carlo and decomposition methods	2020	X								X	X		X					
Hou et al. 2017	Quasi-Monte-Carlo-based probabilistic assessment of wall heat loss	2017									X	X		X					
Hou et al. 2020	Model order reduction for efficient deterministic and probabilistic assessment of building envelope thermal performance	2020				X				X		X	X	X					
IPC et al. 2022	Building Index Resilience	2022	X	X	X	X													
Institute et al. 2013	Climatic Data for Building Design Standards	2013					X												
ji et al. 2021	Building life-span prediction for life cycle assessment and life cycle cost using machine learning: A big data approach	2021	X														X	X	
Kharbouch et al. 2022	Prediction of the impact of climate change on the thermal performance of walls and roof in Morocco	2022																	
Lendrello et al. 2022	Classification of european building stock in technological and typological classes	2022							X										
Lee et al. 2013	Probabilistic risk assessment of the energy saving shortfall in energy performance contracting projects—A case study	2013	X							X	X	X	X	X	X				
Menoni et al. 2012	Assessing multifaced vulnerability and resilience in order to design risk-mitigation strategies	2012	X	X	X														
Moazami et al. 2019	Impacts of future weather data typology on building energy performance – Investigating long-term patterns of climate change and extreme weather conditions	2019					X	X	X	X	X								
Mostafavi et al. 2018	Sustainability of integrated energy systems: A performance-based resilience assessment methodology	2018	X	X	X														
Nahorni et al. 2019	A digital workflow to quantify regenerative urban design in the context of a changing climate	2019	X				X			X	X								
Nik et al. 2021	Towards climate resilient urban energy systems: a review	2021	X	X	X		X				X	X		X					
Overend et al. 2018	Façade 2018-adaptive!	2018	X						X	X									
Panteli et al. 2015	Influence of extreme weather and climate change on the resilience of power systems: Impacts and possible mitigation	2015																	
Panteli et al. 2017	Metrics and Quantification of Operational and Infrastructure Resilience in Power Systems	2017																	
Panteli et al. 2017	Power Systems Resilience Assessment: Hardening and Smart Operational Enhancement Strategies	2017																	
Rad et al. 2021	BIM-based approach to conduct Life Cycle Cost Analysis of resilient buildings at the concept-al stage	2021																	
Reinhorn et al. 2006	Overview of the Resilience Concept Coupled Material and Geometrical Nonlinearity in Frame Structures View project Seismic Retrofit of Electrical Transformer Bushing Systems View project Overview of the Resilience Concept	2006	X																
Scarpa et al. 2021	Financial and energy performance analysis of efficiency measures in residential buildings: A probabilistic approach	2021										X	X	X	X				
Shahandashti et al. 2017	Probabilistic Building Energy Performance Analysis of Ultra-High-Performance Fiber-Reinforced Concrete (UHP-FRC) Façade System	2017						X	X	X	X	X	X	X					
Shamdic et al. 2020	Resilience framework and metrics for energy master planning of communities	2020	X	X	X														
Sharifi et al. 2016	Urban Resilience Assessment: Multiple Dimensions, Criteria, and Indicators	2016	X																
Sharifi et al. 2018	Principles and criteria for assessing urban energy resilience: A literature review	2018	X																
Slamlevic et al. 2018	Comments on the Definition and Quantification of Resilience IEEE Task Force on Definition and Quantification of Resilience	2018	X																
Sozzi et al. 2022	Life cycle assessment approach for the optimization of sustainable building envelopes: An application on solar wall systems	2012	X																
Suarez et al. 2020	Pushing the Envelope: Analyzing Building Envelope Resiliency Using Future Climate Predictions and Rainfall Progressions	2020	X				X												
Sun et al. 2020	Nexus of thermal resilience and energy efficiency in buildings: A case study of a nursing home	2020		X	X	X			X										
Sun et al. 2016	A method of probabilistic risk assessment for energy performance and cost using building energy simulation	2016				X				X	X	X	X	X	X				
Tavakoli et al. 2022	Evaluating the indoor thermal resilience of ventilative cooling in non-residential low energy buildings: A review	2022	X	X		X													
van et al. 2019	Dynamic vulnerability in the pursuit of just adaptation processes: A Bosnian case study	2019																	
Van et al. 2014	Probabilistic design and analysis of building performance: Methodology and application example	2014									X	X	X	X					
Vereecken et al. 2015	Interior insulation for wall retrofitting – A probabilistic analysis of energy savings and hygrothermal risks	2015												X					

Figure D.1: Literature map with the references that were been explored during this research.

Case	Variables	Population/each variable	Number of Simulations	Time / Simulation [s]	Overall time [s]	Overall time [d]	Overall time [y]
	Thickness C						
	Conductivity C		Sim=n^v	Sim whole Building			
	Density C	2	536870912.00	135.00	7.25E+10	8.39E+05	2298.25
	Specific Heat C	5	1.86E+20	135.00	2.51E+22	2.91E+17	7.97E+14
	Thermal Abs C	10	1.00E+29	135.00	1.35E+31	1.56E+26	4.28E+23
	Solar Abs C	20	5.37E+37	135.00	7.25E+39	8.39E+34	2.30E+32
	Vis Abs C	50	1.86E+49	135.00	2.51E+51	2.91E+46	7.97E+43
	Thickness XPS	100	1.00E+58	135.00	1.35E+60	1.56E+55	4.28E+52
1	Conductivity XPS						
(discrete properties)	Density XPS			Sim a floor of Building			
29 variables	Specific Heat XPS	2	536870912.00	8.00	4.29E+09	4.97E+04	136.19
	Thermal Abs XPS	5	1.86E+20	8.00	1.49E+21	1.72E+16	4.73E+13
	Solar Abs XPS	10	1.00E+29	8.00	8.00E+29	9.26E+24	2.54E+22
	Vis Abs XPS	20	5.37E+37	8.00	4.29E+38	4.97E+33	1.36E+31
	Thickness al	50	1.86E+49	8.00	1.49E+50	1.72E+45	4.73E+42
	Conductivity al	100	1.00E+58	8.00	8.00E+58	9.26E+53	2.54E+51
	Density al						
	Specific Heat al			83.00			
	Thermal Abs al			5.00			
	Solar Abs al						
	Vis Abs al			80.00			
	Uvalue gl						
	Gvalue gl						
	Vis trans gl						
	WallWindowRatio						
	AirChange/hour						
	People/m^2						
	Infiltration						
	flow/person						

	Rvalue_C			Sim whole Building			
	Thermal Abs C	2	1.05E+06	135.00	1.42E+08	1.64E+03	4.49
	Solar Abs C	5	9.54E+13	135.00	1.29E+16	1.49E+11	4.08E+08
	Vis Abs C	10	1.00E+20	136.00	1.36E+22	1.57E+17	4.31E+14
	Rvalue_XPS	20	1.05E+26	137.00	1.44E+28	1.66E+23	4.56E+20
2	Thermal Abs XPS	50	9.54E+33	138.00	1.32E+36	1.52E+31	4.17E+28
(R-Uvalues)	Solar Abs XPS	100	1.00E+40	139.00	1.39E+42	1.61E+37	4.41E+34
20 variables	Vis Abs XPS						
	Rvalue_al			Sim a floor of Building			
	Thermal Abs al	2	1048576.00	8.00	8.39E+06	9.71E+01	0.27
	Solar Abs al	5	95367431640625.00	8.00	7.63E+14	8.83E+09	24192651.35
	Vis Abs al	10	1.00E+20	8.00	8.00E+20	9.26E+15	2.54E+13
	Uvalue gl	20	1.05E+26	8.00	8.39E+26	9.71E+21	2.66E+19
	Gvalue gl	50	9.54E+33	8.00	7.63E+34	8.83E+29	2.42E+27
	Vis trans gl	100	1.00E+40	8.00	8.00E+40	9.26E+35	2.54E+33
	WallWindowRatio						
	AirChange/hour						
	People/m^2						
	Infiltration						
	flow/person						

	Building Model	Number of Simulations	Time / Simulation [s]	Overall time [s]	Overall time [h]	Overall time [d]
My Com	1 floor	10000	8	80000	22.22222222	0.925925926
	8 story	10000	40	400000	111.1111111	4.62962963
	15 story	10000	120	1200000	333.3333333	13.88888889
	Opaque params					
VR Lab	1 floor	10000	5	50000	13.88888889	0.578703704
	8 story	10000	27	270000	75	3.125
	15 story	10000	80	800000	222.2222222	9.259259259
	Building params					
	1 floor	16807	5	84035	23.34305556	0.972627315
	8 story	7776	27	209952	58.32	2.43
	15 story	16807	80	1344560	373.4888889	15.56203704
	Apertures params					
	1 floor	3375	5	16875	4.6875	0.1953125
	8 story	8000	27	216000	60	2.5
	15 story	3375	80	270000	75	3.125

Opaque params	3 models
n	10
v	10000	4

Simulations	time [s]
6	240
2*6	267

Building params	1 model
n	7776	6
v	10000	5
v-1	4
Apertures params	**1 model**
n	8000	20
v	10000	3
v+1	4

	time [d]
	0.101

Simulations	time [d]
10000	3.125
5*10000	3.440625

My Com	8 story	45776	40	1831040	508.6222222	21.19259259
VR Lab	8 story	45776	27	1235952	343.32	14.305

My Com	8 story	50000	40	2000000	555.5555556	23.14814815
VR Lab	8 story	50000	27	1350000	375	15.625

Samples			Outputs	EUI	cooling	ventilation	Ec + Ev	Toper
	3125	15625		kWh/m^2	kWh/m^2	kWh/m^2	~~hourly~~	~~hourly~~
	625	625			cumulative	cumulative	cumulative	% 19<>23
		16250		(Ec + Ev)*Toper	PVM			% >23
				~~hourly~~	avg	~~hourly~~		

Figure D.2: Calculation of simulation time for variant number of inputs and variables in the environmental model.

Weather data sources

		CCWorldWeatherGen	WeatherShift	Meteonorm	NEX-GDDP	CEDA Archive	KNMI	EnergyPlus	ClimateOneBuilding	Prometheus	Future Weather Building Simulation
Developer		University of Southampton	Arup and Argos Analytics	Meteotest AG	NASA	NERC Environmental Data Service (EDS)	Koninklijk Nederlands Meteorologisch Instituut	University of Illinois	Climate One Building	University of Exeter	Future Weather BPS
Accessibility	Open source				•	•	•	•	•	•	
	Limited access			•							•
	Must be purchased	•	•	•							
	Complex data sets	•	-	-	•	•	•				
Region	Europe										
	UK					•				•	
	US										
	Worlwide	•	•	•	•		•	•	•		•
Type of weather data	Historical	•	•	•	•	•	•	•	•		•
	Range of projected		•	-		•	•				•
	RCP scenarios	•	•	-	•	•	•			•	•
	Future weather data	•	•	-	•	•	•			•	•
GCM to RCM downscaling process	Morphing	•	•	-	-	-					•
	Statistical			-	-	-	•				•
	Dynamic			-	-	-	•			•	•
Temporal resolution	Annual	•	•	•	-		•	•	•	•	•
	Monthly	•	•	•	-	•	•	•	•	•	•
	Hourly	•	•	•	-		•	•	•	•	•
	Sub-hourly	•					•				
Output formats	EPW	•	•	•	-	-		•	•	-	-
	other	-	-	•	-	•	NetCDF ASCII	•	•	-	-
Link		https://ceda.ac.uk/ccweather	https://www.weathershift.com/he	https://meteonorm.com/	https://www.nccs.nasa.gov/servic	https://data.ceda.ac.uk/badc/ukci	http://climexp.knmi.nl/start.cgi?id	https://energyplus.net/weather	https://climate.onebuilding.org/W	https://emeritus.exeter.ac.uk/r	https://www.futureweatherbps.co

Figure D.3: Mapping different weather data sources.

Weather data sets from CEDA Archive, KNMI and Climate One Building sources meet most of the criteria of the matrix. CEDA Archive contains Historical weather data and future weather projections by taking into account variant probabilistic GHG scenarios. However, the available files are separated into different data lists and the output files are not EPWs. Hence this source leads to complex manipulation of data. Climate One Building source offers a wide range of historical weather data sets but the numerical hourly values are Typical Meteorological Year (TMY) and hence extreme values are neglected. However, according to the literature these historical data could be used for synthesizing future weather data sets by including emission scenarios and temperature extremes. Synthesizing data is a complex process and should be done by a climate researcher. KNMI data sets contain historical hourly data that are downscaled with CORDEX simulations by taking into account different emission scenarios and temperature extremes. Therefore these seem to be the most prominent for working on building simulations with future climate conditions. The main drawback is the lack of EPW files and hence netCDF files need to be converted to EPWs.

E

Equations

The following building physics equations employed for constructing a calculation model to perform sensitivity analysis were utilized in the following manner.

$$T_{facade\,in} = \frac{T_{facade\,out} + T_{air\,in} r_i}{R_{total} - r_e} + T_{air\,in} \tag{E.1}$$

$$T_{facade\,out} = \frac{a_{abs} SOL_{rad}(R_{total} - r_e) + a_e A T_e (r_e - R_{total}) + T_{air\,in} r_i}{a_e A T_e (r_e - R_{total}) + 1} \tag{E.2}$$

$$T_{facade\,out} = \frac{a_{abs} SOL_{rad}(R_{total} - r_e) + a_e A T_e (r_e - R_{total}) + T_{air\,in} r_i}{a_e A T_e (r_e - R_{total}) + 1} \tag{E.3}$$

$$T_{air\,in} = T_e + \frac{W}{H}(1 - e^{-\frac{H}{M}t}) \tag{E.4}$$

$$W = g_{glass} A_{glass} SOL_{rad} + P_{people} Q_{person} + \frac{W}{H}(1 - e^{-\frac{H}{M}t}) \tag{E.5}$$

$$H = \sum U_{mat_{0\ldots i}} A_{mat_{0\ldots i}} + \rho_{air} c_{air} n_{vent} V_{air} \tag{E.6}$$

$$M = \sum \rho_{mat_{0\ldots i}} c_{mat_{0\ldots i}} V_{mat_{0\ldots i}} + \rho_{air} c_{air} V_{air} \tag{E.7}$$

$$R_{total} = r_i + r_{mat_{0\ldots i}} + r_e \tag{E.8}$$

Where:

R_{total}: total thermal resistance of the facade (R-value)

r_i: thermal resistance indoors

r_e: thermal resistance outdoors

$r_{mat_{0\ldots i}}$: thermal resistance of materials and cavity

$\rho_{mat_{0\ldots i}}, \rho_{air}$: material and air density

$c_{mat_{0\ldots i}}, c_{air}$: material and air specific heat

$V_{mat_{0\ldots i}}, V_{air}$: material and air volume

$U_{mat_{0\ldots i}}$: material thermal transmittance (U-value)

$A_{mat_{0\ldots i}}$: material surface

g_{glass}: glass solar heat gain coefficient (SHGC)

A_{glass}: glass surface

SOL_{rad}: solar radiation

P_{people}: number of occupants

Q_{person}: energy demand per person

W: total heat source power

H: heat flow balance

M: thermal mass

a_{abs}: thermal absorptivity coefficient

a_e: radiation heat transfer coefficient outdoors

T_e: exterior temperature

n_{vent}: air change per hour

F

Correlation matrices and Sobol' results

Correlation matrices from simulation results and chart that present the accuracy of the regression model.

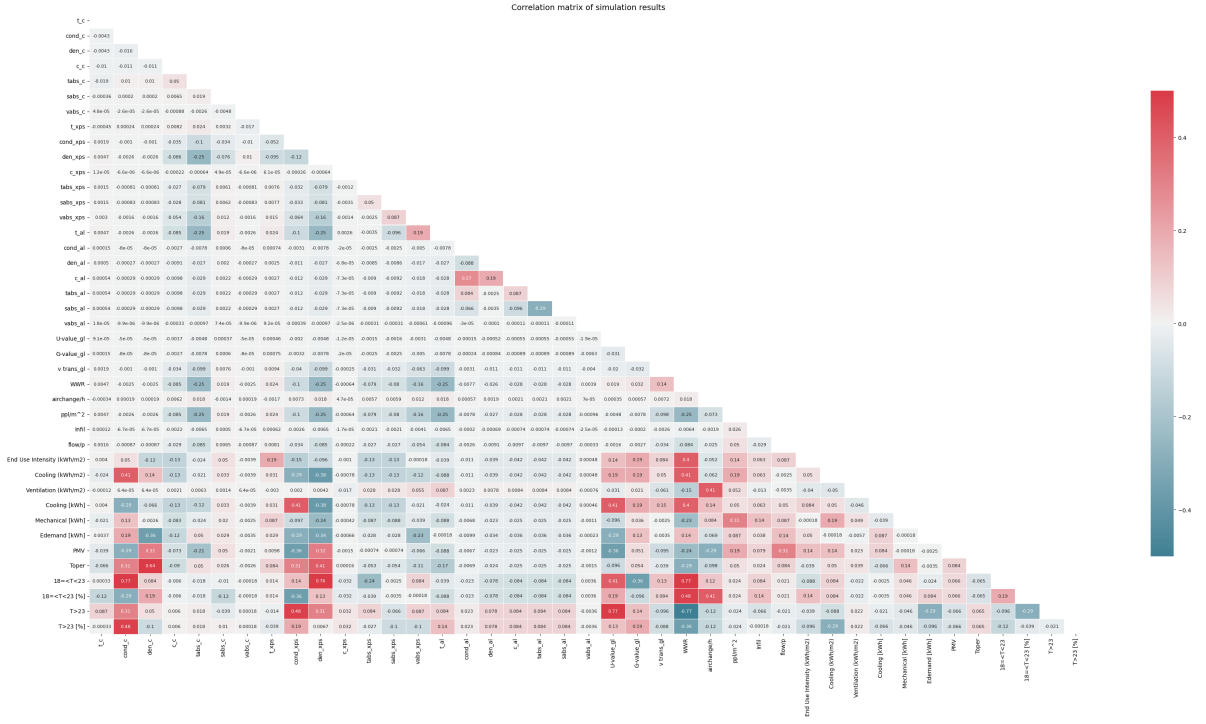

Figure F.1: Correlation matrix of 30 variables and 3470 simulation outcomes (final).

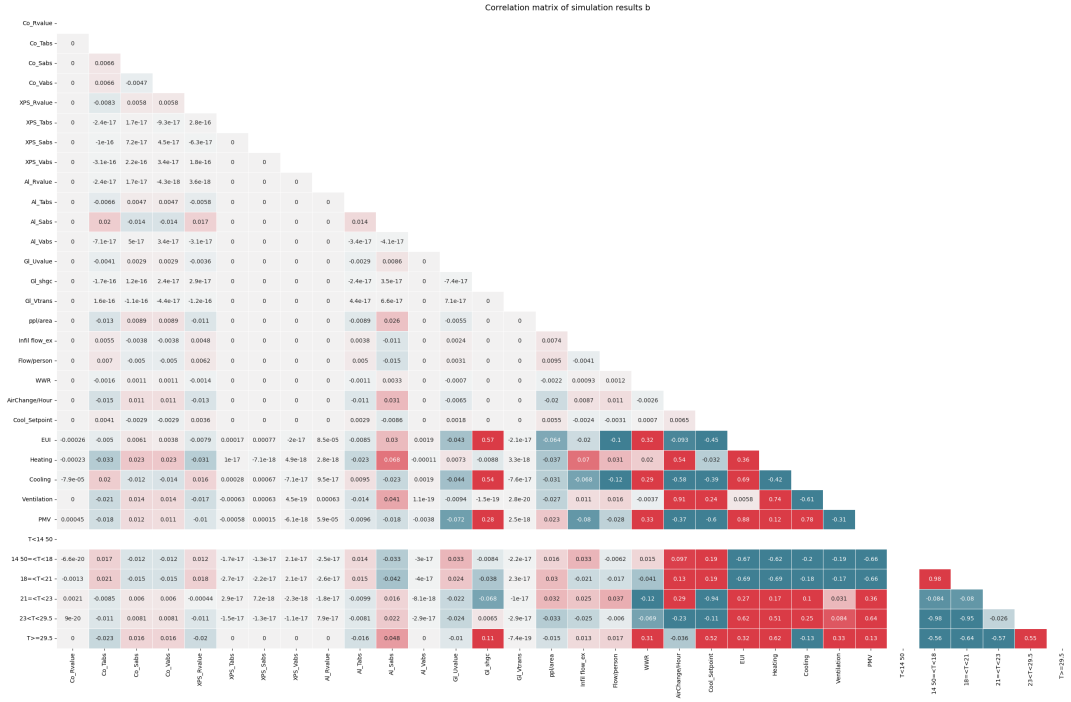

(a) Correlation matrix of 26 variables and 150 simulation results.

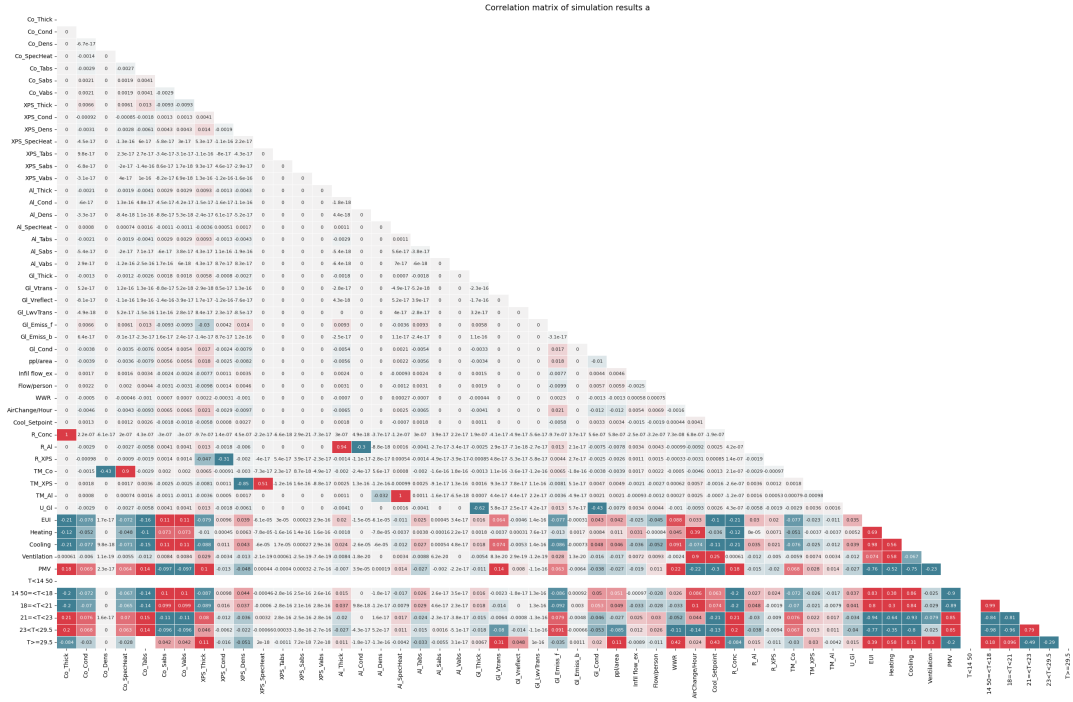

(b) Correlation matrix of 34 variables and 150 simulation results.

Figure F.2: Correlation matrices of one-at-a-time sensitivity analysis.

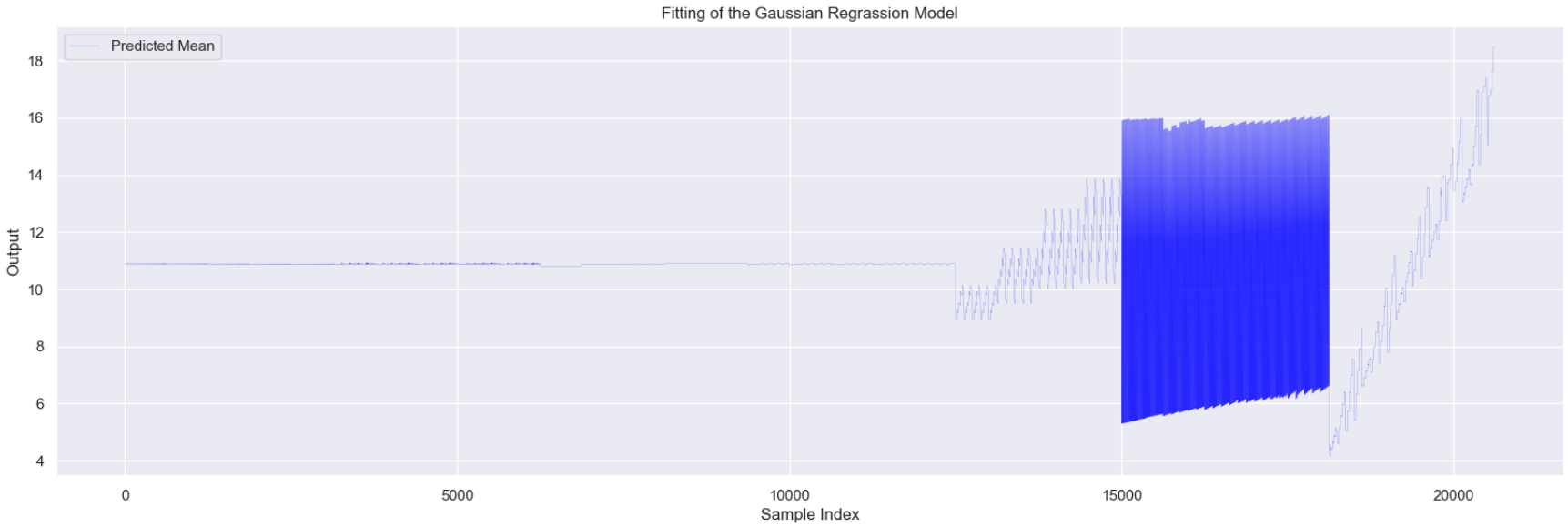

(a) Overview of Gaussian model fitting curve.

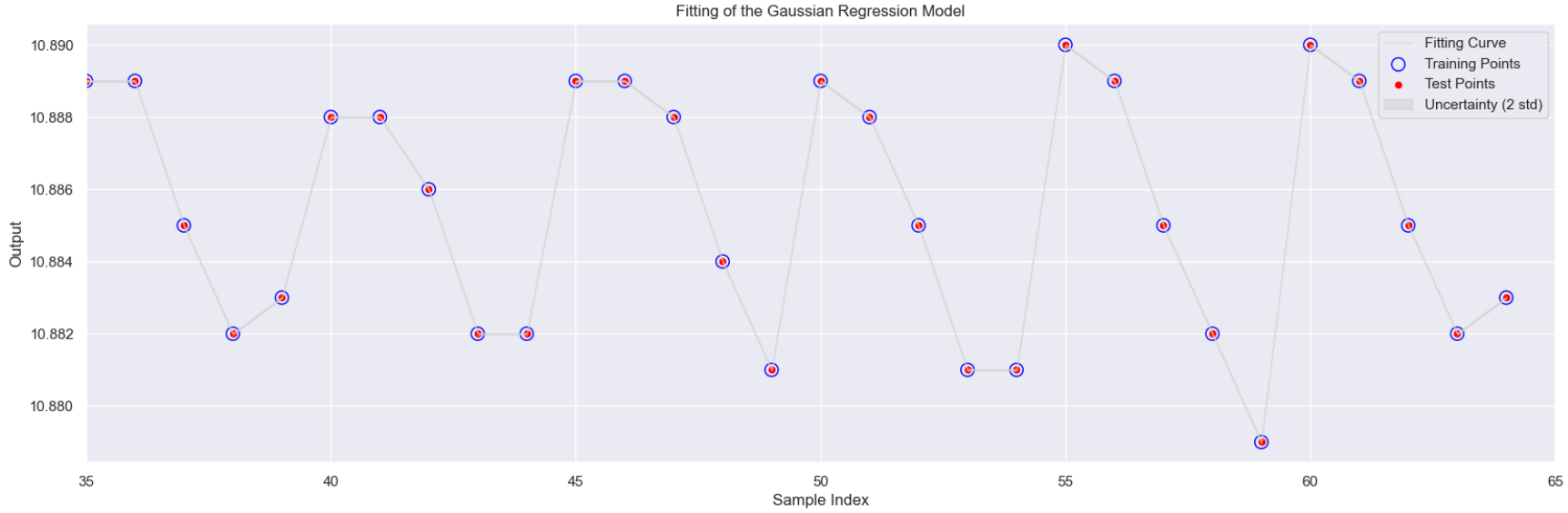

(b) Zoom-in.

Figure F.3: Predicted values of the regression model.